A Study on Augmented Reality for Supporting Decommissioning Work of Nuclear Power Plants

Yan Weida

A Study on Augmented Reality for Supporting Decommissioning Work of Nuclear Power Plants

Contents

Synopsis v

List of Figures ix

List of Tables xiii

Abbreviations xv

Chapter 1 Introduction 1
- 1.1 Background . . . 1
  - 1.1.1 Importance of Nuclear Power . . . 1
  - 1.1.2 Decommissioning of Nuclear Power Plants . . . 1
  - 1.1.3 Augmented Reality . . . 2
- 1.2 Tracking, the Key Technology of AR Support . . . 5
- 1.3 Objective of the Study . . . 9
- 1.4 Configuration of the Thesis . . . 12

Chapter 2 Design of Circular Marker and Development of Marker Automatic Measurement System 15
- 2.1 Introduction . . . 15
- 2.2 Circular Marker for Tracking . . . 18
  - 2.2.1 Marker Design . . . 19
  - 2.2.2 Algorithm to Recognize Circular Markers . . . 20
  - 2.2.3 Algorithm to Calculate Relative Position and Orientation between a Camera and Markers . . . 24
- 2.3 Development of a Marker Automatic Measurement System . . . 26
  - 2.3.1 Requirements for the System . . . 26
  - 2.3.2 System Design . . . 27
  - 2.3.3 Algorithm of the Automatic Marker Measurement . . . 29

2.3.4 System Implementation 35
2.4 Performance Evaluation of MAMS 38
2.4.1 Purpose 38
2.4.2 Method 39
2.4.3 Result 39
2.5 Feasibility Evaluation of MAMS in an NPP Environment 44
2.5.1 Purpose 44
2.5.2 Method 45
2.5.3 Result and Discussion 45
2.6 Improvement of Marker Design 52
2.6.1 Improvement of Marker Design 52
2.6.2 Evaluation of Improved Marker 53
2.7 Summary 59

Chapter 3 A Line Feature-based Tracking Method 61
3.1 Introduction 61
3.2 Development of a Line Feature-based Tracking Method 62
3.2.1 Profile of the Method 62
3.2.2 Initialization 63
3.2.3 Line Detection 65
3.2.4 Line Matching Algorithm 69
3.2.5 RANSAC-based Method 72
3.2.6 New Landmark Registration 78
3.2.7 Accuracy Improvement of Landmarks 78
3.3 Performance Evaluation of the Line Feature-based Method in an NPP Environment 80
3.3.1 Purpose 80
3.3.2 Method 80
3.3.3 Result and Discussion 83
3.4 Summary 86

Chapter 4 Development of Temporary Placement and Conveyance Operation Simulation System 89
4.1 Introduction 89
4.2 Development of TPCOSS 90
4.2.1 System Requirements 92
4.2.2 System Design 93
4.2.3 Implementation of TPCOSS 99
4.3 Feasibility Evaluation of TPCOSS in an NPP Environment 108
4.3.1 Purpose 108

4.3.2 Evaluation Method 108
4.3.3 Result and Discussion 113
4.4 Summary 116

Chapter 5 Conclusion **123**
5.1 Summary of the Study 123
5.2 Applicable Fields 126
5.3 Perspective for Integration of the Researches 126
5.4 Future Perspective 127

Acknowledgment **129**

List of publications **131**

NO TEXT ON THIS PAGE

Synopsis

In the world today, hundreds of nuclear power plants (NPPs) are in operation, several of which are facing imminent expiration of their period of use. An NPP must be decommissioned after its expiration period. Common decommissioning methods of general industrial plants use explosives and disintegrators. However, the decommissioning of an NPP is vastly different because of its residual radioactivity. In every part of an NPP, components must be dismantled one by one according to a planned dismantling procedure. In some cases, large components that are dismantled from their original locations must be cut into small pieces after they are moved to workspaces. Then the small pieces are transported to some other locations for temporary placement before their radioactivity level is checked. In an NPP, passages used for component transportation are invariably narrow, and space for dismantling work and temporary placement is limited. Consequently, large dismantled components might collide with other components in such environments during the temporary placement and conveyance operations. It is important to verify whether the space in a narrow passage is sufficient for transporting large components, whether the workspace is sufficient for field work, and whether the space designated for temporary placement is sufficient. Nevertheless, large volume and various shapes of components in NPP complicate such tasks. It is difficult to do the verification based on a legacy interface as paper documents. Therefore, a simulation system for supporting dismantling work to solved these problems is expected.

Augmented reality (AR) offers great possibility to realize the system. It expands the surrounding real world of the users by superimposing computer-generated information on the users' view. It is broadly used for many applications. Using AR technique, information is represented more intuitively than when using a legacy interface such as paper instruction documents. It is expected that AR system can simulate the dismantling work intuitively to help to make a dismantling plan for actual field work.

The objective of this study is to evaluate the feasibility of AR support system for decommissioning work of an NPP. To apply AR, tracking technology which estimates three dimensional (3D) position and orientation of users in real time is indispensable. Because of the special environment in an NPP, only the tracking methods based on vision sensor, such as camera, can be applied with high accuracy and stability and low cost in NPP environment. The vision sensor based tracking includes two different kinds, one is marker-based tracking, and the other is markerless (natural feature-based) tracking. The marker-based tracking technology has high accuracy and stability, but the preparation workload would

become very heavy if the space of the environment is very large. On the opposite, markerless tracking needs less preparation, but always its accuracy and stability are lower.

In this study, a marker-based method was applied as the primer tracking technology because of its high accuracy and stability. The preparation includes two parts, pasting indispensable markers in the environment, and measuring their 3D position and orientation. To reduce the workload and human error of measuring the markers, a marker automatic measurement system (MAMS) was developed. And then a markerless tracking method (line feature-based tracking method) was proposed as an assistant of the marker-based tracking to decrease the needed marker number, therefore the workload of pasting markers was reduced too. Finally a simulation system for supporting fieldwork was developed and evaluated.

In marker-based tracking method, square markers are widely used, but it is useful only for short distance. Because workers are expected to move throughout capacious space in NPP, the required marker number is large if using square markers. To reduce the marker number, a new type of marker which is applicable for both short and long distance was designed. Compared with the square marker, the required number and size of the new markers are smaller when tracking in a same space.

To apply marker-based tracking, it is necessary to measure the 3D position and orientation of all allocated markers. Manually measurement of the markers is inefficient and difficult to avoid human error. To solve this problem, an automatic marker registration system was developed. This system can measure 3D position and orientation of markers automatically and quickly. The system is composed of a camera which has an interior motion base, a laser rangefinder, a motion base fixed under the laser rangefinder and a PC connected to them. Camera and motion base are both fixed on a tripod. The directions of camera and laser rangefinder can be controlled by PC through motion bases. After setting up the system, it measures the 3D position of each marker automatically. First, all markers are recognized by camera, and then their 3D position and orientation are estimated. According the estimated result, laser rangefinder is then controlled to measure the more accurate 3D position and orientation of every marker, and save the result into database.

A performance evaluation experiment was taken in lab environment to evaluate the accuracy, stability and running time of the system. The result shows that the average system error is 7.6 mm and random error is 3.5 mm. The average time to measure one marker is 21.0 seconds. Another experiment was conducted in the Fugen Decommissioning Engineering Center (Fugen) which was formerly an NPP, and is now beyond its own expiration period, to evaluate the feasibility. The result shows that the system effectively reduces human error and improves measurement efficiency, and some advices on improving the system were given by the evaluaters.

When tracking in the capacious space of NPP, a large amount of markers are indispensable, so that the workload of marker measurement is still heavy even using MAMS. Moreover, in some cases it is difficult to allocate markers, for example, the tracking field

is very narrow or very high. To solve this problem, a markerless tracking method is also necessary as a assistant. The markerless tracking method uses natural features as landmark for tracking. The point feature is the most widely used feature, but it has lower stability than line feature in the NPP environment, and line features are abundant in the NPP environment. Therefore a line feature-based tracking method was developed in this study.

The fieldwork tracking requires miniaturization, real time, and low labor cost. In this study, only a camera was used as a vision sensor for tracking. The position and direction of some 3D lines were measured in advance as initial landmarks. A new random sample consensus (RANSAC) based method for solving perspective 3 Line (P3L) problems, which calculate the position and orientation of a camera through three 3D lines and their projections (2D-lines) on an image, is applied. Compared with existing methods for solving P3L problem, proposed method solves equations with a maximum of two solutions instead of solving an equation with a maximum of eight solutions as the existing method. Therefore the efficiency is improved. To enable tracking in a capacious space, it is insufficient to use only landmarks which position and direction are measured in advance. In this study, new landmarks are registered automatically into a database using a RANSAC-based triangulation method when tracking. An evaluation experiment was conducted using an image series captured in an NPP. The result shows that the tracking frame rate is about 10.4 fps, and the average error of camera position is about 100 mm. The accuracy and speed is sufficient to apply AR to support field work in some cases, such as the dismantling of large equipments.

To evaluate the feasibility of AR system for supporting decommissioning work in an NPP, temporary placement and conveyance operation simulation system (TPCOSS) is developed to support temporary placement and conveyance operations using AR, and it is evaluated by some field workers in an NPP. The system measures dismantling targets and the environment using a laser range scanner to build 3D surface polygon models of actual size. Whereas the obtained models are used to verify the space between dismantling targets and environment, AR technology was used in the temporary placement and conveyance operations simulation in the actual work field to make the information readily comprehensible. If some collision occurs, the collision position is shown in the workers' view. When evaluating the system, the evaluators operated the system according to a scenario, then questionnaires and interviews were administered to evaluate the feasibility and acceptability of the system. Some problems in practical use and improvement advice were also reported by workers. As far as the evaluation result by 4 evaluators is regarded, the system is feasible for supporting the actual conveyance and temporary placement operation in a work field at an NPP, except in some cases. However, some problems remain for practical use. They must be resolved in future work.

Future work of this study includes the following contents:

MAMS : To improve the accuracy and measurement speed, and to add the function for

measuring other type of marker. (Such as linecode marker)

Line-based tracking method : To improve the accuracy and process speed.

TPCOSS : More compact devices such as the iPad2 are expected to be obtained. Simpler operation methods of the virtual dismantling target should also be explored. And it is expected to expanse the system to enable wireless communication among multiple workers.

List of figures

1.1 Conceptual image of augmented reality. 3
1.2 An example of displaying virtual object. 4
1.3 Indication by paper document and AR interface 4
1.4 Support system for water system isolation task. 6
1.5 Indication of target valve. 6
1.6 An example of marker for tracking. 9
1.7 Configuration of the thesis. 12

2.1 Conceptual image of marker-based tracking. 16
2.2 Example of square marker. 16
2.3 Recognition steps of ARToolkit marker. 17
2.4 Dim edges of ARtoolkit marker. 17
2.5 Limitation of large marker in NPP. 18
2.6 Example of circular marker with different ID. 18
2.7 Design example of circular marker. 20
2.8 Example of circular markers patterns (ID=1-4). 21
2.9 An example of marker recognition. (a): Original image. (b): Gray-scale image. (c): Binarized image. (d): Labeled image. (e): Image of detected ellipses. (f): Image of detected markers. 22
2.10 Selection of 3 edge pixels. 25
2.11 Calculated ellipse on image. 25
2.12 Division of a marker when normalization. 25
2.13 Design of MAMS. 30
2.14 Appearance of MAMS. 31
2.15 Relation between diffierent coordinate systems. 32
2.16 Conceptual image of MAMS. 35
2.17 Flow chart of position measurement. 36
2.18 Interface of MAMS. 38
2.19 Experimental environment in lab. 40
2.20 Marker locations on a panel. 41
2.21 System error on panel No.1 (mm). 42
2.22 System error on panel No.2, $x = 2.0 \times 10^3$ (mm). 43
2.23 Random error on panel No.1 (mm). 43
2.24 Random error on panel No.2, $x = 2.0 \times 10^3$ (mm). 44
2.25 Experimental environment in NPP. 46

2.26 Pure-water chamber with marker. 47
2.27 AR experience using the measurement result. 47
2.28 Improvement of marker design. 53
2.29 Examples of misrecognized images. 55
2.30 Example of an image generated using OpenGL. 57
2.31 Points at which tracking can be executed with enough accuracy (top view of the area). 58
2.32 Position errors of tracking. 58

3.1 Flow chart of the proposed method. 64
3.2 Concept of the proposed method. 64
3.3 Rectangle marker. 65
3.4 Initial landmark recognition. 66
3.5 Edge point clusters. 66
3.6 Extreme points of a cluster. 67
3.7 Calculation regions of the rectangle marker. 67
3.8 Curve of $s(r)$. 68
3.9 Concept of IEPF method. 69
3.10 Calculation window of invariant moment. 70
3.11 Line matching with that of previous frame. 71
3.12 Line matching with key frame. 72
3.13 Definition of Plucker line. 74
3.14 A 3D line and its 2D projection on image. 75
3.15 Curve of $f(\theta)$. (Top: $1 - n^2 - c_1^2 = 0$ and $1 - s^2 - t^2 - c_2^2 = 0$. Bottom: $1 - n^2 \sin^2\theta - c_1^2 < 0$ or $1 - (t\sin\theta + s\cos\theta)^2 - c_2^2 < 0$) 77
3.16 Geometry method for new landmark registration. 79
3.17 Re-projection error between estimation and projection of a 2D line. 79
3.18 Rectangle markers in the environment. 81
3.19 Experimental environment. 82
3.20 Processing time of pose estimation. 84
3.21 Estimated trajectory of the camera (XZ-plane). 85

4.1 Outline of TPCOSS. 91
4.2 3D measurement of the modeling subsystem. 94
4.3 Concept of ICP algorithm 95
4.4 Realization of ICP algorithm using randomly chosen part. 96
4.5 Smoothing of a point cloud. 97
4.6 Appearance of the modeling subsystem. 100
4.7 Interface for producing a surface model. 102

4.8 Surface polygon models of the environment (top) and dismantling target (bottom). 103
4.9 Outline of the verification subsystem. 104
4.10 Visualization of collided part. 105
4.11 Appearance of verification subsystem. 106
4.12 Interface of verification subsystem. 107
4.13 Pure-water chamber pasted with markers. 109
4.14 Sketch map of the pasted markers. 110
4.15 Top view of the simulation environment. 111
4.16 Evaluation flow. 112
4.17 Conveyance operation simulation with a dice marker. 113
4.18 Simulation of temporary placement. 114
4.19 Simulation of conveyance. (From left column to right: The dismantling target is moved far away from the evaluator.) 114

5.1 Cooperation system in future. 127

NO TEXT ON THIS PAGE

List of tables

2.1 Hardware specifications of MAMS 37
2.2 Result of function evaluation I 49
2.3 Result of function evaluation II 50
2.4 Result of usability evaluation 51
2.5 Hardware specifications used for evaluation 54
2.6 Maximum and minimum recognition distance (mm) 55
2.7 Necessary tracking time (ms) 56

3.1 Specifications of the IEEE-1394a digital camera 83
3.2 Threshold in the initialization and line detection 83
3.3 Average processing time of one frame (ms) 84
3.4 Errors of the pose estimation 85

4.1 Hardware specifications for the modeling subsystem 100
4.2 Hardware specifications for the verification subsystem 106
4.3 Evaluation result of the verification subsystem (1/5) 117
4.4 Evaluation result of the verification subsystem (2/5) 118
4.5 Evaluation result of the verification subsystem (3/5) 118
4.6 Evaluation result of the verification subsystem (4/5) 119
4.7 Evaluation result of the verification subsystem (5/5) 120

NO TEXT ON THIS PAGE

List of abbreviations

2D 2 Dimensional

3D 3 Dimensional

AR Augmented Reality

BA Bundle Adjustment

CAD Computer Aided Design

CCD Charge Coupled Device

CPU Central Processing Unit

DEXUS Decommissioning Engineering Support System

DOF Degree of Freedom

EKF Extended Kalman Filter

fps frames per second

Fugen Fugen Decommissioning Engineering Center

GPS Global Positioning System

HMD Head Mounted Display

ICP Iterative Closest Point

ID Identification

IEPF Iterative End Point Fit

LAN Local Area Network

MAMS Marker Automatic Measurement System

NPP Nuclear Power Plant

OS Operation System

P3P Perspective 3-Point

P3L Perspective 3-Line

PC Personal Computer

PnP Perspective n-Point

RANSAC Random Sample Consensus

RE Random Error

RFID Radio Frequency Identification

SE System Error

SLAM Simultaneous Localization and Mapping

TPCOSS Temporary Placement and Conveyance Operation Simulation System

VR Virtual Reality

Chapter 1 Introduction

1.1 Background

1.1.1 Importance of Nuclear Power

Nuclear power is the use of sustained nuclear fission to generate heat and electricity. Comparing with other power generation technologies, it has some advantages. Firstly, nuclear power is more efficient. In a nuclear power plant, uranium generates 360,000 kilowatt-hours of electrical energy per kilogram, whereas coal generates about 6.67 kilowatt-hours of electrical energy per kilogram in a thermal plant. Secondly, nuclear power plants emit less greenhouse gas or other pollutants. Thirdly, the running costs of a nuclear power plant are relatively low, although the initial cost of the plant building is high, because a nuclear plant needs only a small amount of uranium to produce a lot of energy.

Now, nuclear power provides about 6% and 14% of the world's energy and electricity, respectively. In sixteen countries, nuclear energy provides at least a quarter of electricity. France gets about 78% of its power from nuclear energy, while Belgium, Bulgaria, Czech Republic, Hungary, Slovakia, South Korea, Sweden, Switzerland, Slovenia and Ukraine get more than 30%[1].

1.1.2 Decommissioning of Nuclear Power Plants

In the world today, hundreds of nuclear power plants (NPPs) are in operation, several of which are facing imminent expiration of their period of use. An NPP must be decommissioned after its expiration period. Especially in Japan, because of the influence of the earthquake and tsunami in 2011, many NPPs has been shutdown, and they have to be decommissioned in future. The decommissioning is the dismantling and decontamination of an NPP site so that it no longer requires measures for radiation protection. The characteristic difference from the dismantling of other power plants is the presence of radioactive material that requires special precautions. Therefore, common decommissioning methods of general industrial plants that use explosives and disintegrators cannot be used for NPPs. There are three options for decommissioning defined by the international atomic energy agency[2] which have been internationally adopted:

Immediate Dismantling : This option begins very soon after shutdown, and lasts for about 2-5 years. In this option, all radioactivity above special levels must be removed from the site. After the immediate dismantling, the unrestricted re-use of the site is then available.

Safe Enclosure : In this option, facility is placed into long-term safe storage, and the dismantling is so deferred in the long period, usually for 10-60 years before the eventual dismantling.

Entombment : This option encases the facility with remaining radioactivity into a long-lived material (such as concrete) on-site, and keep monitoring and maintaining the remaining structures to reduce the size of controlled area. It will last long enough until the remaining radioactivity can be ignored.

Comparing with the other two options, the immediate dismantling is the fastest option to decommission an NPP. Because of the small area and large population of Japan, it is the best option in Japan. In the immediate dismantling, because the radioactive dose rate, the requirements for ensuring safety of fieldwork is much more severer than dismantling other industrial plants, so the dismantling work is very different from other industrial plants. To dismantling an NPP, the components in every part of the NPP must be dismantled one by one according to a planned dismantling procedure. In some cases, large components that are dismantled from their original locations must be cut into small pieces after they are moved to workspaces. Then the small pieces are transported to some other locations for temporary placement before their radioactivity levels are checked. There are two problems in the dismantling work. One is the high dose rate in the NPP environment, which requirement high safety of the dismantling work. Therefore, lots of skilled workers are necessary, and the dismantling work will spent much more time and expense than other industrial plant. Another problem is that there is always only narrow space for maintenance work in an NPP, so passages used for component transportation are invariably narrow, and space for dismantling work and temporary placement is limited. Consequently, large dismantled components might collide with other components in such environments during temporary placement and conveyance operations. To ensure the workers' safety and reduce the dismantling time, it is important to verify whether the space in a narrow passage is sufficient for transporting large components, whether the workspace is sufficient for field work, and whether the space designated for temporary placement is sufficient. Nevertheless, the large volume and various shapes of components in an NPP complicate such verification tasks. It is difficult to do the verification based on a legacy interface as paper documents. Therefore, a simulation system for supporting dismantling work to solved these problems is expected. Augmented reality (AR) offers great possibility to realize the system.

1.1.3 Augmented Reality

AR expands the surrounding real world of the users by superimposing computer-generated information on the users' view[3][4]. The concept of AR is shown in Fig.1.1, virtual objects (vase and chair) are considered being put in a real environment. The virtual objects are displayed on the appropriate position from head mounted display (HMD). The user can

see the virtual object upon the real environment in her view, therefore the virtual objects are combined with the real environment.

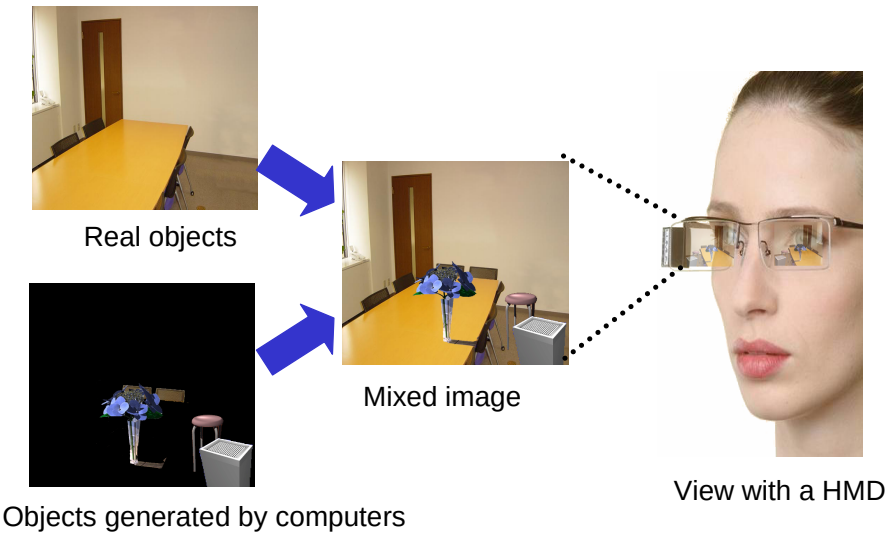

Fig. 1.1: Conceptual image of augmented reality.

AR is applicable in many fields, because it has two advantages:

1. The virtual object appears where it presumed to be as the user's perspective is changed. Fig.1.2 shows an example which a specified bolt to be twist off is indicated AR instruction. Even user's view changes, the indication is still at the correct position as an array.

2. It is more intuitive than using a legacy interface, such as paper instruction documents. Fig.1.3 shows an example: the worker is checking the pressure. When using paper instruction documents, he has to find the instrument, check the pressure, and then compare it with the normal pressure in the paper document. But when using AR, a virtual arrow which indicates the pressure state in the worker's view is intuitive and efficient enough.

AR technology is tried to be used in various fields, such as medical, mobile, industry, edutainment, etc.[5].

In the medical field, AR is widely used for supporting surgery training and education. It can provide the surgeon with information of the blood pressure, the state of the patient's organ, etc. An example is described that a virtual X-ray view based on prior tomography or on real time images from ultrasound and confocal microscopy probes[6]. In another study, 3D computer models were merged with live video to enhance surgeon's understanding[7]. AR is also used for constructing a patient electrophysiological database[8].

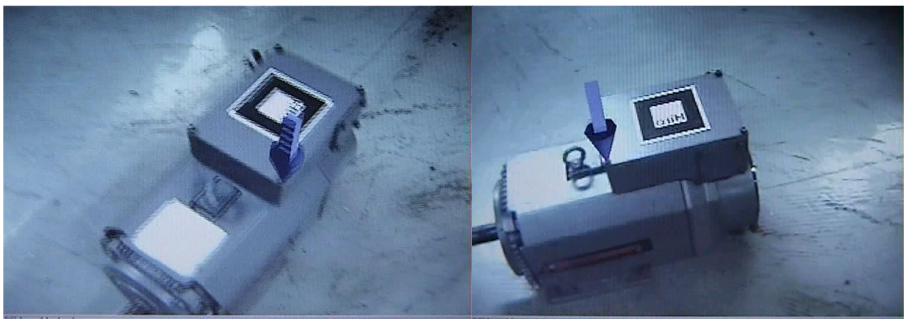

Fig. 1.2: An example of displaying virtual object.

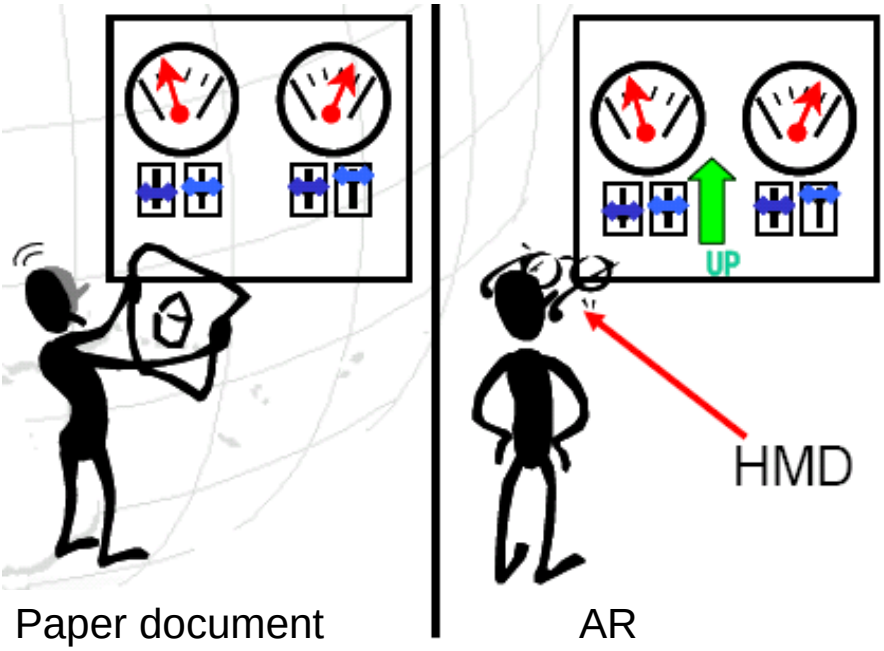

Fig. 1.3: Indication by paper document and AR interface .

The development of hardware and software makes it possible to apply AR on mobile. The AR application on mobile can add virtual information on the real world for collaborative work. An example of collaborative system which supports face to face collaborative AR gaming is described in [9].

In the industry field, AR offers high possibility for supporting the design, maintenance and training task. For example, a product design system was developed for car designers[10], and a navigation and information system which takes AR into large scale industrial environment for spatial data access and on-site navigation was developed[11]. Another example is shown in [12], which workers can complete their job in a much easier way because AR permits them to look through the machine as if it was with x-ray, pointing them to the problem right away.

In the entertainment field, the gaming industry has benefited a lot from the development of AR. A number of complete new games have been developed for prepared indoor environments. A mobile entertainment system is developed based on the interaction between human and computer[13].

In the military field, AR can serve as a networked communication system that renders useful battlefield data onto a soldier's goggles in real time. From the soldier's viewpoint, people and various objects can be marked with special indicators to warn of potential dangers. A battlefield AR system had been realized in a study[14]. Virtual maps and 360 ° view camera imaging can also be rendered to aid a soldier's navigation and battlefield perspective, and this can be transmitted to military leaders at a remote command center[15].

Recently AR is also used for supporting workers in NPPs. In a support system for a water system isolation task[16], AR is used to indicate the 3D position and direction of targets. Fig.1.4 shows the system which comprises a portable computer, camera, display device and radio frequency identification (RFID) reader. Fig.1.5 shows the indication of target valve.

Because informations are represented more intuitively in AR than when using a legacy interface such as paper instruction documents, it is expected that AR system can simulate the dismantling work to help to make a dismantling plan for actual field work. Using AR, many human errors can be avoided. For example, when dismantling a component, some switches must be turn off in order. If this operation is supported by AR, the right switch can be indicated directly in the worker's view so that it is lower possibility to make a mistake.

1.2 Tracking, the Key Technology of AR Support

There are four elementary technologies to realize AR:

Tracking Compute pose (3D position and 3D orientation) of the user in real time.

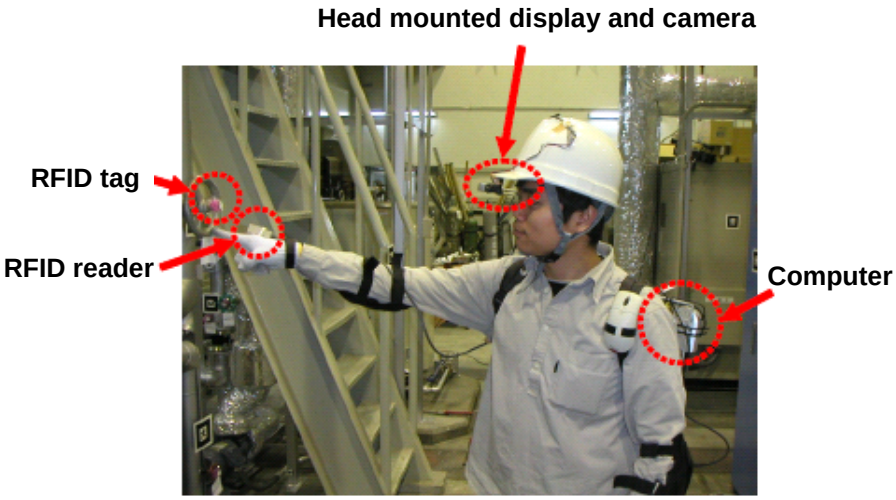

Fig. 1.4: Support system for water system isolation task.

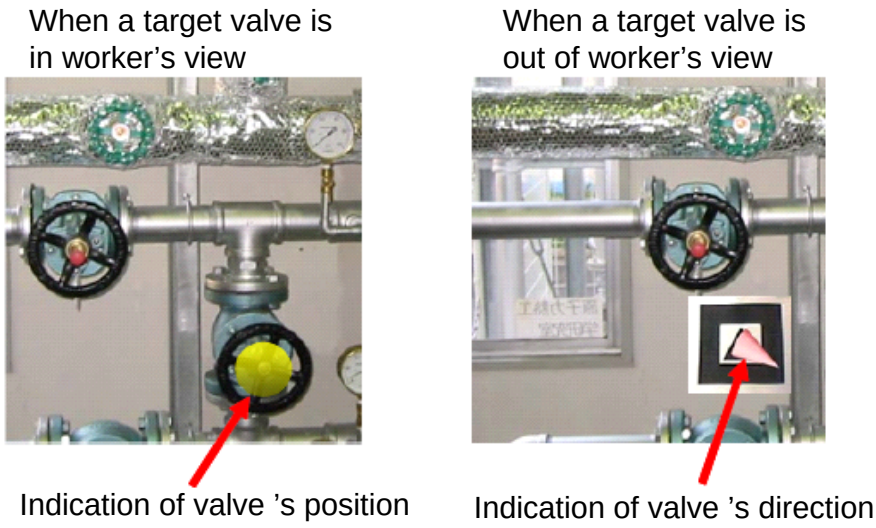

Fig. 1.5: Indication of target valve.

Display Display the virtual objects on the user's view.

Calibration Calibrates the relative position between camera and users' view, and camera distortion etc.

Registration Matches the virtual objects to the real world.

In an NPP, the display, calibration and registration technologies are almost same as other applications of AR, but the tracking technology is quite different from many other application because of the special environment in an NPP. To realize the tracking technology in an NPP, some requirements must be met:

Requirement I The tracking methods which can be used indoor are necessary, because the NPP environment is an indoor environment.

Requirement II The tracking methods which works with long distance movement of workers are necessary, because the NPP environment is a capacious space, there are many types of tasks in dismantling work, such as conveyance of dismantling objects in long distance.

Requirement III The methods which can be used in a complicated environment are necessary because of the complication of NPP field with many equipments and pipes.

Requirement IV The methods which can be used in metal environments are necessary because there are many metal equipments in an NPP.

Requirement V The methods which can estimate both 3D position and 3D orientation of workers are necessary because it is impossible to indicate virtual information correctly with only 3D position of workers.

Requirement VI The tracking methods with high accuracy and stability are necessary, because low accuracy and stability leads to the wrong displaying position of indication, which may cause the danger of error dismantling operation of workers.

Therefore, this study focuses on the problem about the tracking technologies. The widely used tracking technologies includes the following aspects:

Satellite position tracking Satellite position tracking uses multiple satellites to calculate the 3D position of a receiver by estimating the distance between the receiver and satellites. The global positioning system (GPS)[17] is based on this technology. It is a global navigation satellite system. GPS is broadly used in AR applications. But it cannot be used in this study, because NPP field is an indoor environment, it is difficult to receive the satellite signal. Moreover, GPS can only estimate 3D position of the receiver, but 3D orientation of the receiver is also necessary in AR tracking

in an NPP. Therefore, the satellite position tracking cannot meet the Requirement I and V.

Wireless LAN positioning Wireless LAN (Local Area Network) positioning estimates a receiver's position using a wireless LAN signal's fingerprint and strength[18]. Although it can be used in the indoor environment, the accuracy limits its application in NPP for supporting complicated work, it cannot meet the Requirement V and VI.

Inertial sensors Inertial sensors includes two kinds: acceleration sensor and gyro sensor. They are both convenient in practical use because they need few preparation work and additional device. The disadvantage of inertial sensors is that the error will increase over time because of the accumulating error. This makes it difficult to be used in NPP for supporting the complicated work which will take long time, or worker have to move a long distance. Therefore, the inertial sensors cannot meet the Requirement II and VI.

Magnetic sensors Magnetic sensors can offer high accuracy and stability in a specially controlled environment. It estimates 3D position and orientation with only one sensor. The disadvantage of magnetic sensors is that it is easily influenced by metal components. Because there are so many metal components in NPP, magnetic sensors also cannot be used, it cannot meet the Requirement IV.

Ultrasonic sensor Ultrasonic method is also applied in AR tracking[19]. An ultrasonic tracking system comprises a transmitting unit and a receiver. To cover a wide area, the sensor number will become very large to assure the accuracy. This limits its application in the capacious field of NPP. Moreover, it is easily influenced by multiple reflections of ultrasonic on different surface. Therefore ultrasonic also cannot be used in an NPP, it cannot meet the Requirement III.

Vision sensor Usually a video camera is used as a vision sensor. By capturing images of environment using camera, some features which are more distinguishable than other part of the image can be extracted from the images, such as corners, edges, and planes. Then the relative position between the features and the camera can be estimated using a geometric method. Because it is applicable in an indoor environment, and little influenced by other equipment, it is the most appropriate technology to be used in an NPP. The vision sensors-based tracking includes two kinds: marker-based tracking[20][21] and markless tracking[22][23]. Markless tracking uses natural features which originally exist in the environment as landmark for tracking, and marker-based tracking uses artificial markers which are designed with special texture as the landmark for tracking, Fig.1.6 shows an example of circular marker for AR tracking. The marker-based tracking has higher accuracy and stability than markerless tracking. The disadvantage of marker-based tracking is that it is necessary to paste a large

number of markers in a capacious area and measure their 3D positions and orientations before tracking, therefore the preparation work of marker-based tracking is much heavier than markerless tracking.

Fig. 1.6: An example of marker for tracking.

According to the Requirement I-VI, the vision sensor is the most appropriate tracking method in an NPP. In this study, the marker-based tracking technology is chosen as a primer tracking technology because of the requirements on accuracy and stability for the complicated work in an NPP. Although the markerless tracking has lower accuracy and stability than marker-based tracking, it is possible to be used as an assistance method of marker-based tracking in some cases which are difficult to realize the marker-based method, for example, the space is too narrow or the position is too high to paste efficient markers for tracking.

1.3 Objective of the Study

The objective of this study is to evaluate the feasibility of AR system for the decommissioning work of an NPP. To support the dismantling work in an NPP, the feasibility includes the following requirements:

Requirement A AR system must have reliability to ensure safety of the dismantling work. It is the basic requirement, because safety is very important in dismantling work in NPP, the accuracy and stability of tracking must be high enough.

Requirement B AR system must improve the efficiency of the dismantling work. As Requirement A is satisfied, the efficiency is the higher the better.

Requirement C The cost of using AR system must be low. As Requirement A is satisfied, the cost is the lower the better.

In Requirement A, to ensure the sufficient reliability, the accuracy and stability of the tracking must be high enough. The minimum requirement on the accuracy and stability is depend on the concrete task. There are many tasks can be supported by AR in the dismantling work.

In some tasks, the reliability is can be ensured even the accuracy and stability is not so high. For example, the navigation for workers to the destination allows the accuracy with 1-2 m errors, because the navigation only requires the correct indication on direction. The temporary placement of dismantled components allows the accuracy with 0.1-1 m errors, because the space for temporary placement is always with large size, and there are some passages with 0.1-1 m for the workers and the handling machines.

In some other tasks, higher accuracy and stability is required. For example, the conveyance operation of the dismantled target allows the accuracy with less than 0.1 m errors, because in NPP environment, the passages for moving the dismantling target are always narrow, especially for the components with large size. Therefore, in many cases, the spatial clearance for the conveyance is very small (<0.1 m).

Besides the above tasks, there are some tasks which require very high accuracy and stability. For example, the operations of pushing some buttons in order, or rotating some small valves. Because the size of button or valves is very small (<0.02 m), only the accuracy with less than 0.02 m errors is allowed.

As mentioned in section 1.2, tracking is the key technology in NPP for the AR application because the existing tracking method cannot be used directly in the NPP environment. Therefore, feasibility of the tracking must be evaluated in this study. The feasibility of the tracking includes two aspects: (1) The accuracy is enough for the actual use. (2) The stability is enough for the actual use. Here, the stability means the accuracy would not change too much even if the tracking lasts for a long time or the workers have moved a long distance. Because the conveyance operation of the dismantled target requires both high accuracy (<0.1 m) and stability (workers have to move a long distance), it is an appropriate support target to evaluate the feasibility of AR in an NPP.

According to the requirements, the AR system must be designed as the following criterion:

Criterion i Reliability in actual use. The accuracy and stability of tracking result must satisfy Requirement A to ensure safety. It is the basic criterion. In this study, the temporary placement and conveyance is selected as the support target, so the requirement is that the error must be smaller than 0.1 m.

Criterion ii Comprehensibility of user interface and operation. The interface and operation must be comprehensive for easy use to improve the efficiency of operation.

Criterion iii Operability of the AR system. The operation of the AR system must be easily realized by workers to easy use to improve the efficiency of operation.

Criterion iv Effectiveness of the AR system. The designed functions must necessary and useful for supporting the dismantling work.

Criterion v Low cost of realizing and using the AR system.

As the description in the section 1.2, the marker-based tracking technology is chosen as a primer tracking technology in this study. To apply the marker-based tracking method, the following problems must be solved:

Problem 1 Appropriate markers which are applicable in long distance tracking are necessary. The NPP environment is a capacious space, but the space for pasting markers is limited. Therefore, the markers which are applicable in long distance tracking with as small size as possible are necessary. The size of existing markers for long distance tracking is too large to be used in an NPP. In this study, a new circular marker which is applicable in long distance tracking with small size is designed to solve the problem.

Problem 2 Efficiency and low human errors of preparation work for using AR system must be ensured. It is necessary to paste essential markers in the environment, and their 3D position must be measured before applying the marker-based tracking. In the capacious space of the NPP environment, although the space for pasting markers is limited, the needed number of markers is also large. Therefore, the manual work of pasting and measuring has very heavy workload, and the human errors of measuring will influence the tracking accuracy. To solve this problem, a marker automatic measurement system (MAMS) which can measure 3D position of markers automatically and quickly is developed to reduce the preparation workload and human errors of measuring in this study.

Problem 3 In some case, such as the operation task in which workers only move in a small space, the short distance tracking is also important. Consequently, the markers must be applicable in short distance tracking, too. To solved this problem, the circular design is improved to make it applicable in both long and short distance tracking.

Problem 4 In some cases, it is very difficult to paste markers, for example, the space is too narrow or the position is too high. To cover the whole environment, a markerless tracking method is also necessary as an assistant of the marker-based tracking method. To solve this problem, a line feature-based tracking method is proposed in this study.

After solving these problems, an AR system was developed following Criterion i-v, and its feasibility was evaluated to confirm whether the system was effective to satisfy Requirement A-C. The evaluation is based on the actual experience of the evaluators by using the AR system in this study.

1.4 Configuration of the Thesis

Configuration of the thesis is shown in Fig.1.7.

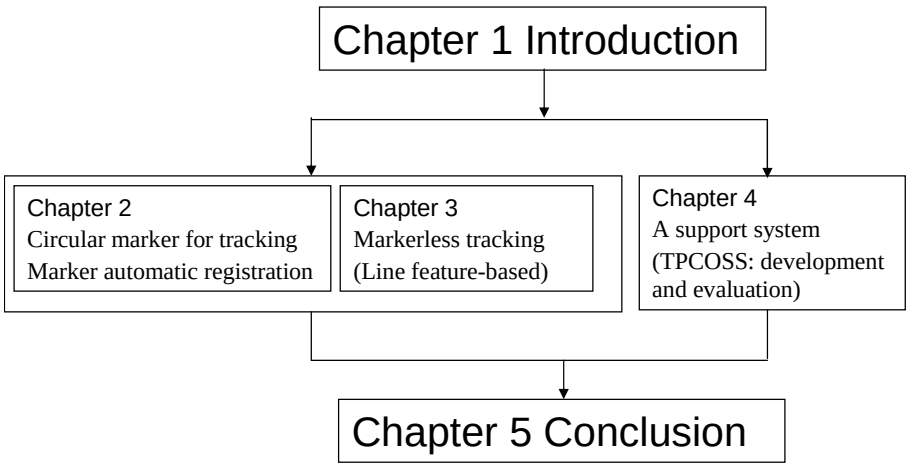

Fig. 1.7: Configuration of the thesis.

In chapter 2, a circular marker is designed for the long distance tracking to solve Problem 1, and then MAMS which can measure 3D position of markers automatically and quickly is developed to solve the Problem 2, so it is convenient for reducing preparation workload and human error in the marker-based tracking. To solve the Problem 3, the circular marker design is improved by adding four small circles as features so that enough point features can be detected even in short distance tracking.

In chapter 3, a line feature based tracking method is proposed to solve the Problem 4. Comparing with the marker-based tracking method, it is less preparation work, but lower accuracy and stability. It is an assistant for marker-based tracking, especially when the needed marker number is too large in case of only use of marker-based tracking.

To evaluate the feasibility of AR system in NPP, temporary placement and conveyance operation simulation system (TPCOSS) is developed in chapter 4. The system simulates the temporary placement and conveyance operation after a component is dismantled. So it is useful for making a dismantling plan which can avoid some possible accidents, for example, the dismantled component collides with other components when it is moved. Then, TPCOSS is evaluated in actual NPP environment to confirm whether the system was effective to satisfy Requirement A-C.

In chapter 5, researches in this thesis are concluded and future works are prospected.

Reference

[1] World Nuclear Association: *Nuclear power in the world today*, 2012

[2] http://www.world-nuclear.org/info/inf19.html, November 1, 2012.

[3] R. Azuma: A survey of augmented reality, *Teleoperators and Virtual Environments*, Vol. 6, No. 4, pp. 355–385, 1997.

[4] R. Azuma, Y. Baillot, R. Behringer, S. S. Feiner, B. MacIntyre: Recent Advances in Augmented Reality. *IEEE Computer Graphics and Applications*, Vol. 21, No. 6, pp. 34–47, 2001.

[5] Y. Donggang, J. Jesse Sheng, L. Suhuai, L. Wei, H. Qingming: A useful visualization technique: A Literature Review for Augmented Reality and Its Application, Limitation & Future Direction, *Visual Information Communication*, pp. 311-337, 2010.

[6] P. Mountney, S. Giannarou, D. Elson, GZ. Yang: Optical Biopsy Mapping for Minimally Invasive Vancer Screening, *Medical Image Computing and Computer-Assisted Intervention*, Vol.5761, pp.483-490, 2009.

[7] W. Lorensen, H. Cline, C. Nafis, R. Kikinis, D. Altobelli, L. Gleason: Enhancing Reality in the Operating Room, *Proceedings of IEEE Visualization Conference*, pp. 410-415, 1993.

[8] Y.P. Starreveld, A.G. Parrent, A.F. Sadikot, T.M. Peters: Three-Dimensional Database of Subcortical Electrophysiology for Image-Guided Stereotactic Functional Neurosurgery, *IEEE Transactions on Medical Imaging*, Vol. 22, No. 1, pp. 93-104, 2003.

[9] A. Henrysson, M. Billinghurst, M. Ollila: Face to Face Collaborative AR on Mobile Phones, *Proceedings of ISMAR 2005*, pp.80-89, 2005.

[10] G. Klinker, A.H. Dutoit, M. Bauer, J. Bayer, V. Novak, D. Matzke: "Fata Morgana", A Presentation System for Product Design, *Proceedings of 1st ISMAR*, 2002.

[11] X. Zhang, Y. Genc, N. Navab: Tracking AR into Large Scale Industrial Environment: Navigation and Information Access with Mobile Computers, *Proceedings of ISAR'01*, pp. 179-180, 2001.

[12] http://www.businessweek.com/stories/2009-11-03/augmented-reality-goes-mobilebusinessweek-business-news-stock-market-and-financial-advice, November 1, 2012.

[13] A.D. Cheok, S.W. Fong, K.H. Goh, X. Yang, W. Liu, F. Fazbiz: Human Pacman: A Sensing-based Entertainment System with Ubiquitous and Computing and Tangible, *Proceedings of NetGame'03*, pp. 106-117, 2003.

[14] S. Julier, Y. Baillot, M. Lanzagorta, D. Brown and L. Rosenblum: Battlefield augmented reality system, *NATO Symposium on Information Processing Techniques for Military Systems*, pp. 9–11, 2000.

[15] http://readwrite.com/2010/06/11/military-grade-augmented-reality-could-redefine-modern-warfare, November 1, 2012.

[16] H. Shimoda, H. Ishii, Y. Yamazaki, H. Yoshikawa: A support system for water system isolation task in NPP by using augmented reality and RFID, *Proceedings of the 6th International Conference on Nuclear Thermal Hydraulics, Operations and Safety(NUTHOS-6)*, 2004.

[17] B. Hofmann, H. Lichtenegger, J. Collins: GPS: Theory and Practice 5th edition, *SPRINGER*, 2001.

[18] Z. Xiang, S. Song, J. Chen, H. Wang, J. Huang, X. Gao: A Wireless LAN-based Indoor Positioning Technology, *IBM Journal of Research and Development*, Vol. 48, pp. 617-626, 2004.

[19] S. Feiner, M. Blair, S. Doree: Knowledge-based augmented reality. *Communications of the ACM*, Vol. 36, No. 7, pp. 52–62, July 1993.

[20] H. Kato, M. Billinghurst: Marker tracking and HMD calibration for a video-based augmented reality conferencing system, *Proceedings of IEEE and ACM International Workshop on Augmented Reality 1999*, pp. 85–94, 1999.

[21] G. Welch, G. Bishop, L. Vicci, S. Brumback, K. Keller: The hiball tracker: high-performance wide-area tracking for virtual and augmented reality environments. *Proceedings of ACM Virtual Reality Software and Technology 1999*, pp. 1–10. 1999.

[22] A. Comport: Real-time markerless tracking for augmented reality–the virtual visual servoing framework. *IEEE Transactions on Visualization and Computer Graphics*, Vol. 12, No. 4, pp.36–45, 2003.

[23] G. Simon, A. Fitzgibbon, A. Zisserman: Markerless tracking using planar structures in the scene, *Proceedings of IEEE and ACM International Symposium on Augmented Reality, 2000*, pp. 120–128, 2000.

Chapter 2 Design of Circular Marker and Development of Marker Automatic Measurement System

In this chapter, firstly a circular marker which is applicable for long distance tracking is developed. Then a marker automatic measurement system (MAMS) is developed, and its performance and feasibility is evaluated. Finally, the design of the circular marker is improved to make it applicable in both short and long distance tracking.

2.1 Introduction

The marker-based tracking method calculates the 3D position and orientation of a camera by estimating the relative position between the markers and the camera. The conceptual image of the marker-based tracking is shown in Fig.2.1. The main steps of the marker-based tracking include two parts: preparation work (the following Step 1-1 and Step 1-2) and tracking (the following Step 1-3 and Step 1-4).

Step 1-1 Paste a number of markers in the tracking environment.

Step 1-2 Measure 3D positions and orientations of all the markers.

Step 1-3 Capture some markers by a camera, and recognize them in the captured image.

Step 1-4 Calculate the position and orientation of the camera.

In usual marker-based AR applications, because the motion distance of users is limited in a small space, short distance tracking is enough to meet the requirements of the system. For example, the necessary recognition and tracking distance of an AR system for supporting surgery simulation is only 2-3 m (the size of operating table). Another application of the MagicBook project[1] even needs only 1-2 m for tracking because its tracking area is only limited around a book. In the existing marker-based tracking method, square markers, such as in ARToolkit[2] are widely used[3]-[7]. Fig.2.2 shows an example of ARToolkit marker. The marker is recognized by the following steps (as shown in Fig.2.3):

1. Detect edges of the marker.

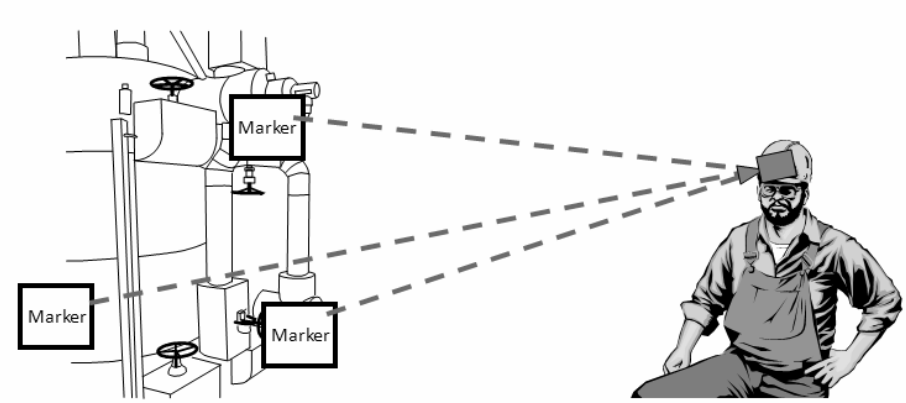

Fig. 2.1: Conceptual image of marker-based tracking.

2. Extract four lines from the edges.

3. Calculate the four intersection between the 4 lines. The four intersection points are the feature points which will be used for estimating the 3D position and orientation of the camera.

Fig. 2.2: Example of square marker[2].

However, workers in an NPP usually need long distance motion as long as 10 m in the inspection task. Existing paper-based markers, including the square markers are inapplicable in NPP field work because their recognition distance are too short. For example, the edges of a square marker become dim (Fig.2.4) when the distance from a camera and the marker becomes longer, which amplifies recognition error of feature point positions. Experiments conducted using ARToolkit marker with 80 mm of side length[2] show that ARToolkit markers' error of position increases with the distance from a camera and the markers becomes longer, and the maximum error is about 30 mm when the distance is 600

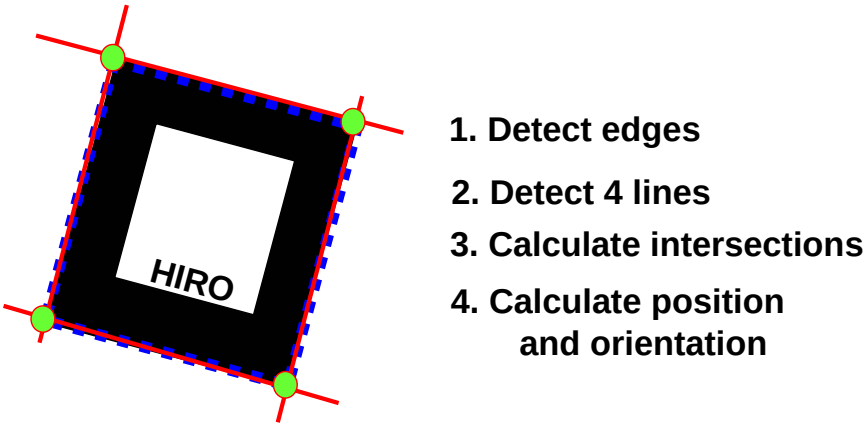

Fig. 2.3: Recognition steps of ARToolkit marker.

mm. The distance and the accuracy are unacceptable for NPP field work support, which requires at least 10 m recognition and tracking distance and higher accuracy. One solution is to make the markers with larger size. However, the space for pasting large marker is limited because of the complicated NPP environment, as shown in Fig.2.5. Another problem is that if the marker size is too large, it may become undetectable when the distance between the camera and the markers becomes short, because it is difficult to capture the whole marker under a short distance. If the number of detectable feature points on the markers is smaller than 4, the tracking will fail[9]. In other words, large markers easily leads to tracking failures in short distance tracking.

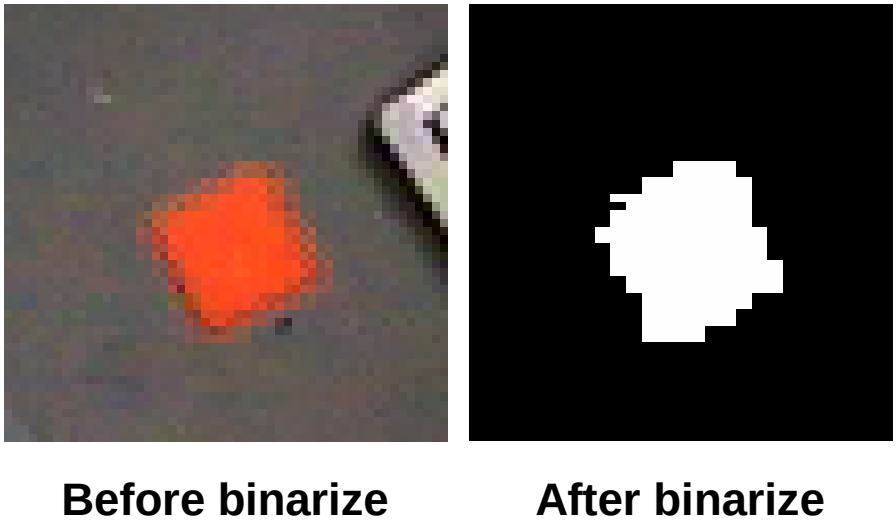

Fig. 2.4: Dim edges of ARtoolkit marker.

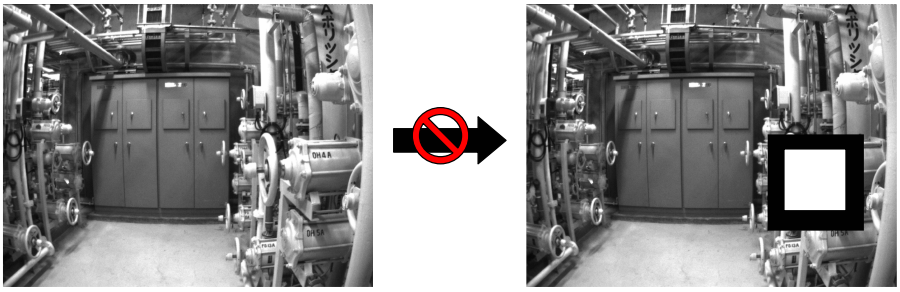

Fig. 2.5: Limitation of large marker in NPP.

Circular markers are also used in AR systems. Fig.2.6 shows an example of circular markers with different ID (identification). Compared with the square markers, it has the advantage that the center of it is centroid, invariant to the view angle. It is more detectable than square marker even the edges become dim when the distance between the camera and the marker increase. However, the design of the marker includes some shapes with relative small area (the small circular in Fig.2.6), which makes it difficult to be recognized correctly in the long distance. To solve this problem, a new circular marker which is applicable in long distance tracking is designed for the marker-based tracking method in this study.

Fig. 2.6: Example of circular markers with different ID[8].

To apply marker-based tracking, another important problem is the preparation work before tracking. It is necessary to measure the 3D positions and orientations of all allocated markers in the environment. Manually measurement of the markers is inefficient and difficult to avoid human error, especially in the capacious space of NPP where needs more markers. To solve this problem, MAMS was developed in this study. The system uses a computer to control the direction of a laser ranger finder to measure 3D positions and orientations of markers automatically and quickly with high accuracy.

2.2 Circular Marker for Tracking

Circular markers are used for tracking as the follow steps:

Step 2-1 Capture circular markers pasted in the environment using camera.

Step 2-2 Recognize the markers with their ID and positions on the image.

Step 2-3 Calculate 3D position and orientation of the camera using the result obtained from Step 2-2 and the corresponding 3D position information of the recognized markers.

To be distinguished from other patterns, every marker must have a unique ID. Therefore, it is necessary to design the circular marker to make it available with enough patterns. The details of the design should be described in section 2.2.1.

2.2.1 Marker Design

Following the Criterion i mentioned in chapter 1, the circular marker must be reliably recognized in long distance tracking. Therefore, the design of circular marker proposed in this study is shown in Fig.2.7. It consists of one large circle located in the marker's center. The large circle is composed of one black outer circle, one white center circle, and one middle circle. The thickness of the outer circle, center circle and middle circle are respectively 30%, 30% and 40% of the large circle's radius. The center of the large circle are used as a feature point of the marker which would be used for the tracking calculation. Comparing with the existing circular marker, the new designed marker has no relative small area, therefore it is more reliable recognition in long distance. Moreover, the ID recognition is based on a threshold which can be changed when the illumination changes (the details will be described in section 2.2.2), it is more reliable recognition in different environment. To obtain a unique solution, four or more feature points must be recognized simultaneously on the camera image[9]. The middle circle consists of 10 black or white fans, which represent a binary code through their color (white is 1 and black is 0). In practical use, the marker patterns and their corresponding ID are decided by the following steps:

Step 3-1 Represent from 1 to 1022 in binary code. 0 and 1023 are not used, because in the case of 0 and 1023, the ten fans would become all black or all white, respectively.

Step 3-2 Root shift the binary one bit, and repeat 10 times, then choose the minimum of the 10 shifted result. For example, 0110110000 would be shifted to 0000011011.

Step 3-3 Sort all result code obtained from Step 3-2 in ascending order. If the result codes of multiple code are same, the result code should only be sorted once. Finally 99 patterns can be obtained.

Step 3-4 The ID of the 99 patterns are 1-99 as the ascending order of their binary code.

Fig.2.8 shows the example patterns which ID is from 1 to 4 respectively. Combined with other tracking method, 99 patterns are enough for cover the whole field of NPP. For example, using the inertial sensors or wireless LAN positioning, the position of the workers can be estimated firstly in a small area, and then the small area can be covered by less than 99 patterns to use the marker tracking.

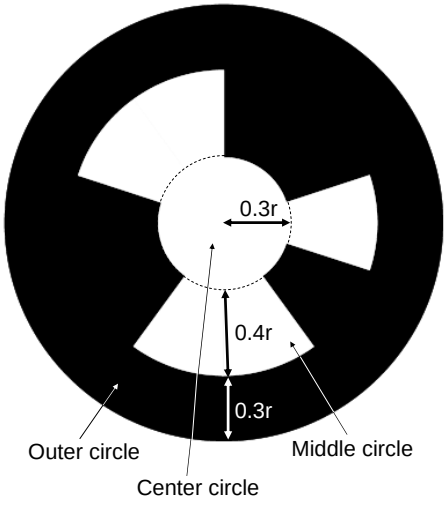

Fig. 2.7: Design example of circular marker.

2.2.2 Algorithm to Recognize Circular Markers

The basic recognition procedure is as follows:

1. Detect the edge of the large circle of a marker on image. A circle would become a ellipse on image.
2. Extract an ellipse from the detected edge.
3. Calculate the center point of the ellipse.
4. Recognize the ID of the marker.

Fig.2.9 shows an example of the recognition result of the circular markers. The details are described in the following. It is assumed that the markers are printed out on white paper with printers and that the image obtained from a camera is in gray-scale format: each image pixel $I(x, y)$ has a gray-scale value ranging from 0 to 255.

Step 4-1 If the environment is too dark or too light, the difference between the white part and the black part of the original image becomes small. It is necessary to enhance the contrast in the high and low gray-scale area of the image. To solve this problem, each

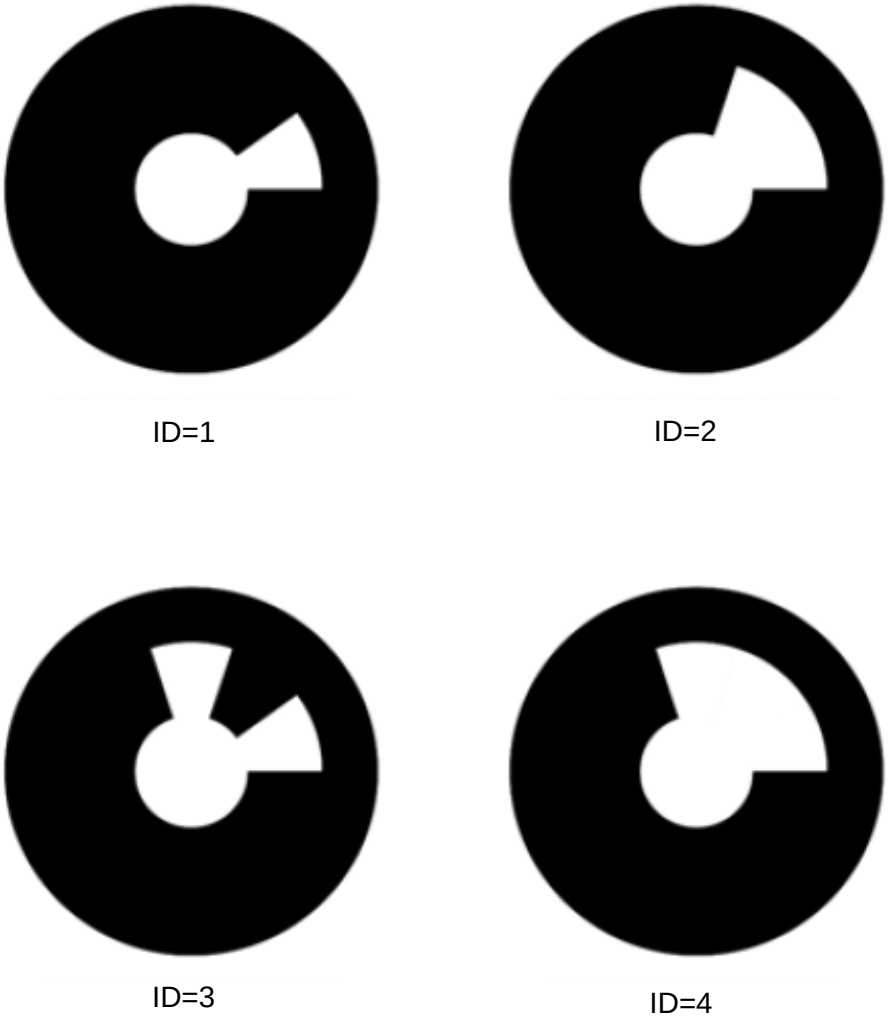

Fig. 2.8: Example of circular markers patterns (ID=1-4).

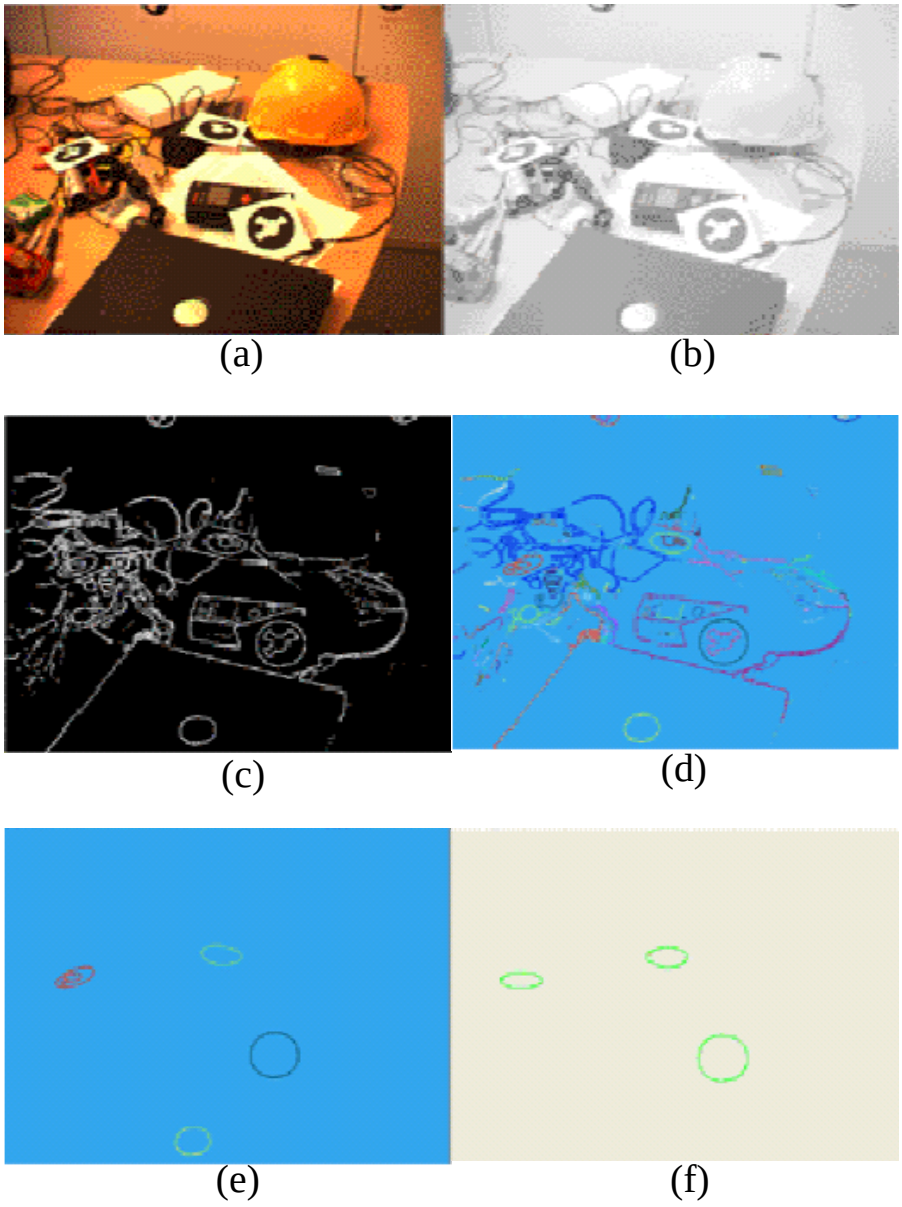

Fig. 2.9: An example of marker recognition. (a): Original image. (b): Gray-scale image. (c): Binarized image. (d): Labeled image. (e): Image of detected ellipses. (f): Image of detected markers.

pixel $I(x, y)$ is converted using Equation (2.1) and (2.2). This transform enhances the contrast of the image where the gray-scale is very high or very low. The result is shown as Fig.2.9(b).

$$J(x, y) = \log_{10}(I(x, y) + 1), (0 \leq I(x, y) \leq 127) \tag{2.1}$$

$$J(x, y) = 4.243 - \log_{10}(266 - I(x, y)), (128 \leq I(x, y) \leq 255) \tag{2.2}$$

Step 4-2 Apply a 3×3 Sobel edge detector[10] to the image obtained in Step 4-1 and binarize the result with a threshold value (0.8 in this study). The result is shown as Fig.2.9(c).

Step 4-3 Label the binarized image by collecting the connected pixels and assigning a unique label to them. Eliminate candidates with an area narrower than 10 or wider than 100,000 to remove the noise which are not markers. The result is shown as Fig.2.9(d).

Step 4-4 Choose one labeled area.

Step 4-5 Trace the edges of the chosen area and number each edge pixel.

Step 4-6 As shown in Fig.2.10, select one edge pixel($\mathbf{P}$) randomly and two other edge pixels($\mathbf{P}_1$, $\mathbf{P}_2$) so that the differences between the pixel numbers are all equal. Furthermore, calculate the ellipse that passes through the selected three edge pixels. Repeat this calculation 150 times and calculate the average of the center(x_{ell},y_{ell}), major radius r_a, minor radius r_b, and rotation angle θ_{ell} (angle of major radius and horizontal line on the camera image, Fig.2.11), respectively.

Step 4-7 Eliminate the ellipse candidates for which the major radius r_a is smaller than 10 pixels or for which the ratio of the major radius to the minor radius is larger than 3.5 to remove the noise which are not markers.

Step 4-8 Calculate the average of the squared distance between the ellipse calculated in Step 4-6 and each edge pixel. Eliminate candidates for which the average is greater than 0.02.

Step 4-9 Normalize the recognized ellipses to a circle using the ratio of the major axis to the minor axis, and the rotation θ_{ell} of the ellipse, as depicted in Fig.2.12. Set the baseline on the major radius of the ellipses. The outer circle and the center circle of the marker are divided into five rings along with the radius, and each ring is divided into 20 pixels along with the arc. The middle circle is divided into 100 elements along with the arc. Each element is divided into 10 pixels along with the radius.

Step 4-10 To make the recognition stabler even if the brightness of the environment changes, calculate the variance v_{out} and average a_{out} of pixels in the black outer circle, as well as the variance v_{in} and average a_{in} of pixels in the white center circle using the original image captured by the camera. Eliminate candidates for which v_{out} is larger than 5×10^8 or for which v_{in} is larger than 5×10^7. Set the average of a_{out} and a_{in} to a threshold th.

Step 4-11 For each element of the middle circle divided in Step 4-9, count pixels for which the brightness is greater than th and less than th. Set the results as s_w and s_b, respectively. (The processing of Step 4-10 and Step 4-11 make the recognition stabler even if the brightness of the environment changes.)

Step 4-12 Find an element of the middle circle which $s_w > s_b$. Perform the search from the baseline shown in Fig.2.12 in counterclockwise order.

Step 4-13 Starting from the element isolated in Step 4-12, look in counterclockwise order for an element which $s_w < s_b$ in the middle circle. The element found in this step is set as the basis for analyzing the binary code of the middle circle. Calculate N_{scn} by counting the elements between the baseline and the element found in this step. The element found is considered as a boundary between two fans of the middle circle.

Step 4-14 Starting from the element found in Step 4-13, count in counterclockwise order the number of elements which $s_w > s_b$ and $s_w < s_b$, respectively, for each fan. Set the results as S_w and S_b , respectively.

Step 4-15 Eliminate candidates which have a fan verifying $|S_w - S_b| < 3$.

Step 4-16 In total, 10 bits are obtained from the middle circle, assuming that a fan for which $S_w > S_b$ has a binary value of 0, whereas a fan for which $S_w < S_b$ has a binary value of 1.

Step 4-17 Shift the 10 bits obtained in Step 4-16 10 times (circular shift in 1 bit step) and find the smallest value. Set the result as the number (ID) of the marker. Set the number of the shift operation when the smallest value appears as N_{sft}.

2.2.3 Algorithm to Calculate Relative Position and Orientation between a Camera and Markers

If enough markers are recognized on image which means there are enough feature points, the relative 3D position and orientation between the camera and the markers can be estimated using perspective n-point method (PnP)[9], while the 3D positions of the n points and their 2D positions on image are known. The details is described as following algorithm.

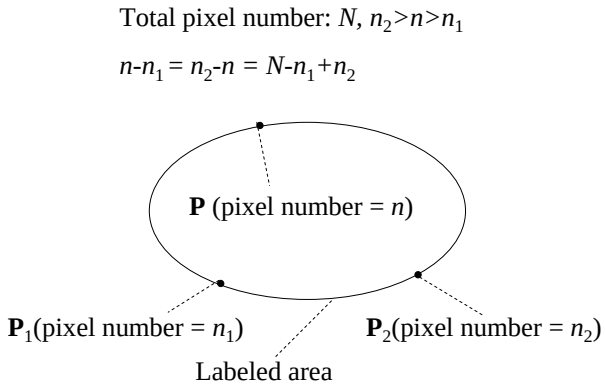

Fig. 2.10: Selection of 3 edge pixels.

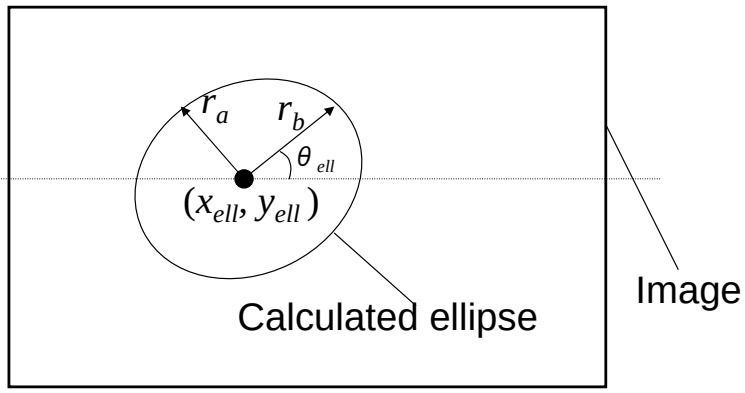

Fig. 2.11: Calculated ellipse on image.

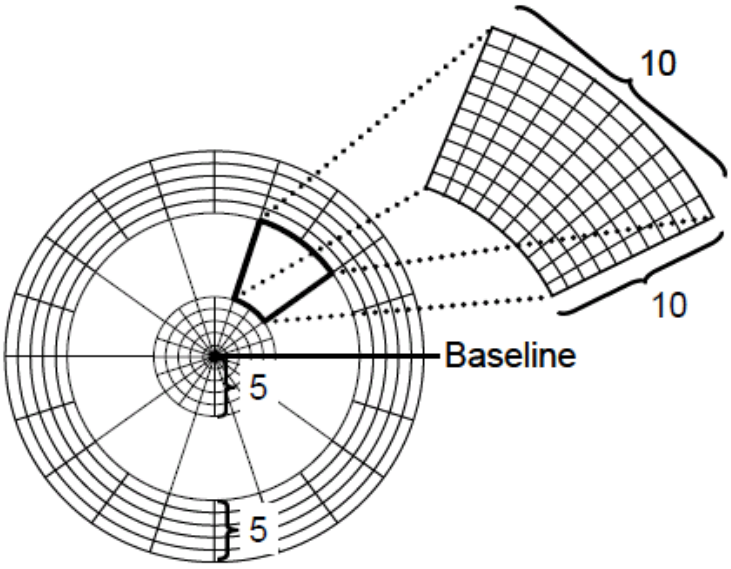

Fig. 2.12: Division of a marker when normalization.

Step 5-1 If four or more markers are recognized, select the two markers that are the most distant from each other on the image. Then calculate a line which passes through the two markers and select the marker that is the most remote from the line, because the accuracy decreases the smaller the distances are between the selected markers. Solve the perspective 3-point (P3P) problem using the three markers selected, and obtain a maximum of four possible solutions. The tracking fails if fewer than four markers are recognized.

Step 5-2 Estimate the positions of all feature points recognized on the image using the four solutions obtained in Step 5-1, inertial parameters (focal length, vertical and horizontal view angle and resolution) of the camera, and the three-dimensional position of the feature points, which were measured in advance. Then calculate the difference between the estimated positions and the recognized positions. That difference is called the re-projection error. Select the solution for which the re-projection error is smallest.

Step 5-3 The estimated result obtained from Step 5-2 including some errors, especially rotation error. To reduce the errors, obtain 12 new solutions by rotating the solution by ± 0.01 ° around the x, y, and z axes (defined in advance) and shifting the solution by ± 10 mm along the x, y, and z axes. Calculate the re-projection error for all new solutions. Then select the solution with the smallest re-projection error. This step remove some estimated errors because it reduce the re-projection error.

Step 5-4 Repeat Step 5-3 a maximum of 30 times until the re-projection error becomes less than 20 pixels.

After these steps, the 3D position and orientation of camera are estimated.

2.3 Development of a Marker Automatic Measurement System

2.3.1 Requirements for the System

In an NPP, because of the complexity and expanse of environment, the needed number of markers is always large. It is very difficult to measure them manually and avoid human errors. Therefore, MAMS is developed to improve the efficiency of preparation work before marker-based tracking and reduce human error. For practical application of the system in the complicated environment of an NPP, the Requirement A-C mentioned in chapter 1 must be satisfied. To develop MAMS, the following concrete requirements should be fulfilled:

I Measure the 3D positions of markers as quickly as possible (Requirement B).

If the measurement time is too long, the labor cost would become large because the worker may feel tired. The measurement time includes not only the marker measurement, but also the installation and remove of the system.

II Accuracy and stability should be enough to apply AR in field work(Requirement A).

If the measurement result is not accurate enough, the indication may be displayed at wrong position, which causes the operation mistake.

III Workers can master the operation of this system easily (Requirement B).

To reduce the cost of the training for using the system, the interface must be designed as comprehensive as possible to make it easily used, even for beginners.

IV Low price of hardware (Requirement C).

The dismantling work of NPP requires as low cost as possible. Therefore, existing hardware is used in the system instead of special development of some hardware.

V Can be fixed even in narrow space (Requirement B).

There are a lot of narrow spaces in an NPP. Therefore, the system must be as miniature as possible for using in these space.

VI Can be used in the environment with obstacles (Requirement B).

Because there are a lot of components in an NPP, the pasted markers may be occluded by the components. It is necessary to make it possible to measure the occluded markers.

2.3.2 System Design

To meet the requirements mentioned in section 2.3.1, the system is designed following the Criterion i-v mentioned in chapter 1, as shown in Fig.2.13. The system is composed of a camera which has an interior motion base, a laser range finder, a motion base fixed under the laser range finder and a PC connected to them. The camera and motion base are both fixed on a tripod. The directions of camera and laser range finder can be controlled by PC through the motion bases.

The system is used as following steps:

Step 6-1 Users select the world coordinate system (right hand system), and collocate the circular markers. (No.1 marker is at origin, No.2 is on $+x$ axis, and No.3 is on a plane xOy.).

Step 6-2 The system is set up at where it can capture the images of most of the markers.

Step 6-3 The system measures the 3D positions of selected markers automatically.

Step 6-4 If there are any markers which are not recognized, repeat Step 6-2 at where the most of these markers can be captured, and then repeat Step 6-3.

Step 6-5 Results are saved in a file, which can be used in AR application.

The above Step 6-3 is automatically executed. Its details are described as following steps:

Step 7-1 Camera rotates and captures images in the environment (It is controlled by PC through a motion base), and after recognizing the markers, estimate markers' positions.

Step 7-2 As the estimated result in Step 7-1, the system changes the direction and zoom of the camera to enlarge the marker image at screen center.

Step 7-3 As the estimated result in Step 7-1, the system controls the laser range finder to point to the marker. Here the result in Step 7-1 is always with large errors, so the laser dot is always distant from the marker center at first.

Step 7-4 Compare two images captured before and after laser shooting to find the laser dot.

Step 7-5 Control the laser range finder to shoot at marker center. Then measure the relative 3D position between laser range finder and marker.

Step 7-6 Transfer information of the 3D position into world coordinate system.

Above steps from Step 7-1 to Step 7-6 is controlled by PC automatically, so it is much more efficient and less human error than manual measurement. In additional, if the circular markers for defining world system (No.1, No.2, No.3 markers) are not moved away, the result obtained from Step 7-6 is based on the same coordinate system. Therefore the system can be set up at any place where it can capture the circular markers. So even if some markers are measured unsuccessfully, they can be measured again through changing the position of the system.

The system appearance is shown as Fig.2.14. To meet the requirements and realize Step 6-1 to Step 6-5, the following main functions are designed in MAMS:

1. Measure and calculate the 3D position of every marker automatically (Function 1). To realize this function, the marker automatic recognize (Function 2) and 3D position measurement of markers using laser range finder (Function 3) are also necessary.

2. To meet the Requirement I, the hardware of the system must can be arranged in boxes (Function 4) for easily moving of the system and reducing the installation and

remove time. The functions of camera initialization (Function 5), laser range finder initialization (Function 6) and system initialization (Function 7) are also necessary because it is efficient when workers want to measure some (or all) markers again.

3. To meet the Requirement II, the circular marker was used for tracking, so the position of circular marker must can be measured by the system (Function 8).

4. To meet the Requirement III, the comprehensive user interface is necessary. Therefore, the buttons of the interface must be as large as possible (Function 9), and its color must can be changed when operating (Function 10). To make the state of the measurement comprehensive, the following functions are also necessary: display the recognized marker ID (Function 11), display the log of the system actions (Function 12), display the past time of measurement (Function 13), inform when the measurement is end (Function 14), display the total number of recognized markers (Function 15), display the total number of measured markers (Function 16), display the total number of the markers to be measured (Function 17), display the area which is being captured by the camera (Function 18), control the camera direction using slide bar (Function 19), control the camera direction using angle map (Function 20), and represent the measurement result based on world coordinate system (Function 21).

5. To meet the Requirement VI, the functions that allow the manual measurement (Function 22) and allow the different automatic measurement model according to the different distance between MAMS and marker (Function 23) are necessary. Moreover, the functions of measuring one marker automatically (Function 24), measuring the markers which is being captured by camera automatically (Function 25), deleting the result of selected measured marker (Function 26) and stopping the measurement (Function 27) are also realized.

Experiments were conducted to evaluate that whether the realized functions can meet the requirements. It will be described in later sections.

2.3.3 Algorithm of the Automatic Marker Measurement

Definition of Coordinate Systems

7 coordinate systems are defined as shown in Fig.2.15. In this study, translation and rotation from system 1 to system 2 are represented as $\mathbf{T}_{12}$ and $\mathbf{R}_{12}$ respectively.

1. World system W. It is defined by 3 circular markers (No.1, 2, 3) as Step 6-1. The center of No.1 marker is the origin O, the direction from the center of No.1 to No.2 is the $+x$ direction. The plane composed by the centers of the 3 circular markers is the xOy plane.

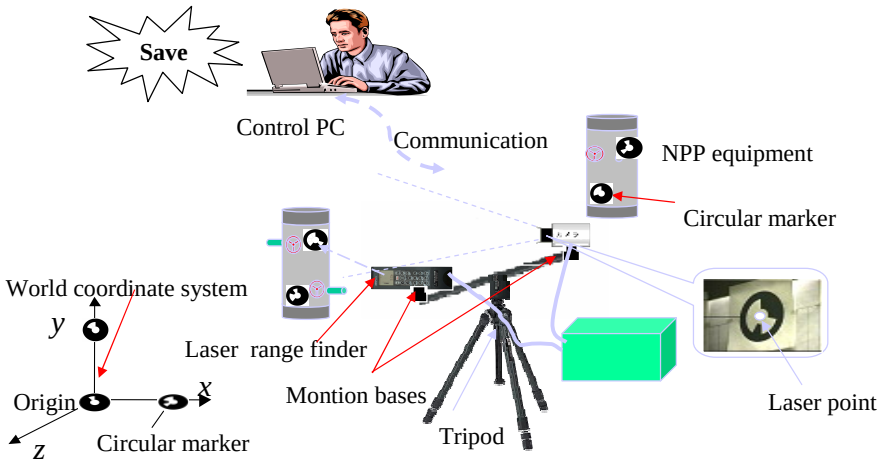

Fig. 2.13: Design of MAMS.

2. Motion base system A. For the motion base fixed under the laser range finder, the intersection of its pan and tilt axes is origin, the up direction and front direction of its initial position is $+z$ and -x respectively.

3. Laser system L. The projection of the origin of A on the rotation plane of laser range finder is origin. The directions of axes are same as A.

4. Screen system S. In the image plane, the up-left corner is the origin, right direction is $+x$ and down direction is $+y$.

5. Motion base system B. For the camera's interior motion base, the intersection of its pan and tilt axes is origin. The up direction and front direction of its initial position is $+z$ and $-x$ respectively.

6. Camera system C. Focal point of camera is origin. The direction from the center of image plane to origin is $+x$. The direction parallel with the x axis of S is $+y$.

7. Marker system M. Marker center is origin. The border of two fans which represent the first bit and the last bit of marker ID respectively is x axis, The normal of marker plane is z axis.

In this study, the origins of B and C are assumed to place at a same point. In the laser system L, when it rotates in tilt direction, its origin moves on a circle with radius of d_{AL}, which rounds the rotation axis.

Marker Position Estimation by Camera

Before measuring markers using the laser range finder, rough estimations of markers' 3D positions are necessary to control the laser range finder turn to the correct direction. To

Fig. 2.14: Appearance of MAMS.

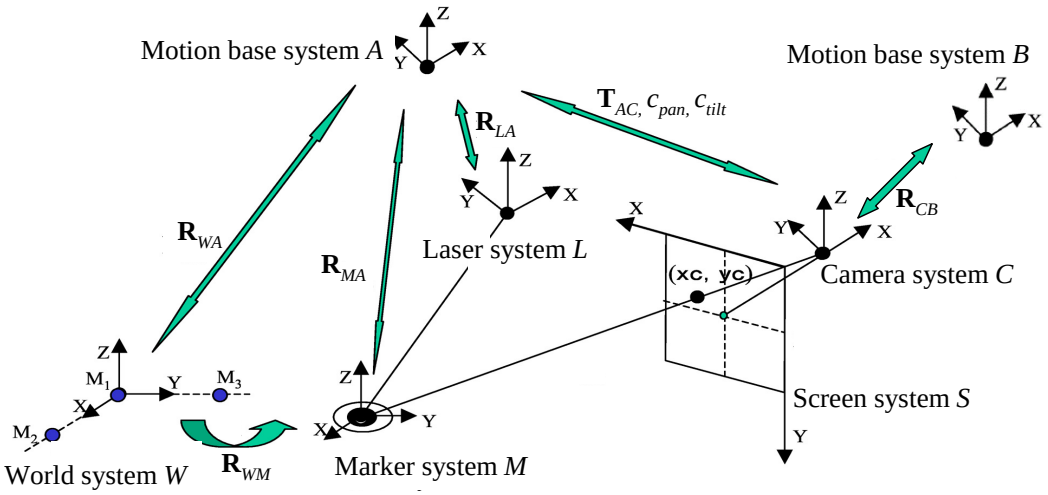

Fig. 2.15: Relation between diffierent coordinate systems.

estimate the 3D position vector of marker $\mathbf{T}_{AM}$ in motion base system A, the following parameters are used: radius of marker pasted in environment r_{real}, marker position in screen system (x_S,y_S), major radius of marker image r_{image}, and camera parameters (Internal parameters: focal length f, camera CCD chip width w_{CCD}, resolution w_{reso}, h_{reso}. External parameters: camera position $\mathbf{T}_{AC}$ in motion base system A, pan direction c_{pan} and tilt direction c_{tilt} in motion base system B). Camera internal parameters and $\mathbf{T}_{AC}$ are obtained in advance, and direction parameters are obtained from the communication between motion base and PC. After starting the system, camera rotates automatically to recognize markers in the environment. When a marker image is captured by camera, the parameters (x_S,y_S) and r_{image} are obtained as described in section 2.2.2.

The distance between the camera and a marker d_{CM} is estimated as Equation (2.3), where d is the distance between the marker image center and the screen center. Here d_{CM} may have large error.

$$d_{CM} = \frac{r_{real}}{r_{image}} \sqrt{d^2 + \frac{w_{reso}^2}{w_{CCD}^2}} \tag{2.3}$$

Pan and tilt coordinates of the marker m_{pan} and m_{tilt} in camera system C are:

$$m_{pan} = \frac{v_h}{w_{reso}} \left(\frac{w_{reso}}{2} - x_S \right) \tag{2.4}$$

$$m_{tilt} = \frac{v_h}{w_{reso}} \left(\frac{h_{reso}}{2} - y_S \right) \tag{2.5}$$

where $v_h = \arctan(w_{CCD}/2f)$.

Finally, the marker's estimated 3D position vector $\mathbf{T}_{AM}$ in motion base system A is:

$$\mathbf{T}_{AM} = \mathbf{T}_{AC} + \mathbf{R}_z(m_{pan} + c_{pan})\mathbf{R}_y(m_{tilt} + c_{tilt})\mathbf{D}_M \tag{2.6}$$

where $\mathbf{D}_M = (-d_{CM}, 0, 0)$, and $\mathbf{R}_y(\alpha)$, $\mathbf{R}_z(\beta)$ are rotation matrix with the angle α, β around the axis y, z of motion base system B respectively, as shown in Equation (2.7) and (2.8).

$$\mathbf{R}_y(\alpha) = \begin{pmatrix} \cos\alpha & 0 & \sin\alpha \\ 0 & 1 & 0 \\ -\sin\alpha & 0 & \cos\alpha \end{pmatrix} \tag{2.7}$$

$$\mathbf{R}_z(\beta) = \begin{pmatrix} \cos\beta & -\sin\beta & 0 \\ \sin\beta & \cos\beta & 0 \\ 0 & 0 & 1 \end{pmatrix} \tag{2.8}$$

Position Measurement Using Laser Range Finder

When laser range finder is turned on, the distance between laser dot and laser rangefinder d_{LD} is measured. Using d_{LD} and the direction parameters of laser rangefinder in motion base system A (obtained from communication between computer and motion base), s_{pan} and s_{tilt}, 3D position vector of the laser dot $\mathbf{T}_{AD}$ in motion base system A is calculated as:

$$\mathbf{T}_{AD} = \mathbf{R}_z(s_{pan})\mathbf{R}_y(s_{tilt})\mathbf{D}_r \tag{2.9}$$

where $\mathbf{D}_r = (-d_{LD}, 0, d_{AL})$, and $\mathbf{R}_y(\alpha)$, $\mathbf{R}_z(\beta)$ are rotation matrix with the angle α, β around the axis y, z of motion base system A respectively.

The conceptual image of automatic measurement of the system is shown as Fig.2.16. Fig.2.17 shows the main flow of position measurement using laser range finder. The details about how to automatically measure a recognized marker are described as following steps.

Step 8-1 Calculate d_{CM}, m_{pan}, and m_{tilt} of the marker as Equation (2.3), (2.4) and (2.5).

Step 8-2 According to the result, camera pose is adjusted to move the marker image center to be coincided with the screen center.

Step 8-3 Adjust focal length to resize the major radius r_{image} to be 30% of h_{reso}. If the ratio a% of major radius r_{image} vs. h_{reso} is smaller than 20% before adjusting focal length, adjust camera focal length to increase the ratio from a% to 20%, and repeat from Step 8-1 to Step 8-3.

Step 8-4 Repeat Step 8-1 and Step 8-2 to move the marker image center to be coincided with the screen center again. Now the focal length $f_{a\%}$ is:

$$f_{a\%} = \frac{afh_{reso}}{100r} \tag{2.10}$$

Where f is the focal length and r is the major radius of marker image when the marker was recognized. Record the marker center (x_S, y_S) and the minor radius of marker image b.

Step 8-5 Repeat Step 8-1 to calculate d_{CM}, m_{pan}, and m_{tilt}, then calculate the vector $\mathbf{T}_{AM} = (x_M, y_M, z_M)$ as Equation (2.6).

Step 8-6 Calculate the directions t_{pan} and t_{tilt} of marker in motion base system A as Equation (2.11) and (2.12). Then adjust the laser range finder to point to marker center according to the result.

$$t_{pan} = \arctan(y_M/x_M) \tag{2.11}$$

$$t_{tilt} = \arctan\left(\frac{z_M}{\sqrt{x_M^2 + y_M^2}}\right) \tag{2.12}$$

Step 8-7 Shorten the shutter speed of camera to reduce the brightness of image, so the laser dot on image is easier to be detected.

Step 8-8 Turn off the laser.

Step 8-9 Save the image captured by camera as I_{off}.

Step 8-10 Turn on the laser.

Step 8-11 Save the image captured by camera as I_{on}.

Step 8-12 Calculate the gray-scale difference between I_{on} and I_{off}, and then compute the area s_{diff} of pixels whose difference is larger than a threshold.

Step 8-13 If s_{diff} is smaller than a threshold, it means that the laser dot is not found in image, go to Step 8-14. Else go to Step 8-15.

Step 8-14 Equi-spaced adjust the laser range finder direction along a spire curve whose center is the direction obtained in Step 8-6. Then repeat from Step 8-8 to Step 8-13. If the iteration number is larger than a threshold, the marker measurement is failure. (Turn to next marker measurement.).

Step 8-15 Calculate the center of gravity $\mathbf{G} = (x_G, y_G)$ of pixels which are picked in Step 8-12.

Step 8-16 Calculate the relative vector between G and marker image center (x_S, y_S). If the length of the vector is larger than $1.5b$ (b is obtained in Step 8-4), go to Step 8-14. Else go to Step 8-17.

Step 8-17 If the length of the vector obtained in Step 8-16 is smaller than a threshold, it means that the laser dot is shot at the marker center, go to Step 8-19. Else go to Step 8-18.

Step 8-18 Adjust the laser range finder direction to point to the marker center, and go to Step 8-8. The adjusting parameters are calculated by Equation (2.13) and (2.14), where v_h is the horizontal view angle of camera when Step 8-11, t'_{pan} and t'_{tilt} are laser range finder directions when Step 8-12.

$$t_{pan} = t'_{pan} + (v_h/w_{reso})(x_G - x_S) \tag{2.13}$$

$$t_{tilt} = t'_{tilt} + (v_h/w_{reso})(y_G - y_S) \tag{2.14}$$

Step 8-19 Calculate the marker position $\mathbf{T}_{AM}$ as the algorithm described in Equation (2.6).

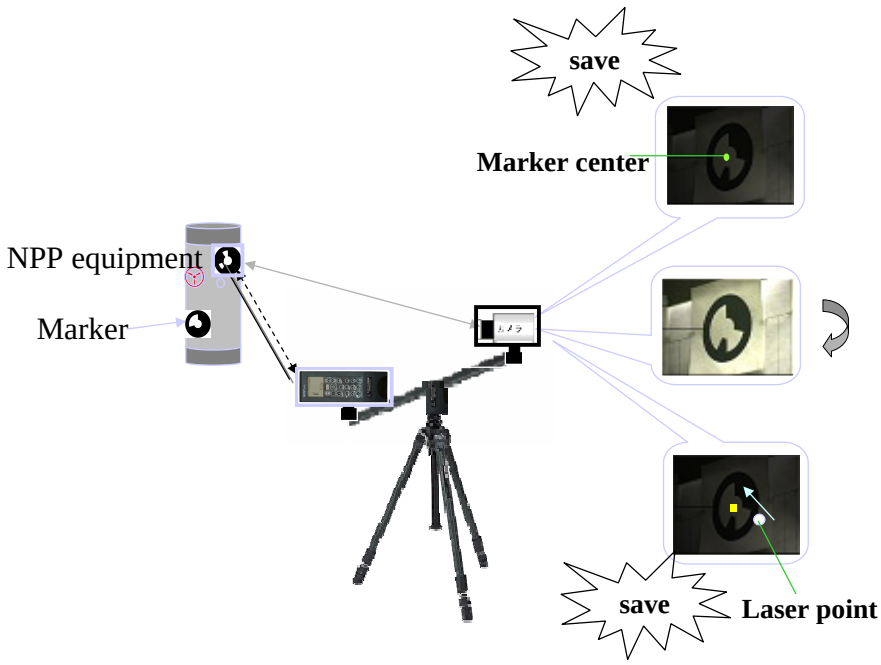

Fig. 2.16: Conceptual image of MAMS.

2.3.4 System Implementation

Table 2.1 displays the specifications of the hardware. The minimum error about 1 mm of the laser range finder ensures the accuracy (Requirement II). And the motion base

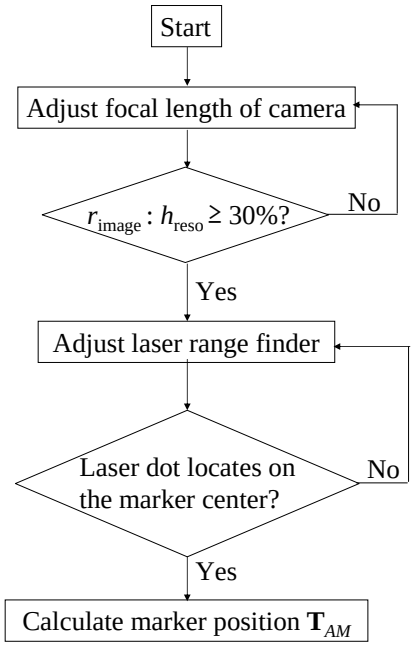

Fig. 2.17: Flow chart of position measurement.

ensures the accurate control of the laser range finder and camera (Requirement II). They can be fixed together and moved easily (Requirement V), and available as commercial products (Requirement IV). Whether they can meet the requirements will be evaluated in the feasibility experiment.

The program and user interface of MAMS were developed by Microsoft Visual C++ 2005 on Microsoft Windows XP. During the automatic measurement, some markers may fail to be measured if their positions relative to the system are not so well, for example, the marker is blocked by some components, or at a position which is out of the rotation range of motion based. In this case, it is necessary to measure these markers manually. So the function of marker manual measurement was also developed. User interface of operating MAMS is shown in Fig.4.7.

I Image displaying interface. Here current image captured by camera is displayed, so workers can understand the current measurement intuitively.

II Marker auto-measurement interface. Here are the buttons to start or cancel the marker automatic measurement for easy operation of workers.

III Camera control box. Camera can be controlled manually here (pan, tilt and zoom), so workers can manually control the camera to capture the selected markers.

IV Laser range finder control box. Laser range finder can be controlled manually here (pan, tilt, laser dot on or off), so workers can manually control the laser range finder to measure the selected markers.

Table 2.1: Hardware specifications of MAMS

Video camera	Type	Sony EVI-D30
	Video signal	NTSC
	Focus	5.4mm〜64.8mm
	Horizontal Angle of View	48.8 °〜4.3 °
	Pan/Tilt	Horizontal ± 100 °, Vertical ± 25 °
	Resolution	640 × 480
	Control Terminal	RS-232C
	Weight	1.2kg
Laser range finder	Type	Leica Geosystems DISTO Pro 4a
	Range	0.3m〜40m
	Accuracy	Typical: ± 1.5mm, Max: ± 2mm
	Φ Laser dot (at distance)	6/30/60mm (10/50/100m)
	Control Terminal	RS-232C
	Weight	0.44kg
Motion base	Type	Directed Perception PTU-D46-70
	Position resolution	0.012857 °
	Max speed	60 °/s
	Pan/Tilt	Horizontal ± 159 °, Vertical -31 °〜+48 °
	Control Terminal	RS-232C
	Weight	1.5kg
PC	Type	ASUS M5N
	CPU	Pentium M 1.4GHz
	Memory	DDR333 768MB
	OS	Microsoft Windows XP Home Edition
	Weight	1.55kg

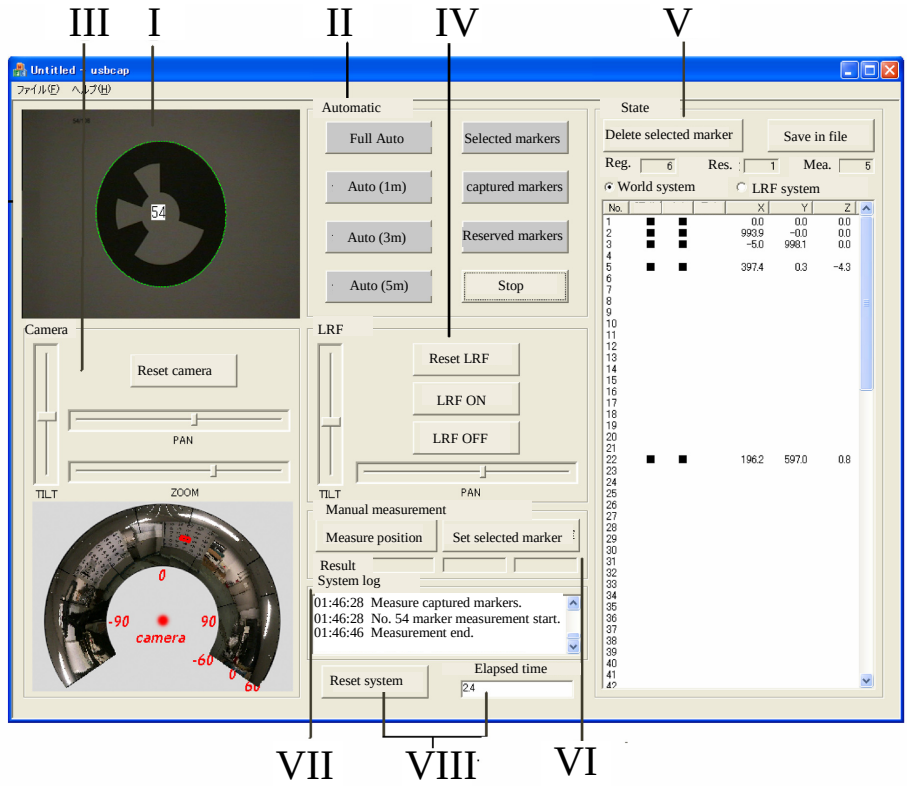

Fig. 2.18: Interface of MAMS.

V Measurement state display box. Each marker's information is displayed here (ID, 3D position, etc.), so workers can understand the measurement progress.

VI Manual measurement control box. The 3D position of laser dot can be measured manually here.

VII Actions log of the system. It is necessary for recording the system and measurement state.

VIII Others. System can be initialized for re-measurement, and measurement time is displayed here.

2.4 Performance Evaluation of MAMS

2.4.1 Purpose

Evaluations are necessary to examine that whether the developed system meets the Requirement I-VI, therefore a performance experiment was carried out to evaluate the

accuracy, stability and running time of the system to examine that whether the system meets the Requirement I and II.

2.4.2 Method

Experimental Environment

The size of experimental field in lab is about 5.0 m × 5.0 m, as shown in Fig.2.19. To evaluated the measurement accuracy and stability of MAMS, the accurate 3D position of the markers to be measured must be obtainable in advance. Therefore, 72 circular markers which diameters are 100 mm were neatly arranged with 200 mm's equidistance on two panels, as shown in Fig.2.20. The panel width is 1.24 m and height is 2.0 m. Center of No.1 marker pasted on the down-left corner of No.1 panel was origin. Center of No.2 marker pasted on down-right corner of No.1 panel was located at (1.0×10^3 mm, 0 mm, 0 mm). Center of No.3 marker pasted on up-left corner of No.1 panel was located at (0 mm, 1.0×10^3 mm, 0 mm). So world coordinate system is defined, and then the accurate 3D positions of the 72 markers can be easily calculated. No.1 panel was fixed but No.2 panel was moved with experimental process to evaluate the difference performance when the distance between MAMS and the markers changes.

Experimental Flow

The No.2 panel was placed at the positions where x=2.0×10^3 mm, 2.4×10^3 mm, 2.6×10^3 mm, 2.8×10^3 mm and 3.0×10^3 mm respectively, and the down left marker located at (x, 0 mm, 4.0×10^2 mm). At every position, the automatic measurement by the system was repeated 20 times.

2.4.3 Result

System error means that average of many separate measurements differs significantly from the actual value. It is caused by the measurement instruments. Random error means the errors in measurement that lead to measurable values being inconsistent when repeated measures of a constant attribute or quantity are taken. Random error is caused by unpredictable fluctuations in the readings of a measurement apparatus, or in the experimenter's interpretation of the instrumental reading. These fluctuations may be in part due to interference of the environment with the measurement process. In this study, system error (SE) was used to evaluate the accuracy, and random error (RE) was used to evaluate the stability. Here, SE and RE are estimated as:

$$SE = \sqrt{(\overline{x} - x_0)^2 + (\overline{y} - y_0)^2 + (\overline{z} - z_0)^2} \tag{2.15}$$

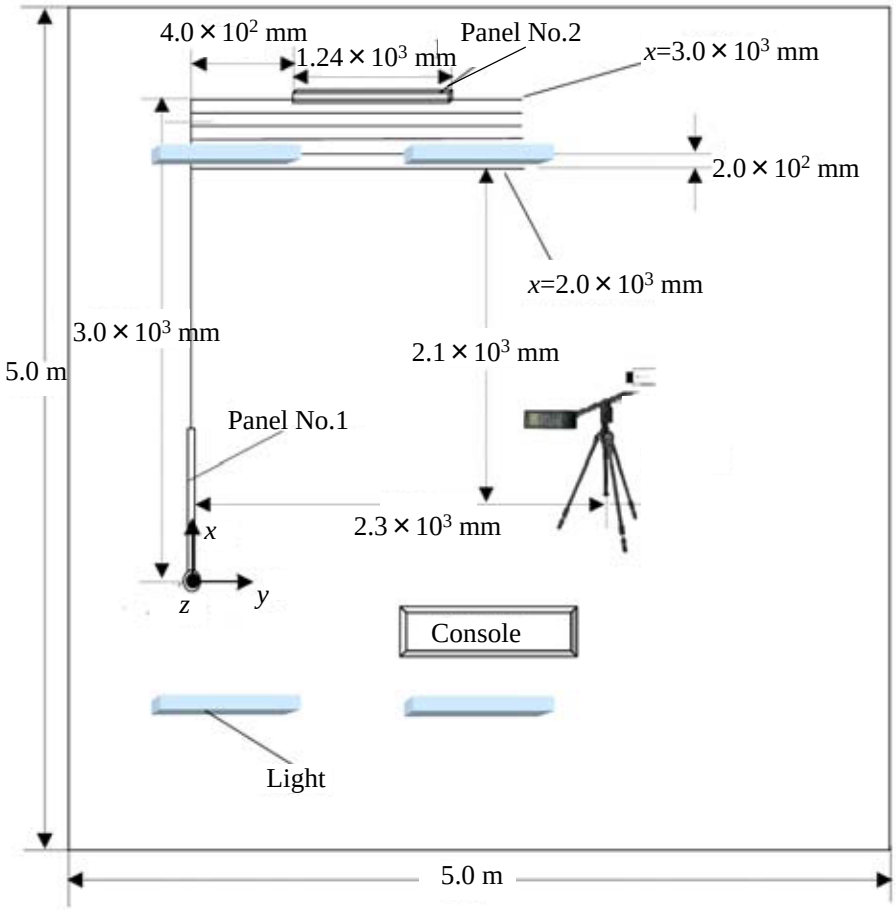

Fig. 2.19: Experimental environment in lab.

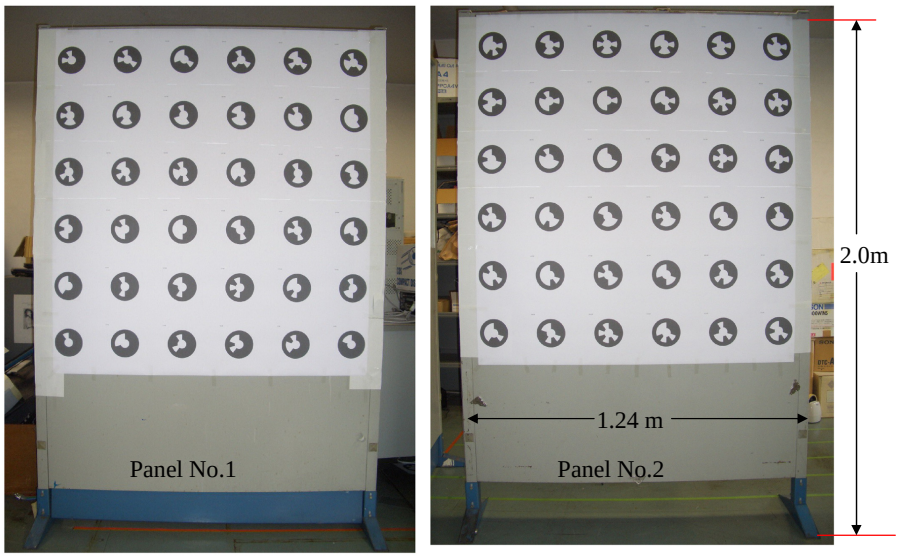

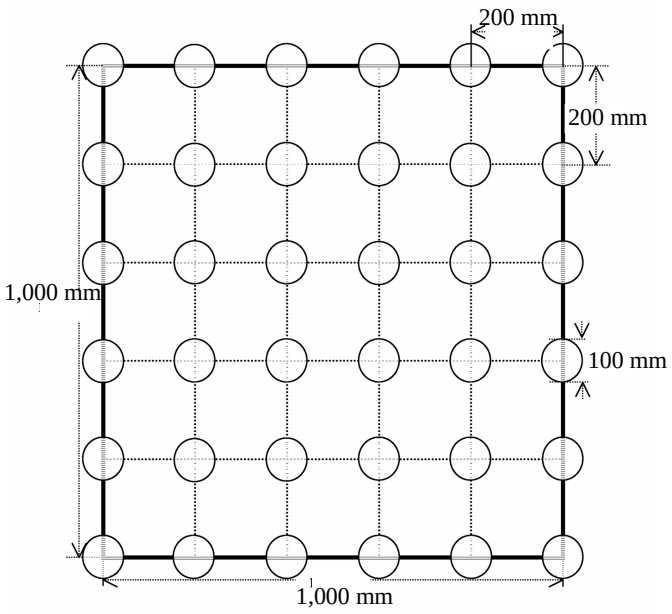

Fig. 2.20: Marker locations on a panel.

$$RE = \sqrt{\frac{1}{n-1}\sum_{i=1}^{n}\{(\overline{x}-x_i)^2+(\overline{y}-y_i)^2+(\overline{z}-z_i)^2\}} \tag{2.16}$$

where (x_0, y_0, z_0) is the real position of marker, and $(\overline{x}, \overline{y}, \overline{z})$ is average position of measure values. (x_i, y_i, z_i) is the ith measurement position of marker. (There are n=20 measurement positions of each marker in total)

Accuracy

System error of each marker is shown in Fig.2.21 and Fig.2.22. Total 8,640 results (marker number 72 $\times$ No.2 panel position number 6 $\times$ repeat times 20) show that the maximum error between measurement value and real value is 27.6 mm, average error is 7.6 mm. As shown in Fig.2.22, the error increases from down-left to up-right on the No.2 panel when $x = 2.0 \times 10^3$ mm, and much lager than the No.1 panel. Same trends of system error on the No.2 panel at other positions are also found. The reason is that panel No.2 has a deviation from its ideal position, so the real position is with errors itself.

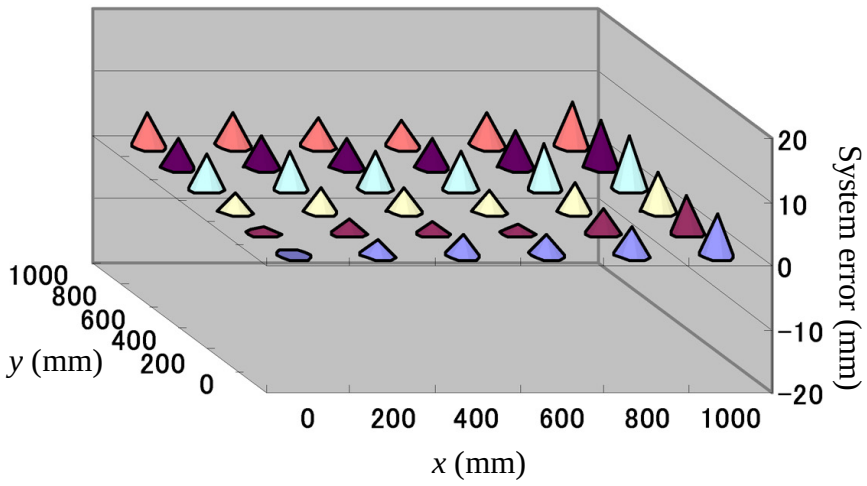

Fig. 2.21: System error on panel No.1 (mm).

Stability

The random error of each marker is shown in Fig.2.23 and Fig.2.24. The trends of random error on No.2 panel at other positions are very same as $x = 2.0 \times 10^3$ mm. Maximum of random error is 6.2 mm, and average is 3.5 mm. As the result, random error is much smaller than system error (The measurement error by laser range finder, and the rotation error of motion based.). Therefore, system error is the main error. In other words, the repetition of measurement affects less on accuracy.

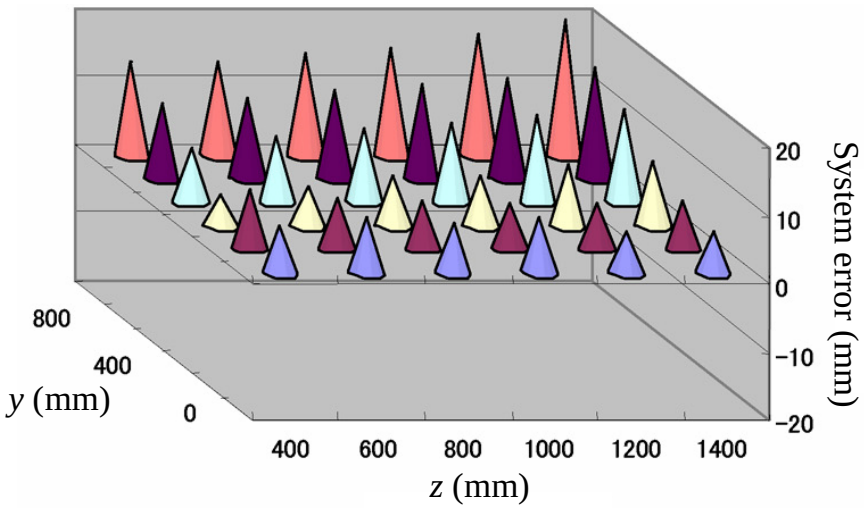

Fig. 2.22: System error on panel No.2, $x = 2.0 \times 10^3$ (mm).

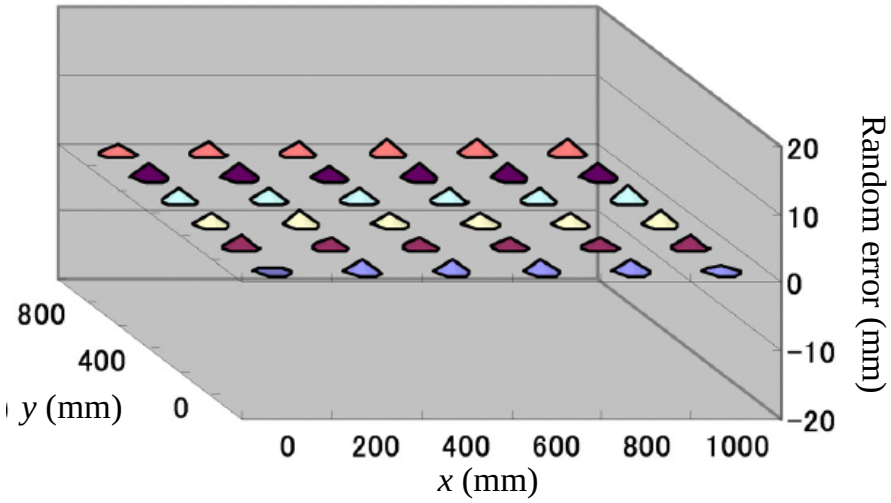

Fig. 2.23: Random error on panel No.1 (mm).

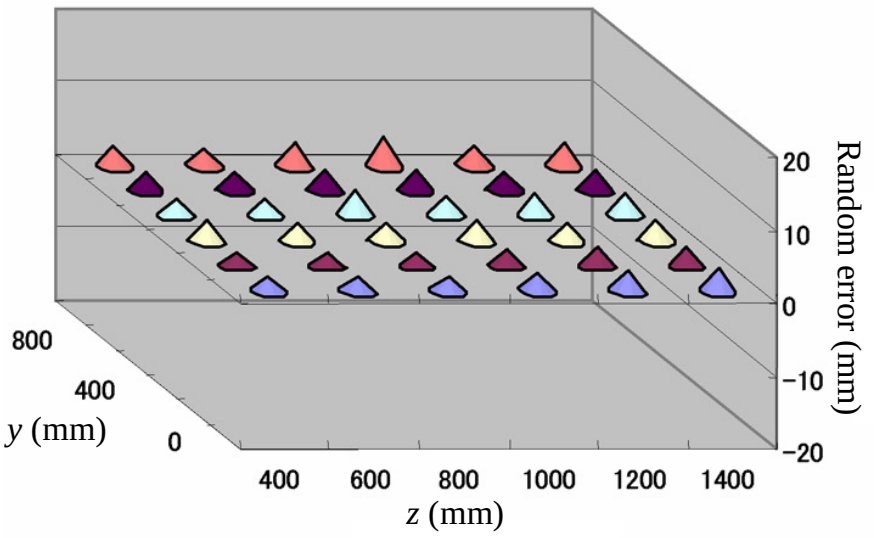

Fig. 2.24: Random error on panel No.2, $x = 2.0 \times 10^3$ (mm).

Measurement Time

It took 25.2 minutes in average for 1 successful experiment (72 marker were measured automatically successfully, 21.0 seconds in average for measuring one marker). When distance between laser range finder and No.2 panel increased, measurement time became longer. Because the accuracy of marker position estimation in Equation (2.6) reduces with the distance increases, it would take more time to match the laser dot with marker center automatically.

2.5 Feasibility Evaluation of MAMS in an NPP Environment

2.5.1 Purpose

An experiment was conducted in Fugen NPP to evaluate the feasibility, including that whether the system meets the 6 requirements mentioned at the beginning of section 2.3.1, whether it can work successfully in NPP environment, whether NPP workers master this system quickly, and what should be improved.

2.5.2 Method

Evaluation Environment

Evaluation field in Fugen was in a pure-water chamber whose size was about 9.5 m × 8.0 m. In the chamber, there are many components, such as tanks and pipes, as shown in Fig.2.25. The luminance was 200-500 Lux, so markers were recognized easily by MAMS.

Evaluation Flow

First, the system operation was demonstrated in front of two evaluators who had never used this system before. One of the evaluators is a Fugen NPP worker who is accomplished in NPP field work (evaluator A), the other is a human interface expert (evaluator B). Then two evaluators operated the system by themselves to evaluate the system usability for beginners. 3 markers (No.1 to No.3) were pasted to define the world coordinate system. Other 20 markers were pasted at where the evaluators thought they were needed for tracking, as shown in Fig.2.26. To make it more easily to paste markers, a magnet was pasted on the back of each marker, and the markers are pasted on iron equipment. After the system finished the measurement, to check that whether the result obtained by MAMS is accurate enough for actual AR application, the evaluators used a small PC to experience an AR application using the measurement result. The real time tracking of position and orientation of the PC was realized through a camera. As shown in Fig.2.27, the tracking result was used in AR to display important information for workers, such as fluid state in pipes (with green frame in Fig.2.27), and guidelines (with red frame in Fig.2.27). The 3D positions to display virtual information were prepared in advance, therefore if tracking successes, the information is indicated correctly. Finally, the evaluators answered a questionnaire about feasibility evaluation. The evaluation items are shown in Table 4.2, 4.3 and 4.4. They are decided based on the Requirement I - Requirement VI and the Function 1 - Function 27. For every evaluation item, one of 5 options (1 - disagree, 2 - disagree a little, 3 - neither, 4 - agree a little, 5 - agree) can be chosen, and evaluator would tell his reason if necessary.

2.5.3 Result and Discussion

Running Time

It took 85 seconds to paste markers, 350 seconds to fix the system, 75 seconds to start the system. Then 640 seconds was spent for measurement. Including 240 seconds of the system removed time, totally it took 1,390 seconds (23.2 minutes).

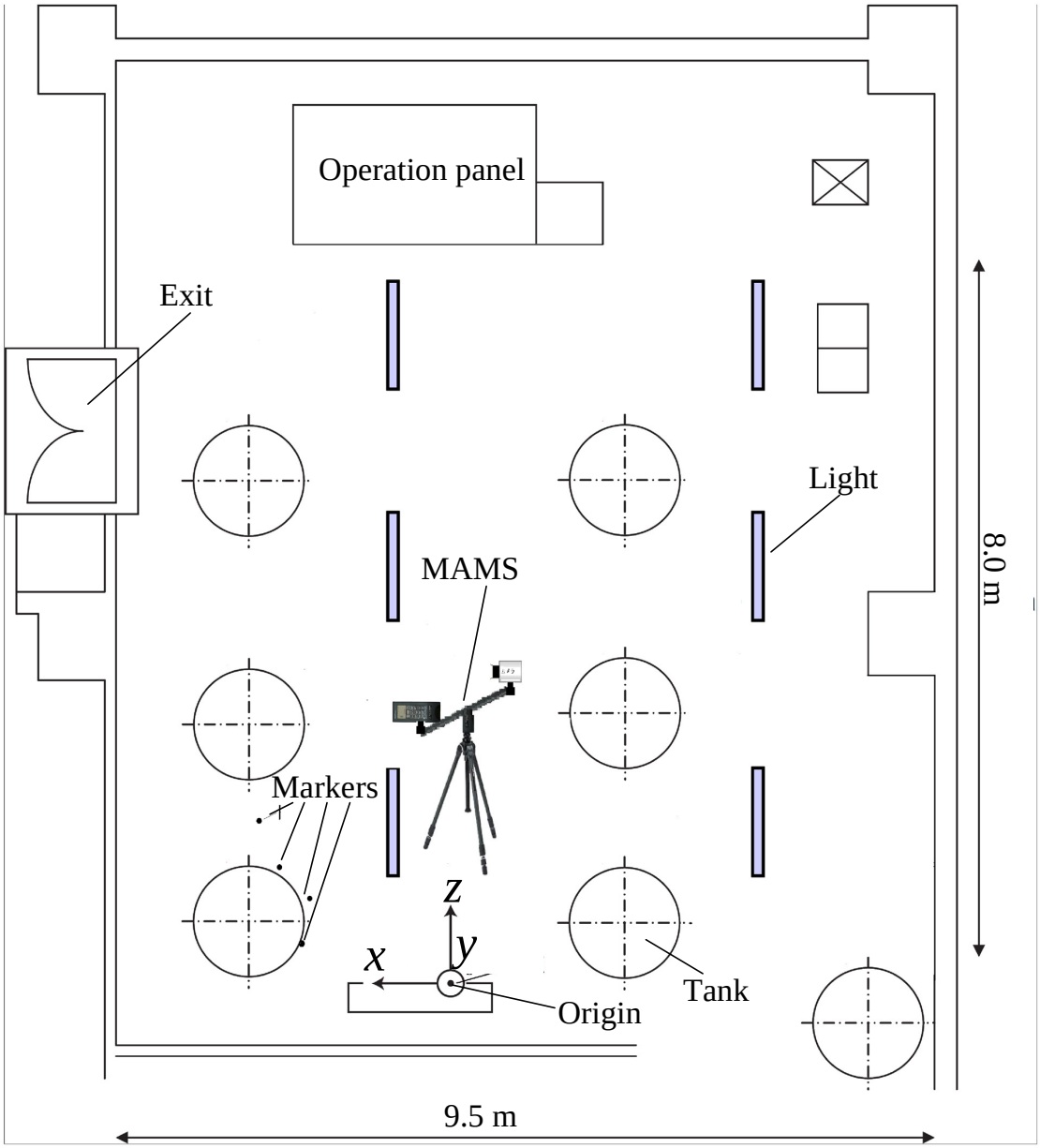

Fig. 2.25: Experimental environment in NPP.

Fig. 2.26: Pure-water chamber with marker.

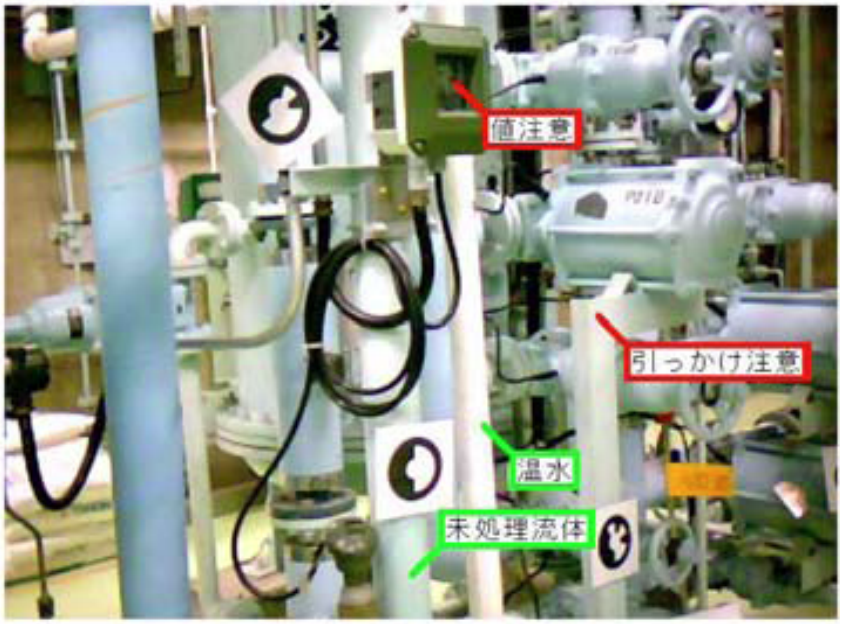

Fig. 2.27: AR experience using the measurement result.

About System Function

Table 4.2 and 4.3 shows the evaluation result. The items from A-1 to A-5 and A-8 which are corresponding to automatic measurement functions have high evaluation. It means that the automatic measurement functions are useful when measuring. The item A-6 has low evaluation. Although evaluators thought that it was faster than any other existing measurement methods, measurement speed should still be improved for practicality. The item A-7 has low evaluation. Evaluators thought that the accuracy requirement depended on different cases, so it was difficult to evaluate whether the accuracy was enough. In other words, the accuracy is not so good in some cases. The item A-9 has low evaluation, because the experimental environment is very bright in NPP, it is difficult to evaluate whether the system can work in low luminance environment. Considering that the performance evaluation in lab environment mentioned in Chapter 4 is with lower luminance, the items may have higher evaluation in fact. The items A-10 and A-12 have very low evaluation. In evaluators' opinion, the system cannot be fixed in very narrow space, and markers would be occluded by obstacles. To solve these problems, the system miniaturization and some aid technology which can avoid pasting markers in obstacle area should be realized, such as inertial sensors, natural feature points. Oppose to the case in item A-10, the item A-11 has high evaluation. Evaluators thought the system could be used in capacious space. The item A-13 has low evaluation. Evaluator A thought the hint sound was easily interfered by noise, and evaluator B thought this function was not very necessary. The items from A-14 to A-19 are corresponding to manual measurement. From A-14 to A-17 and A-19 have high evaluation. Evaluators thought the functions were useful, especially when there was any marker with unsuccessful automatic measurement. But A-18 has very low evaluation because evaluators thought the function was not very necessary. At the items A-20 and A-21, two evaluators gave different evaluation, so availability cannot be estimated. The items from A-22 to A-29 have high evaluation. It means these functions are useful. The items A-30 and A-31 have low evaluation. Evaluators thought they were not necessary.

About System Usability

The evaluation result about system usability is shown in Table 4.4. At the items B-1 and B-2 which are corresponding to the field fixing of system, two evaluators gave different evaluation. Considering that evaluator A understood the decommissioning work in NPP field better as a NPP work, his answer was more believable. So B-1 and B-2 have low evaluation. It means that the system fixing and removing are not very easy. From B-3 to B-8 corresponding to the user interface, evaluator A gave all high evaluation, but evaluator B gave low evaluation at B-4 and B-8. As a human interface expert, B's answer was more believable. He thought that the measurement interface was not so easy to understand for beginner when manually measurement. B-9 has low evaluation. The evaluators thought that it was difficult for beginner to operate the system without any manual book

Table 2.2: Result of function evaluation I

No.	Survey item	Requirements and functions	Evaluation	
			A	B
A-1	When marker is measured, the marker automatic recognition by camera is available.	Function 2	4	5
A-2	When marker is measured, the automatic measurement by laser rangefinder is available.	Function 3,22	4	5
A-3	When marker is measured, the direction control by motion base is available.	Function 22	5	5
A-4	Automatic recognition of all markers pasted in environment is available.	Function 2	5	5
A-5	Automatic measurement of all markers pasted in environment is available.	Function 1	5	5
A-6	Spent time for automatic measurement of marker is very short.	Requirement I	3	4
A-7	The measurement accuracy is enough for AR application.	Requirement II	4	3
A-8	The efficiency of preparatory for AR is raised by using the automatic measurement.	Requirement I, Function 23	5	5
A-9	System can be used at where luminance is low.	Requirement II, Function 8	3	4
A-10	System can be used in environment with obstacles.	Requirement VI	3	1
A-11	System can be used in capacious space.	Requirement V	5	5
A-12	System can be used in narrow space.	Requirement V	3	2
A-13	The hint sound after finishing marker measurement is available.	Requirement III	3	4
A-14	The control of camera's pan, tilt and zoom using a slider is available.	Function 19,20	5	5
A-15	Automatic measurement of markers only in current image is available.	Function 25	5	5
A-16	The function of deleting measurement result of one marker is available.	Function 26	5	5
A-17	The switch function between marker measurement state (measurement finished or not) is available.	Function 11	4	5

Table 2.3: Result of function evaluation II

No.	Survey item	Requirements and functions	Evaluation	
			A	B
A-18	The switch function between marker preparatory state (will be measured or not) is available.	Function 11	3	2
A-19	The switch function between measurement results in different coordinate system (world system or laser system) is available.	Function 21	5	5
A-20	The function of displaying system states by words is available.	Function 12	3	5
A-21	System initialization is available.	Function 7	5	1
A-22	The function that using a red frame on angle map to represent the current view range of camera is available.	Function 20	5	4
A-23	The function of changing camera direction by clicking at angle map is available.	Function 20	5	5
A-24	The stop function during automatic measurement is available.	Function 27	4	5
A-25	Automatic measurement of markers which are selected is available.	Function 22	5	5
A-26	The function of displaying the total number of recognized markers is available.	Function 15	5	5
A-27	The function of displaying the total number of markers which will be measured is available.	Function 17	5	5
A-28	The function of displaying the total number of measured markers is available.	Function 16	5	5
A-29	The function of displaying each marker's state (recognition, measurement and preparatory) is available.	Function 15,16,17	5	5
A-30	The function of dividing camera zoom in 3 ranges to automatically measure respectively is available.	Function 23	3	2
A-31	Initialization of camera direction is available.	Function 5	3	2

Table 2.4: Result of usability evaluation

No.	Survey item	Requirements and functions	Evaluation	
			A	B
B-1	It is easy to set up the system.	Function 4	1	4
B-2	It is easy to remove the system.	Function 4	3	5
B-3	It is easy to read the words and numbers from the user interface.	Function 9	4	4
B-4	It is easy when manually operation.	Function 22	5	2
B-5	It is easy to understand the interface.	Requirement 3	5	4
B-6	It is easy to push the software buttons.	Function 10	5	5
B-7	It is easy to understand the display measurement result.	Requirement 3	5	4
B-8	It is easy to control the pan, tilt and zoom manually.	Function 9,19	5	2
B-9	It is easy to operate the system for a beginner.	Requirement 3	3	2
B-10	System response to the operation is immediate.	Function 7	4	5
B-11	It is easy to understand the marker's state.	Function 12	5	5
B-12	It is frustrated to operate the system.	Function 1	1	1

or preparatory training. The items from B-10 to B-12 have high evaluation.

About Improvement Points

According to the evaluation result, there are some improvements which should be developed.

1. Improve the speed of system actions to shorten the measurement time.
2. Improve measurement accuracy for more widely application of the system.
3. Miniaturize and lighten the system.
4. Improve user interface for easily understanding.
5. Display some help information which are related to current operation actions for beginner to easily operate.

2.6 Improvement of Marker Design

According to the evaluation result of section 2.5.3, some items such as A-6 and A-10 have low evaluation. The large number of pasted markers is one of the reasons that causes the low evaluation of the items A-6 and A-10. Moreover, in actual application, if the distance between markers and camera is too short, the projection of a marker on the image would become large. In other words, there are few markers detectable in the image, which means the detected feature points are few. If the number of detected feature points are smaller than 4, the tracking would fails. Therefore, it is necessary to improve the marker design to reduce the needed number of markers in the same case, and improve the stability in the short distance tracking when using the markers. The circular marker was so improved and its performance was evaluated in this study.

2.6.1 Improvement of Marker Design

The circular marker was improved by adding four additional small circles, as shown in Fig.2.28. If the camera is closed to the markers, the four small circles are easily recognized, and then there will be at least 5 feature points even if only one marker is detected on the image. Therefore it is not necessary to change the marker size even in the short distance tracking. The four small circular can be recognized after the center of the whole circular marker is recognized. The algorithm to recognize the small circular markers is described as following steps. It is executed after Step 4-17 mentioned in the section 2.2.2.

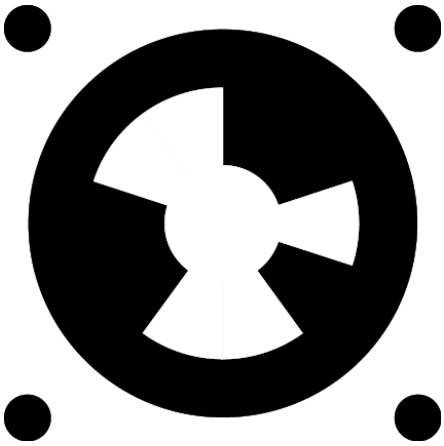

Fig. 2.28: Improvement of marker design.

Step 9-1 Estimate four vectors ($x_{cnr}(i)$,$y_{cnr}(i)$) (i=0,1,2,3) from the center of the marker to the four small circles using (2.17).

$$\begin{aligned} x_{cnr}(i) &= x\cos(\theta_{ell}) - y\sin(\theta_{ell}) \\ y_{cnr}(i) &= x\sin(\theta_{ell}) - y\cos(\theta_{ell}) \\ x &= \cos(\theta_{ell})\sin(\alpha) + \sin(\theta_{ell})\cos(\alpha) \\ y &= (\cos(\theta_{ell})\cos(\alpha) - \sin(\theta_{ell})\sin(\alpha))r_b/r_a \\ \alpha &= \theta_{ell} + 3.6N_{scn} + 36N_{sft} + 45 + 90i \end{aligned} \tag{2.17}$$

Step 9-2 Calculate the distance l between the center of the marker and each ellipse, which were recognized in Step 4-8 described in section 2.2.2 but not identified as a marker yet. Furthermore, find ellipses that are $r_b < l < 1.7r_a$.

Step 9-3 Calculate a vector from the center of the marker to the center of the ellipses found in Step 9-2. Find four ellipses for which the angle between v_e and ($x_{cnr}(i)$,$y_{cnr}(i)$) is at most 60 °. and the distance between the center of the marker and the center of the ellipse is the shortest. The four ellipses are inferred to be the four small circles of the marker.

2.6.2 Evaluation of Improved Marker

Purpose and method

To evaluate that whether the improvement is effective in short distance tracking, and whether the marker is recognized reliably in NPP environment, some experiments were conducted to evaluate the tracking method using the improved marker. The tracking method performance changes according to the radius of the large circle r_1, the radius of the

Table 2.5: Hardware specifications used for evaluation

PC	CPU	Pentium Core2Duo 2.66 GHz
	Memory	DDR2 800 MHz, 2 GB
Camera	Vendor	Point Gray Research Inc.
	Model	Dragonfly2 XGA Black& White
	Interface	IEEE1394a
	Resolution	1,024 × 768
	Frame rate	30 fps
	Focal length	8.00 mm

small circle r_2, and the distance between the large circle and the small circle d. However, it is difficult to evaluate the relationship between these parameters and the tracking performance in detail. In this study, therefore, one design of a multi-range marker (r_1=50 mm, $r_2 = 0.12r_1$, $d = 1.42r_1$) was evaluated. In this case, the gap separating the contour of the small circle and the large circle is equal to the outer black circle's thickness; the small circle and each fan of the middle circle are almost equal in size. The marker is about 142 mm large including the white area allocated outside of the small circles, which is meant to stabilize the recognition of the marker. (The thickness of the white area is the same as the one of the outer black circle.)

Table 2.5 shows the main specifications of the hardware used for the evaluation. The program was built under Microsoft Visual C++ 2005 on Microsoft Windows XP. The camera shutter speed was fixed to 10 ms; the gain was adjusted automatically during the evaluation.

Result

Recognition Range To evaluate the performance under the short distance tracking, one marker was located in front of the camera so that the camera would capture the marker at the center of the image. The distance between the camera and the marker was changed to evaluate the maximum and minimum distance at which the system could flawlessly recognize the marker ID and the four small circles 1000 times consecutively. The brightness on the marker was 700 lux. Table 2.6 presents the results, the minimum distance of recognizing the small circles is 289 mm, which means that in a short distance over 289 mm, there are still enough feature points (5 points) can be detected for tracking.

Recognition Reliability To evaluate whether the algorithm described in section 2.2.2 misrecognizes non-marker objects as markers, images captured in a water purification

Table 2.6: Maximum and minimum recognition distance (mm)

Marker ID		Small circles	
Max.	Min.	Max.	Min.
5344	251	4980	289

room of the Fugen nuclear power plant were processed using the algorithm. The images were captured by a camera held by a worker according to a scenario in which the worker walked around the water purification room to check instruments. 19,742 images were processed; for 121 of them (0.61%), the algorithm misrecognized objects that were not markers as markers. To compare the result with existing markers, 99 patterns (euqal to the pattern number of the new designed circular marker) of ARToolkit marker was registered in the database, and the same images were also processed using the ARToolkit marker recognition algorithm. The misrecognition rate of ARToolkit marker is 15.77%. Therefore, the new designed circular is much reliably recognized than ARToolkit marker.

In all the misrecognized cases, only the large circle was recognized; the small circles were not recognized. Fig.2.29 depicts two images in which the algorithm misrecognized the centers of circular valves and “ 0 ” character as markers. To avoid the misrecognition, the markers which ID is 1 and 2 should not be used for the tracking because in 59.5% of the misrecognition, non-marker objects were misrecognized as these two markers, which design seems to be too simple to be used in NPPs.

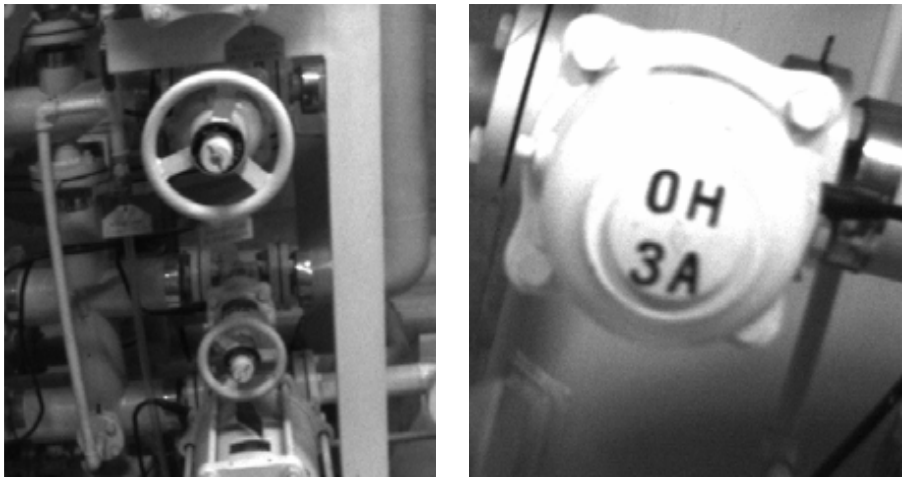

Fig. 2.29: Examples of misrecognized images.

Processing Speed of Tracking One marker was located in front of the camera so that

Table 2.7: Necessary tracking time (ms)

Process	Required time	
	1 marker	9 markers
Step 4-1 to Step 4-2	8.5	8.5
Step 4-3 to Step 4-4	2.9	3.4
Step 4-5 to Step 4-17	0.4	3.9
Step 9-1 to Step 9-3	0.01	Not used
Step 5-1 to Step 5-4	11.9	15.9

the camera would capture the marker at the center of the image. The distance between the camera and the marker was fixed at about 1.5 m. The time necessary for executing each process described in sections 2.2.2, 2.2.3 and 2.6.1 were measured with the marker. Then, nine markers were placed in front of the camera on a 3×3 grid (0.5 m vertical step, 1.0 m horizontal step); the distance between the camera and the marker was fixed at about 5.0 m. The time necessary for executing each process described in sections 2.2.2, 2.2.3 and 2.6.1 were measured with the nine markers. Table 2.7 presents the results. The additional four circles affect little on the processing speed.

Area within Which Tracking Can Be Executed It is difficult to check whether the tracking can be executed at every point in a real environment if the environment is large. For this study, therefore, the area within which tracking can be executed with enough accuracy was evaluated using computer simulation. In a virtual environment, nine markers were placed on a 3×3 grid (x = -1.0, 0.0, 1.0 m; y = -0.5, 0.0, 0.5 m; z = 0.0 m). The textures of nine markers were generated at a resolution of 512×512 pixels, and they were pasted on the virtual markers. A virtual camera for which inertial parameters (focal length, vertical and horizontal view angle and resolution) were set referring to the camera in Table 2.5 was moved in 10 mm steps in an area ($-3.0 \leq x \leq 3.0$ m; $-0.5 \leq y \leq 0.5$ m; $0.0 \leq z \leq 6.0$ m) in front of the markers. The camera direction was fixed to -z direction. Then it is checked that whether tracking can be executed at every point by generating the camera image using the OpenGL library and applying the algorithm described in sections 2.2.2, 2.2.3 and 2.6.1 (Total $601 \times 101 \times 601 = 36{,}481{,}301$ points). Fig.2.30 shows an image generated using the OpenGL library. In this image, the imperfection of the distortion correction and the illumination variance were not accurately simulated. Still, we could roughly estimate the area within which the tracking can be executed, Fig.2.31 shows a performance evaluation result of the improved marker. The points at which the position and orientation error of the tracking is less than 200 mm and 20 °respectively was shown

in the figure when the camera was moved on a plane ($y = 0$). When the distance between the marker and the camera is greater than about 3 m, the accuracy and stability of the tracking is not good enough if the camera can capture less than four markers. When the distance is greater than about 5 m, the accuracy and stability is not good enough even if the camera can capture not less than four markers. This means that tracking with the small circles is effective at less than 3 m whereas tracking with the large circle is effective at less than 5 m. The number of points at which the algorithm used not less than four markers at a distance ranging from 3 m to 5 m, and at a range shorter than 5 m were, respectively, a = 4,269,416 and b = 4,898,851. The number of points at which the tracking can be executed with a single marker at less than 3 m distance was c = 5,635,046. Therefore, the area within which the tracking can be executed using multi-range markers is (c-b+a)/a $\times$ 100 = 117.2% larger than that of the normal circle marker. In other words, to cover a same area, the necessary number of the improved markers is smaller than the normal circle marker with the same size.

A similar experiment using nine markers with the same arrange in the actual environment was also conducted. By moving a camera in 0.5 m step, the distance between the camera and the markers was from 0.5 m to 5.0 m. Fig.2.32 shows the position errors of the computer simulation and the actual experiment. Because the computer simulation and the actual experiment have the same trend of the position errors, therefore the computer simulation was used to check the area within which tracking can be executed.

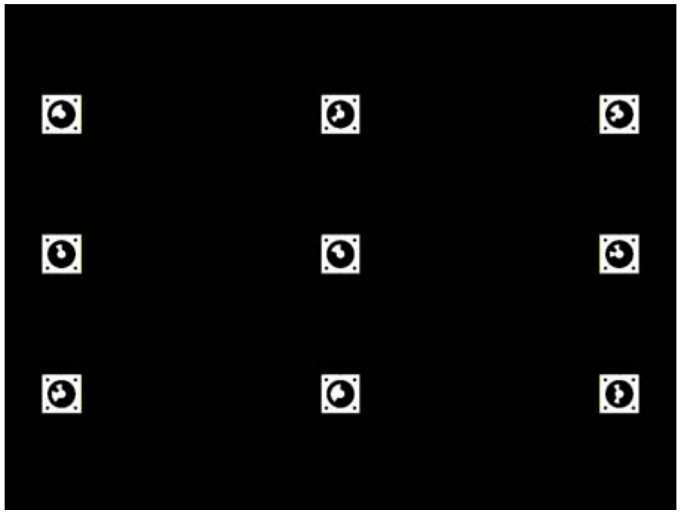

Fig. 2.30: Example of an image generated using OpenGL.

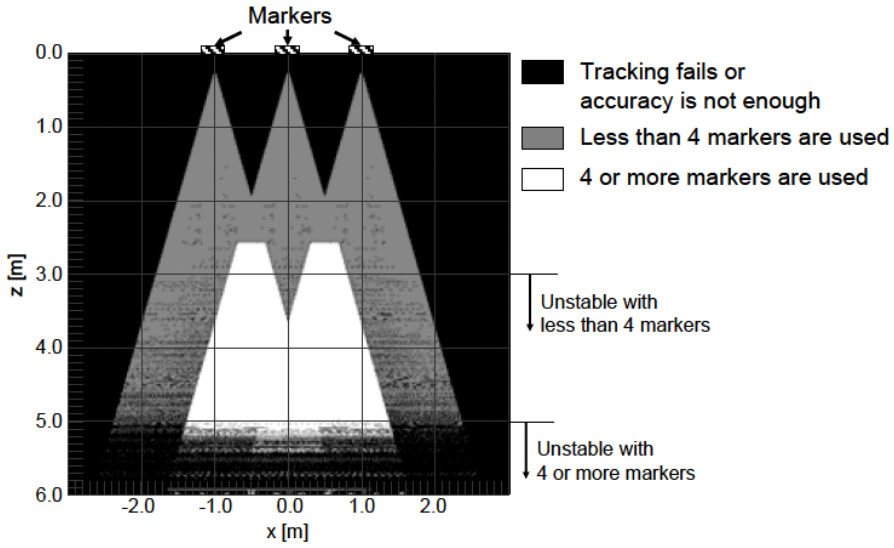

Fig. 2.31: Points at which tracking can be executed with enough accuracy (top view of the area).

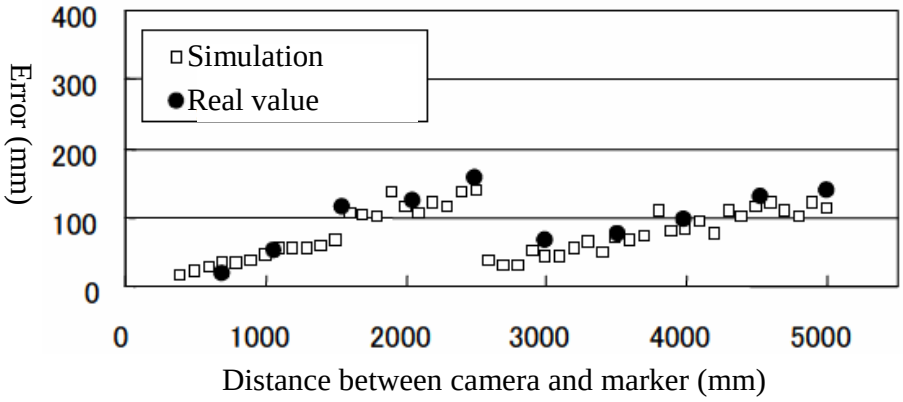

Fig. 2.32: Position errors of tracking.

2.7 Summary

In this study, firstly a new circular marker was designed which is useful in long distance tracking in NPP environment. Then, a marker automatic measurement system was developed so as to measure the 3D position of each circular marker automatically. The system is composed of a camera, a laser range finder and a motion base, which is used to control the pose of the laser range finder. A computer, connected to them, is used for controlling the system and for data transport. The results of the experimental evaluations show that the measurement takes about 21 seconds per marker and that the root mean square error of the position measurements is 3.5 mm. The feasibility evaluation of the system was conducted in Fugen nuclear plant. The results show that the system can largely reduce the preparatory workload of an AR application in an NPP.

However, some items have low evaluation because the evaluators thought that the number of pasted marker is still large. Moreover, when a camera is with short distance with markers, there are fewer detectable marker, which means there are no enough feature points for tracking, the tracking will fails. Therefore, the marker design is improved by adding four additional small circles on the marker. In this case, if the distance between camera and markers are short, the projection of the marker on image is with large area, and its four small circle can be easily detected as feature points. If the distance between camera and markers are long, although the small circles are difficult to be detected, the detectable marker number become large. Therefore there are always enough feature points. The performance evaluation of this marker shows that it is effective in both long distance and short distance tracking.

Reference

[1] M. Billinghurst , H. Kato , I. Poupyrev: The MagicBook: Moving Seamlessly between Reality and Virtuality, *IEEE Computer Graphics and Applications*, Vol. 21 No.3, pp.6-8, 2001.

[2] H. Kato, M. Billinghurst: Marker Tracking and HMD Calibration for a Video-based Augmented Reality Conferencing System. *Proceedings of International, Workshop on Augmented Reality 1999*, pp.85-94, 1999.

[3] DF Abawi, J. Bienwald, R. Dorner: Accuracy in Optical Tracking with Fiducial Markers: An Accuracy Function for ARToolKit, *IEEE and ACM International Symposium on Mixed and Augmented Reality 2004*, pp. 260–261, 2004.

[4] H. Kato, K. Tachibana, M. Billinghurst, M. Grafe. A Registration Method Based on Texture Tracking Using ARToolKit, *IEEE International Augmented Reality Toolkit Workshop 2003* , pp. 77–85, 2003.

[5] H. Slay, B. Thomas, R. Vernik. Using ARToolkit for Passive Tracking and Presentation in Ubiquitous Workspaces, *IEEE International Augmented Reality Toolkit Workshop 2003*, pp. 46–53, 2003.

[6] D. Wagner and D. Schmalstieg. ARToolKit on the PocketPC Platform, *IEEE International Augmented Reality Toolkit Workshop 2003*, pp. 14–15, 2003.

[7] W. Piekarski, B. Thomas. Using ARToolKit for 3D Hand Position Tracking in Mobile Outdoor Environments, *IEEE International Augmented Reality Toolkit Workshop 2002*, p. 2, 2002.

[8] L. Naimark, E. Foxlin: Circular Data Matrix Fiducial System and Robust Image Processing for a Wearable Vision-inertial Self-tracker, *Proceedings of International Symposium on Mixed and Augmented Reality 2002*, pp. 27–36, 2002.

[9] L. Quan, Z. Lan: Linear N-point Camera Pose Determination, *IEEE Transactions on Pattern Analysis and Machine Intelligence*, Vol. 21, No. 8, pp. 774–780, 1999.

[10] H. Farid, E. P. Simoncelli: Optimally Rotation-Equivariant Directional Derivative Kernels, *International Conference of Computer Analysis of Images and Patterns*, pp. 207–214, 1997.

Chapter 3 A Line Feature-based Tracking Method

3.1 Introduction

When tracking in the capacious space of NPP, a large amount of markers are indispensable even using the improved circular marker, so that the workload of marker measurement is still heavy even using MAMS. Moreover, in some cases, it is difficult to allocate markers, for example, the tracking field is very narrow or very high. To solve this problem, a markerless tracking method is also necessary as an assistant of the marker-based tracking.

In the markerless tracking methods, point features, such as the corner points of actual objects in the environment, are most widely used as natural features in tracking[1][2][3] because it is the simplest feature and always abundant in most environment, but many occlusions exist in an NPP environment. Therefore point features are occluded easily, and many pseudo-points are detected. Moreover, some real feature points are not stable when the illumination or view angle changes. Compared with point features, line features such as the boundary of pipes and cables are abundant. Furthermore, the line feature has more pixels on an image, so it can be detected more reliably than point features because even a part of a line is occluded, it is still detectable as a line. Therefore, in this study a line feature-based tracking method is developed and evaluated whether it is applicable in NPPs for supporting fieldwork. As the assistant of the marker-based tracking, whether it is feasible in a markless environment must be examined.

Some related studies have examined a tracking technology using line features. A structure-from-motion system[4] was proposed using both point and line features extracted from omni-directional video sequences. A trinocular stereo camera was used to estimate a map based on 3D line segments[5]. Eade et al. used local edge segments in monocular SLAM system[6]. Vertical lines were used as landmarks for tracking in another study[7] , whereas the robot movement is similar on a ground plane. A monocular extended Kalman filter (EKF) SLAM using line landmarks was presented in [8]. Similar research was presented in a recently report by L. Zhang et al.[9]. A method to incorporate 3D line segments in vision-based SLAM was proposed in [10]. Recently, G. Zhang et al.[11] proposed a method to build 3D map based on vertical and floor line using monocular SLAM.

However, the methods described above entail some disadvantages if they are applied in the NPP environment. For example, only parallel lines or floor lines are used, as in some studies[4][7][11], but many line features in an NPP do not have parallel lines. In one earlier study[5], a trinocular camera was used, which increases the cost of the system,

and less convenience than using monocular vision in some narrow spaces. In another investigation[6], the center point of a line segment was used to represent the line segment. However, because the line segment length always changes, the center point of the line segment might be very different in different images. It is therefore difficult to match the line features accurately. The two reports of studies[8][10] describe a camera that is controlled by a robot to move along an accurately determined trajectory, which is impossible for workers when moving in an NPP environment. In the reports[8][9], the estimation of camera position and orientation is based on EKF, in which the accuracy is very rely on the initial guess and some prior prediction. The method is effective in a simple indoor environment, as the result shown in[9]. But it is difficult to keep the accuracy level using the prediction-based method when moving a long distance during the field work in an NPP environment. Moreover, the number of line features in an NPP is much larger. Therefore the computation cost would become higher if using EKF.

In this study, a monocular camera was used as the vision sensor, and infinite line is used as the line feature instead of line segment. Because the two endpoints of a line segments is difficult to be recognized stably when the view angle or illumination changes, but the infinite line is much more stably in the same cases. The camera position and orientation was estimated by solving P3L problem using a RANSAC (random sample consensus) based method which is independent of any prediction. The maximum possible solution is eight in a P3L problem. In the two studies[12][13], the P3L problem is transferred to solving a polynomial equation with one unknown, but the distribution of the eight solutions remains unclear. In other words, the solutions must be sought in the whole field of real numbers. In this study, a new method was proposed for solving P3L problems, which solves four equations with one unknown in four parallel threads respectively to improve the processing speed. An image series captured from an NPP environment was used to evaluate this method. No report in the relevant literature describes a similar study using line features for SLAM in an NPP environment.

3.2 Development of a Line Feature-based Tracking Method

3.2.1 Profile of the Method

In this section, the method for calculating the camera pose (position and orientation) and registering 3D line landmarks into the database was described. Two rectangular markers for which four edges were registered as initial line landmarks were measured in advance for the initialization. The main flow of the method is depicted in Fig.3.1. Using the initial landmarks, the method starts tracking, and registers new landmarks from environment while the camera is moving. The 3D lines which positions and directions are measured in

advance are registered into databases as initial landmarks. The concept of the method is shown as Fig.4.1. The main steps of the method are the follows.

Step 1-1 At first image frame, 2D lines are detected on the image, and the correspondence of the initial line landmarks are found from the detected 2D lines.

Step 1-2 Detect 2D line features from next image using image processing.

Step 1-3 Match the detected 2D line features with 3D landmarks registered in the database.

Step 1-4 Estimate the camera pose using RANSAC-based method.

Step 1-5 Register new landmarks into database, and then go to Step 1-2. New landmarks were registered from unknown environment. A triangulation method is applied to estimate the corresponding 3D line of a 2D line that is not matched with any landmark. If the estimated 3D line satisfies some constraints which mean that it is sufficiently reliable, then it will be registered as a new landmark.

To satisfy Requirement A mentioned in chapter 1, the method must be designed with enough accuracy and stability. Therefore, RANSAC method is used for reduce the error of camera pose estimation. Moreover, the registered landmarks always includes errors of their position and direction, which increases the tracking error of camera. Therefore, bundle adjustment[14] is used to update the registered landmarks to improve the accuracy of their position and direction. Because the computation of bundle adjustment is large, it is executed in a parallel thread to improve the speed of the main thread.

3.2.2 Initialization

In this study, two rectangle markers were used as initial landmarks. (In theory, one rectangle is sufficient to calculate the 3D position and orientation of a camera. However, the tracking accuracy very depends on the initial tracking accuracy of camera, therefore more rectangle markers are necessary for improving the accuracy.) The rectangle marker is depicted in Fig.3.3. At first frame, the corresponding 2D lines of the eight registered initial 3D landmarks must be extracted from the image. An example of the initialization is shown as Fig.3.4. It is realized as the following steps:

Step 2-1 Undistortion is applied to cancel the camera lens distortion. Fig.3.4(a) is the original image. The result of undistortion is shown in Fig.3.4(b).

Step 2-2 Binarization of the image. In this study, grayscale images were captured in which each image pixel has a value ranging from 0 to 255. If the pixel grayscale is larger than a threshold value th_1, then it would be changed to 255, otherwise it would be changed to 0. The result of the binarization is shown in Fig.3.4(c).

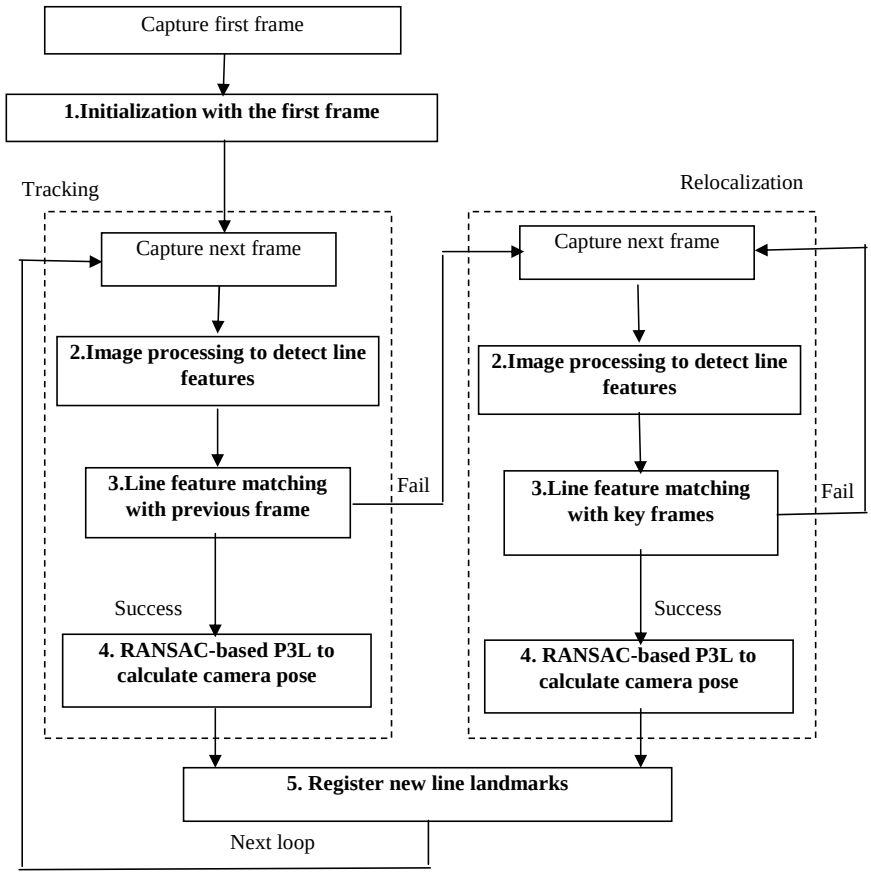

Fig. 3.1: Flow chart of the proposed method.

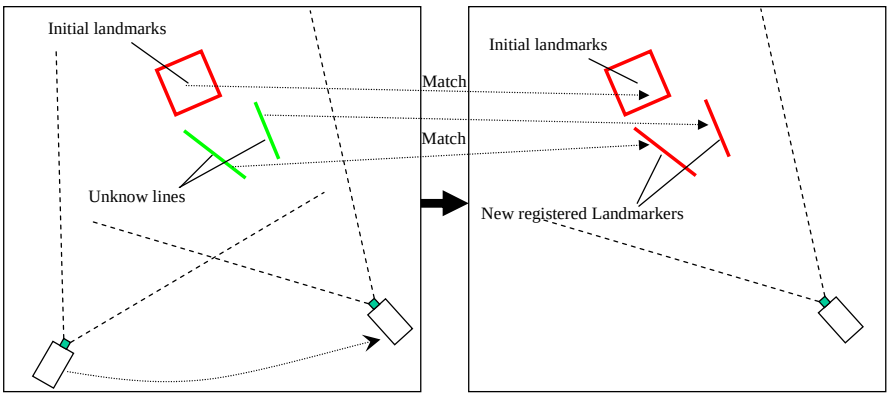

1. Register initial landmarks (red rectangle)
2. Detected 2D lines (red lines)
3. Matching 2D lines
4. Estimate the 3D position and orientation of camera
5. Register 2d lines as new landmarks into database

Fig. 3.2: Concept of the proposed method.

Step 2-3 Detect edge points using Canny operator[15]. Then for every edge point, any edge point in its adjacent eight pixels would be classified in the same cluster (Fig.3.5).

Step 2-4 For each point cluster, find the four points with extreme coordinate values at x and y directions, respectively (Fig.3.6).

Step 2-5 Check whether the four points are located on a parallelogram. If yes, then check whether or not all the points in the cluster are located on the four edges of the parallelogram. If yes, then this parallelogram is a candidate of initial landmarks.

Step 2-6 Check the grayscale of the pixels of part A (black part) and part B (shadow part), respectively, as depicted in Fig.3.7. The width of part B is set to 5 in this study. If the average value of part B is higher than a given threshold th_2 larger than that of part A, then four edges of the parallelogram are regarded as the corresponding lines of an initial marker.

The final result of the recognition of the initial landmarks is shown in Fig.3.4(d).

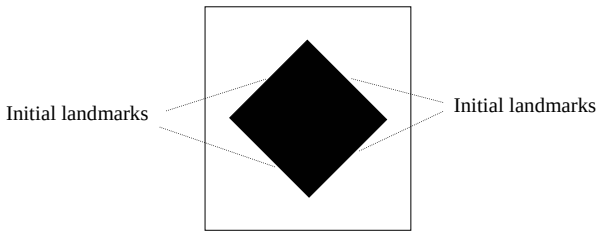

Fig. 3.3: Rectangle marker.

3.2.3 Line Detection

In an NPP, the edges of much equipment are lines. Image processing is intended to extract 2D line features from an image captured from the NPP environment. Line features on an image are one kind of edge feature, which indicates pixels with a large gradient of grayscale. Image processing consists of the following steps:

Step 3-1 After capturing a raw image, undistortion is applied to cancel the camera lens distortion.

Step 3-2 A contrast enhancement method that enhances the difference of the grayscale when the grayscale is very high or very low is applied. Assuming that the grayscale of a pixel is r, $0 \leq r \leq 255$, then the new grayscale $s(r)$ after transformation is as Equation (3.1) and (3.2). The gradient of grayscale will become larger after the logarithmic transformation, where r is very small or very large. In other words, the

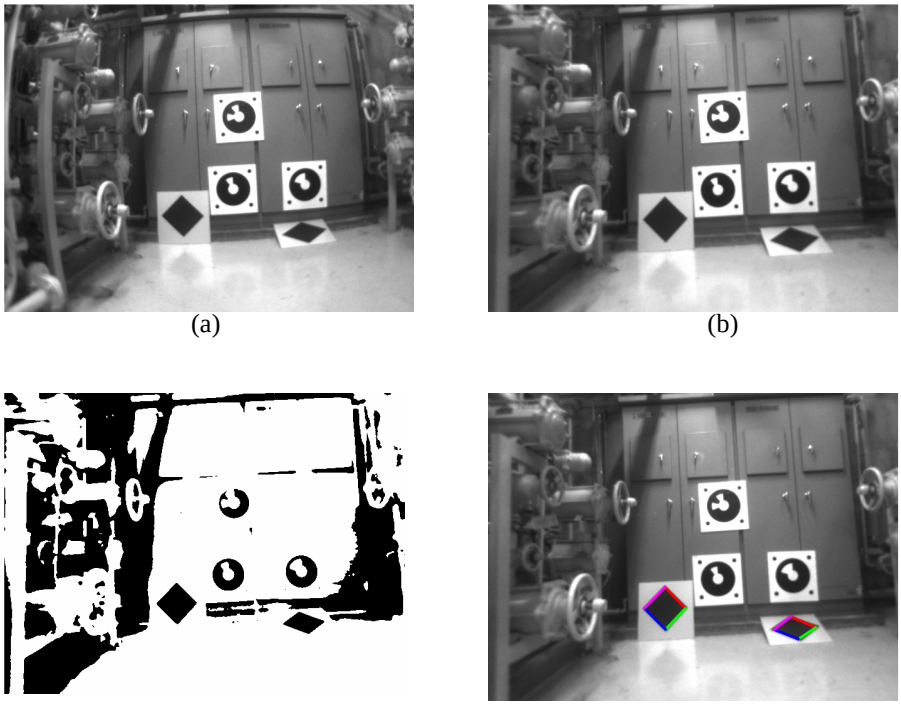

Fig. 3.4: Initial landmark recognition.

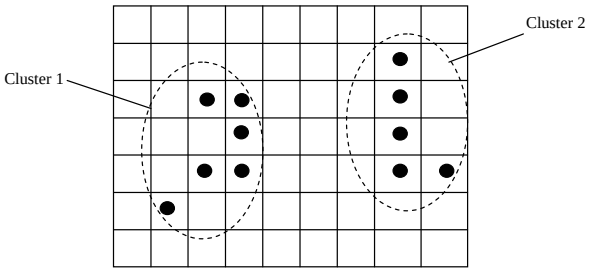

Fig. 3.5: Edge point clusters.

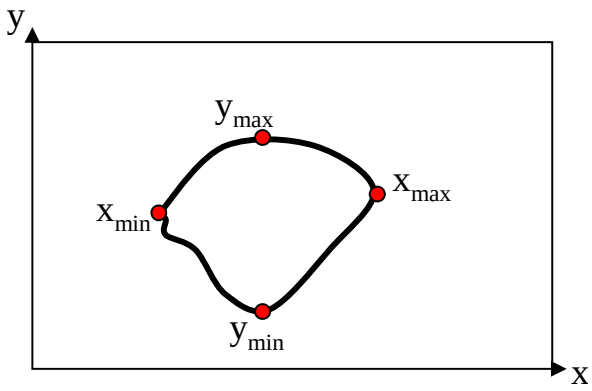

Fig. 3.6: Extreme points of a cluster.

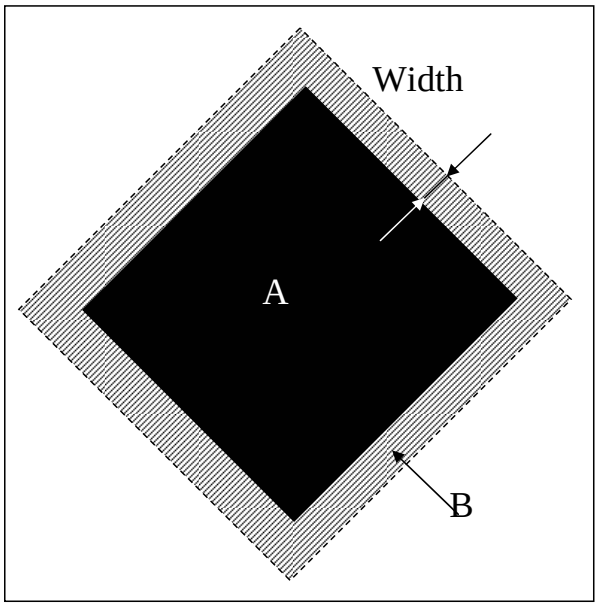

Fig. 3.7: Calculation regions of the rectangle marker.

contrast will enhance areas where the pixel is either very dark or very bright, as shown in Fig.3.8.

$$s(r) = 1000 \log_{10}(r+1), (0 \leq r \leq 127) \tag{3.1}$$

$$s(r) = s(127) + 1000(\log_{10}(137) - \log_{10}(266 - r)), (128 \leq r \leq 255) \tag{3.2}$$

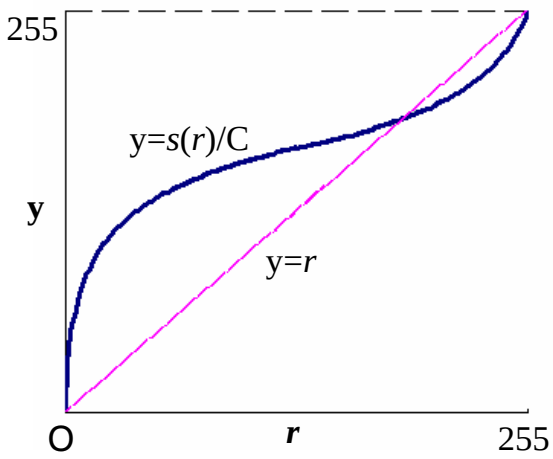

Fig. 3.8: Curve of $s(r)$.

Step 3-3 Apply Gaussian smoothing to remove the image noise.

Step 3-4 Detect edge point clusters. (Same as the Step 2-3 of the initialization)

Step 3-5 Iterative end point fit (IEPF)[16] method is applied to extract line features from the edge point cluster. Assuming that an edge point cluster exists, as portrayed in Fig.3.9 (thick solid line). Search for point $\mathbf{P}$, which has the longest distance d to the line through the two endpoints $\mathbf{P}_1$ and $\mathbf{P}_2$. If d is larger than a threshold th_3, then divide the cluster into two clusters at $\mathbf{P}$, and repeat this step on each. When d is smaller than th_3, the corresponding cluster is then regarded as a line feature. Least-squares error optimization is applied to find the optimal line (dashed line l). Finally, some lines might be mutually connected if the difference of their inclinations are smaller than a threshold th_4 and the distance between their endpoints are smaller than a threshold th_5.

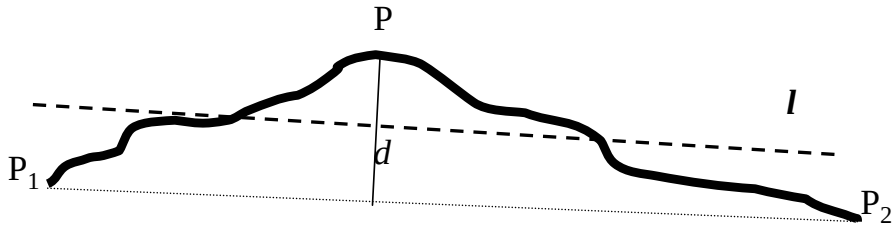

Fig. 3.9: Concept of IEPF method.

3.2.4 Line Matching Algorithm

To solve P3L problem, the correspondences between 3D lines (landmarks) and 2D lines (projection of landmarks) are necessary. In this study, detected 2D line features are matched with that of previous frame or key frames to find out which are the projection of 3D landmarks. If a 2D line on the image is a correspondence of a 3D landmark, then it would be used for calculating the position and orientation of the camera in this frame. Otherwise it would be a candidate line, which has the possibility to be registered as a new landmark through a triangulation method. If matching fails, (The number of 2D lines which are matched with 3D landmarks is smaller than 4. Because the P3L problem has a maximum of eight solutions, more than 4 landmarks are necessary to obtain the best solution.) the line features of current frame would be matched with that of key frames, which are saved when the movement of camera between the current frame and last key frame is larger than a threshold.

Invariant Moment

Because of the instability of Canny operator and IEPF, the same 2D line might be detected with different lengths at different frames. The typical for matching features between different frames is to produce a template around the feature as a patch. By comparing the patches of the features, the corresponding features can be matched. But it is difficult to produce a template of the line with determined width and length of a window as a matching patch. Therefore, a general patch method using normalized cross correlation for matching features is difficult to apply. The histogram invariant moment[17] of landmarks is used for tracking in this study. The invariant moment represents the average grayscale of an image. Therefore it is not necessary to define a window of fixed size and shape in advance, and it is invariant when the image is zoomed or rotated. The definition of the invariant moment of a line is described as the follows:

For a 2D line, a window (dash frame) with width of 15 pixels was defined as presented in Fig.3.10. If the absolute value of the slope to the x axis is greater than 1, then the width is along the x direction. Otherwise it is along the y direction.

In the window, n is the total number of pixels, and $n(r)$ is the number of pixels with

grayscale r ($0 \leq r \leq 255$). The probability function $P(r)$ is defined as $P(r) = n(r)/n$. Then the k-order moment m_k is $m_k = \Sigma r^k P(r)$, and the k-order central moment is $u_k = \Sigma(r - r_a)^k P(r)$, where $r_a = m_1/m_0$. Finally, invariant moment h is defined as $h = \eta_5/\eta_2\eta_3$, where $\eta_k = u_k/u_0^{k+1}$.

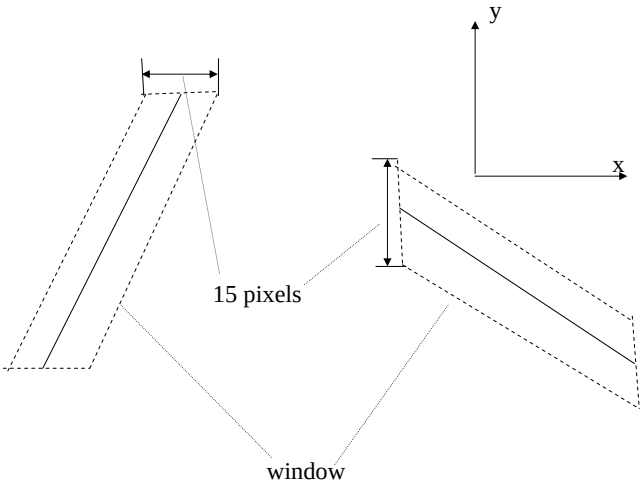

Fig. 3.10: Calculation window of invariant moment.

Line Matching with That of Previous Frame

When the camera moves slowly and smoothly, and the capturing frame rate is sufficiently high, the movement of a line between consecutive frames would be sufficiently small. It can therefore be matched in the previous frame in a small zone round the line, and will not be confused with other lines. In this study, the camera pose is estimated from the correspondences between registered landmarks and their projections at every frame. Therefore, after image processing, the corresponding 2D lines of registered landmarks must be found from extracted lines features. At first frame, the initial correspondences are created as described in section 3.2.2. Then every extracted line feature of the current frame can be matched with that of previous frame to find the correspondences between landmarks and detected 2D lines at the current frame. As depicted in Fig.3.11, **l** and **l'** are two detected line segments (Thick solid line segments. Dash lines are their extended lines) in previous frame and current frame respectively. If their difference of invariant moment is sufficiently small ($< 20\%$ in this study), then the minimum distance d between two points located on segments **l** and **l'** respectively and the angle θ between them are checked. If they are both sufficiently small ($d < 20$ pixel, $\theta < 5\,^\circ$ in this study), then **l'** is considered as the same feature of **l**. If **l** is the corresponding 2D line of a landmark, **l'** will be the corresponding 2D line of the landmark too. If more than one line is matched with **l**, the line is considered not so reliable. Therefore, only the lines which have only one matched line are picked out

as matched lines. At every frame, the correspondences between the landmarks and their projections are ascertained.

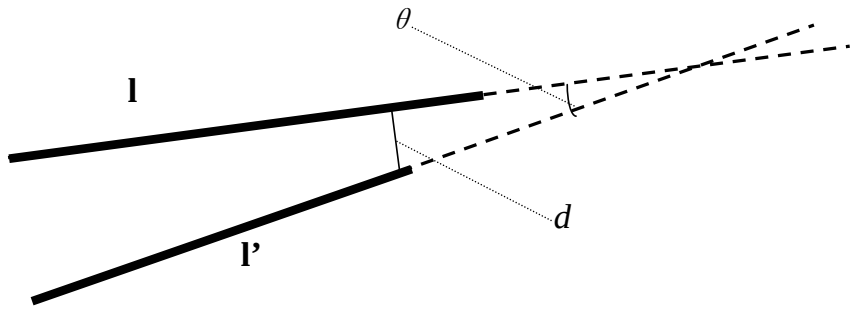

Fig. 3.11: Line matching with that of previous frame.

Relocalization Using Key Frames

If line matching with the previous frame fails, then the tracking also fails at the current frame. A relocalization method to estimate the position and orientation of a camera after tracking failure is necessary. General relocalization[18] compares current frame and key frames at low resolution to find the key frame that is most similar to the current frame, and the position and orientation of the camera at the current frame is then estimated based on the key frame. However, the error might be large even if relocalization succeeds in the general method. To solve this problem, a different method that matches the line features between the current frame and key frames was proposed. If the matching succeeds, then the position and orientation of the camera can be estimated using RANSAC-based method, which is the same with the tracking method. Therefore the accuracy level would not decrease.

A 2D infinite line can be decided uniquely using a point that is located on the line and with the smallest distance to the origin. Therefore, the line can be uniquely represented by the point. The concept of the line matching with key frames is shown as Fig.3.12. By replacing a 2D line with a point, the details of the relocalization are as the follows:

Step 4-1 For every point $\mathbf{p}$ corresponding to a landmark in a key frame, a circle with radius of 40 pixels, and center at point $\mathbf{p}$ is defined. Then in the current frame, the invariant moment of points located in the circle are checked. If the difference of the invariant moment between $\mathbf{p}$ and a point is smaller than a given threshold, then the point would be chosen as a candidate that is matched to $\mathbf{p}$.

Step 4-2 In the key frame, choose a point as $\mathbf{p}_0$, other points are $\mathbf{p}_i$, and $l_i = ||\mathbf{p}_0\mathbf{p}_i||$ (i=1,2,3$\cdots$k-1, k is the point number in the key frame).

Step 4-3 In the current frame, choose a candidate of $\mathbf{p}_0$ as $\mathbf{p'}_0$ and a candidate of $\mathbf{p}_i$ as $\mathbf{p'}_i$, as portrayed in Fig.3.12. If $|l_i - ||\mathbf{p'}_0\mathbf{p'}_i|||$ is smaller than a threshold (20 pixels), and if the angle between the lines $\mathbf{p}_0\mathbf{p}_i$ and $\mathbf{p'}_0\mathbf{p'}_i$ is smaller than a threshold (5 $^\circ$), then $\mathbf{p'}_0$ and $\mathbf{p'}_i$ are regarded as matched respectively with $\mathbf{p}_0$ and $\mathbf{p}_i$. Repeat this step until all candidates of $\mathbf{p}_i$ in the current frame are checked in order. If $\mathbf{p}_i$ is matched with more than one candidate, then choose the candidate for which the distance between it and $\mathbf{p}_i$ is the minimum. This is a matching result.

Step 4-4 In the current frame, choose another candidate of $\mathbf{p}_0$ as $\mathbf{p'}_0$ and repeat Step 4-3 until all candidates of $\mathbf{p}_0$ are checked in order. The case with the maximum number of matched pairs between $\mathbf{p}_i$ and $\mathbf{p'}_i$ is regarded as the best matching result based on $\mathbf{p}_0$.

Step 4-5 Choose another point in key frame as $\mathbf{p}_0$, repeat Step 4-2 to Step 4-4 until all points in the key frame are checked in order as $\mathbf{p}_0$.

Step 4-6 Choose the case with the maximum number of matched pairs ($\mathbf{p}_i$ and $\mathbf{p'}_i$) as the final matching result. If the number is smaller than 4, then the matching is regarded failure; then the current frame would be matched with another key frame. Otherwise the matching result would be used to calculate the camera position and orientation.

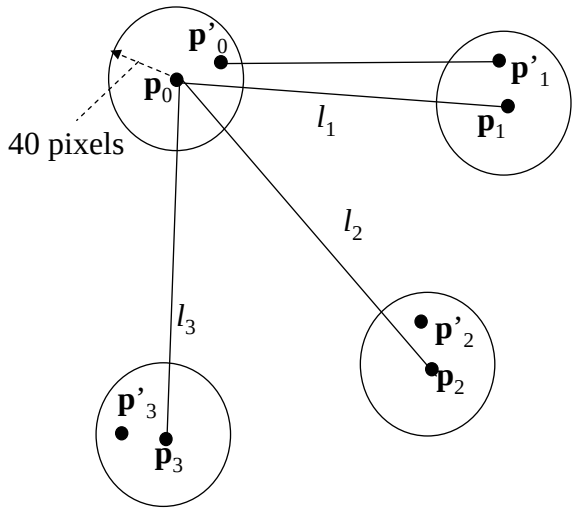

Fig. 3.12: Line matching with key frame.

3.2.5 RANSAC-based Method

In this study, a RANSAC-based method was used to estimate the camera pose. In general, the P3L problem has maximum eight solutions. The existing methods in [12][13]

must search all the solutions in the whole field of real numbers by solving an eight-degree equation with a single unknown. In this study, four equations which are solvable in the field $[0, \pi)$ with maximum two solutions were solved instead of solving the eight-degree equation, they are solved in four different threads to improve the processing speed. Details of the RANSAC-based method are as the following steps:

Step 5-1 Randomly choose three line correspondences.

Step 5-2 Use the correspondences to estimate the position and orientation of the camera through solving P3L problem.

Step 5-3 Based on the result obtained from Step 5-2, check the re-projection error of all line correspondences. The line correspondences for which the re-projection error is smaller than a threshold are inliers.

Step 5-4 Repeat Step 5-1 to Step 5-3 by min(n, 100) times, where n is the number of line correspondences. Choose the result with the maximum number of inliers.

The details of solving P3L problem are described as follows.

Coordinate System

In this study, subscript represents a vector or matrix in different coordinate systems. For example, $\mathbf{t}_A$ is a vector in system A, and $\mathbf{t}_{AB}$ and $\mathbf{R}_{AB}$ respectively denote the translation vector and rotation matrix from system A to system B. Subscripts W and C respectively signify the world system and camera system.

3D line Representation

It is extremely convenient to represent a 3D line using Plucker coordinates[19]. A Plucker line is:

$$\mathbf{L}_{6\times1} = (\mathbf{n}^T, \mathbf{u}^T)^T = (n_1, n_2, n_3, n_4, n_5, n_6)^T \tag{3.3}$$

Therein, $\mathbf{u}$ is the unit directional vector of the 3D line and $\mathbf{n} = \mathbf{p} \times \mathbf{u}$, where $\mathbf{p}$ is an arbitrary point on the line. As presented in Fig.3.13. $h = ||\mathbf{n}||$ is the distance from origin to the 3D line. Considering the constraints as Equation (3.4) and (3.5), there are only 4 degrees of freedom (DOF).

$$\mathbf{n} \cdot \mathbf{u} = 0 \tag{3.4}$$

$$\| \mathbf{u} \| = 1 \tag{3.5}$$

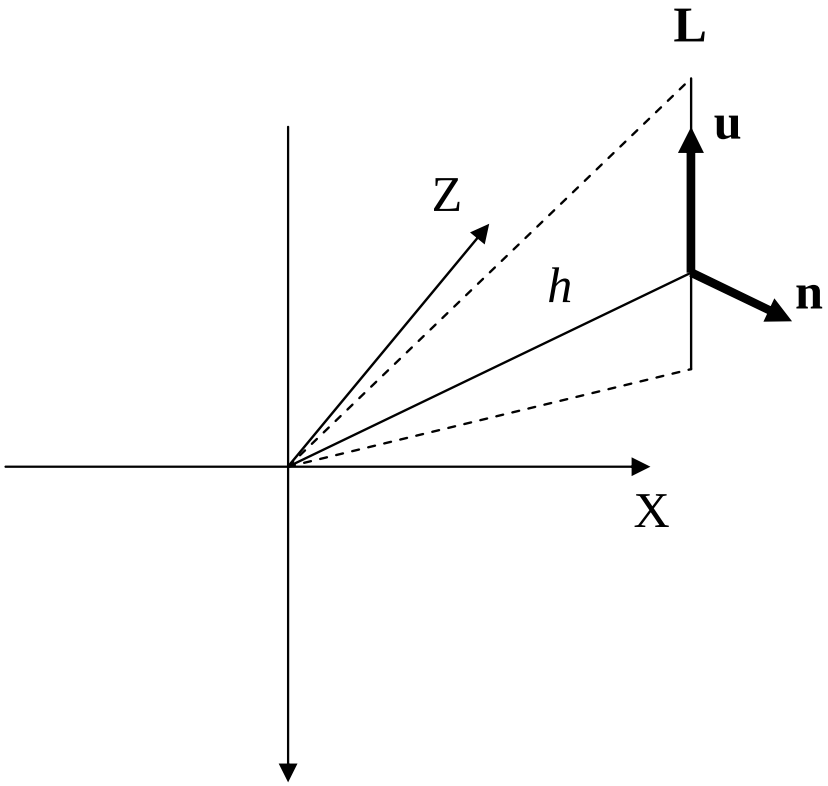

Fig. 3.13: Definition of Plucker line.

Method for Solving P3L Problem

The line projection is depicted in Fig.3.14. Assuming that $\mathbf{p}$ is an arbitrary point on line $\mathbf{L}$. For convenience, it is defined as $\mathbf{p} = \mathbf{u} \times \mathbf{n}$. $\mathbf{v}$ is the unit normal vector of the plane (the shadow plane in Fig.3.14), which contains the origin of camera system and the 3D line. The 2D projection of the line is also placed on this plane, so $\mathbf{v}$ is obtainable by $\mathbf{v} = \mathbf{a} \times \mathbf{b}$, where $\mathbf{a}$ and $\mathbf{b}$ are the two endpoints of the detected 2D line. The directional element of $\mathbf{L}$ and the vector $\mathbf{p}$ in the camera system are:

$$\mathbf{u}_C = \mathbf{R}_{WC}\mathbf{u}_W \tag{3.6}$$

$$\mathbf{p}_C = \mathbf{R}_{WC}(\mathbf{p}_W - \mathbf{t}_{WC}) \tag{3.7}$$

Because $\mathbf{u}_C \perp \mathbf{v}_C$, $\mathbf{p}_C \perp \mathbf{v}_C$, Equation (3.8) and (3.9) are deduced as shown below.

$$(\mathbf{R}_{WC}\mathbf{u}_W) \cdot \mathbf{v}_C = 0 \tag{3.8}$$

$$\mathbf{R}_{WC}(\mathbf{p}_W - \mathbf{t}_{WC}) \cdot \mathbf{v}_C = 0 \tag{3.9}$$

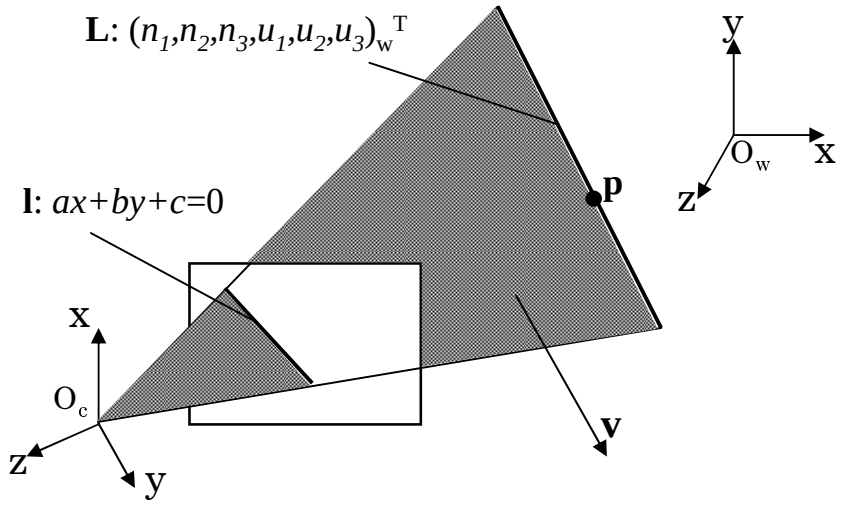

Fig. 3.14: A 3D line and its 2D projection on image.

Equation (3.8) includes only three unknown parameters related to rotation. Therefore the rotation information is solvable first if there are three line correspondences when the three lines are not parallel. Assuming that the unit direction vectors of the three lines are $\mathbf{u}_{1W}$, $\mathbf{u}_{2W}$, and $\mathbf{u}_{3W}$ respectively in the world system, then their corresponding unit vectors $\mathbf{v}_{1C}$, $\mathbf{v}_{2C}$, and $\mathbf{v}_{3C}$ in the camera system are obtainable from the two detected endpoints of their corresponding 2D lines and camera intrinsic parameters. For convenience, a local system A was defined in which $\mathbf{v}_{1A} = (1,0,0)^T$, $\mathbf{v}_{2A} = (m,0,n)^T$, and $\mathbf{v}_{3A} = (r,s,t)^T$.

Therein, $\mathbf{v}_{2A} = \mathbf{R}_{CA}\mathbf{v}_{2C}$, $\mathbf{v}_{3A} = \mathbf{R}_{CA}\mathbf{v}_{3C}$, and $\mathbf{R}_{CA} = [\mathbf{v}_{1C}, (\mathbf{v}_{1C}\times\mathbf{v}_{2C})/||\mathbf{v}_{1C}\times\mathbf{v}_{2C}||, (\mathbf{v}_{1C}\times(\mathbf{v}_{1C}\times\mathbf{v}_{2C}))/||\mathbf{v}_{1C}\times(\mathbf{v}_{1C}\times\mathbf{v}_{2C})||]^T$. Moreover, it might be readily apparent that $m^2+n^2 = r^2+s^2+t^2 = 1$. Then the problem is equal to solve the unit direction of the three lines $\mathbf{u}_{1A}$, $\mathbf{u}_{2A}$ and $\mathbf{u}_{3A}$ in local system A. Because $\mathbf{u}\cdot\mathbf{v} = 0$, it can be assumed that $\mathbf{u}_{1A} = (0,\cos\theta,\sin\theta)^T$,$\mathbf{u}_{2A} = (x,y,z)^T$, and $\mathbf{u}_{3A} = (x',y',z')^T$.

According to the geometry relation, Equation (3.10) and (3.11) can be obtained, where c_1 is a constant decided by $\mathbf{u}_{1W}$ and $\mathbf{u}_{2W}$, as shown below.

$$\mathbf{u}_{1A}\cdot\mathbf{u}_{2A} = \mathbf{u}_{1W}\cdot\mathbf{u}_{2W} = c_1 \tag{3.10}$$

$$\mathbf{u}_{2A}\cdot\mathbf{v}_{2A} = 0 \tag{3.11}$$

From Equation (3.10) and (3.11), consider that $||\mathbf{u}_{2A}||$=1, then x, y and z is solvable as Equation (3.12), (3.13) and (3.14). Two maximum solutions exist (double sign in same order).

$$x = \frac{-mnc_1\sin\theta \mp n\cos\theta\sqrt{1-n^2\sin^2\theta-c_1^2}}{1-n^2\sin^2\theta} \tag{3.12}$$

$$y = \frac{c_1 \cos\theta \mp m \sin\theta \sqrt{1 - n^2 \sin^2\theta - c_1^2}}{1 - n^2 \sin^2\theta} \tag{3.13}$$

$$z = \frac{m^2 c_1 \sin\theta \pm m \cos\theta \sqrt{1 - n^2 \sin^2\theta - c_1^2}}{1 - n^2 \sin^2\theta} \tag{3.14}$$

Similarly, $\mathbf{u}_{3A} = (x', y', z')^T$ is solvable as Equation (3.15), (3.16) and (3.17), where c_2 is a constant decided by $\mathbf{u}_{1W}$ and $\mathbf{u}_{3W}$. Two maximum solutions exist (double sign in same order).

$$x' = \frac{-c_2 r(s\cos\theta + t\sin\theta) \mp (s\sin\theta - t\cos\theta)\sqrt{1 - (t\sin\theta + s\cos\theta)^2 - c_2^2}}{1 - (t\sin\theta + s\cos\theta)^2} \tag{3.15}$$

$$y' = \frac{-c_2((1-s^2)\cos\theta - st\sin\theta) \pm r\sin\theta\sqrt{1 - (t\sin\theta + s\cos\theta)^2 - c_2^2}}{1 - (t\sin\theta + s\cos\theta)^2} \tag{3.16}$$

$$z' = \frac{c_2((1-t^2)\sin\theta - st\cos\theta) \mp r\cos\theta\sqrt{1 - (t\sin\theta + s\cos\theta)^2 - c_2^2}}{1 - (t\sin\theta + s\cos\theta)^2} \tag{3.17}$$

Then, according to the constraint $\mathbf{u}_{2A} \cdot \mathbf{u}_{3A} = \mathbf{u}_{2W} \cdot \mathbf{u}_{3W} = c_3$ (c_3 is a constant decided by $\mathbf{u}_{2W}$ and $\mathbf{u}_{3W}$), the nonlinear Equation (3.18) with one unknown parameter θ is obtainable.

$$f(\theta) = \mathbf{u}_{2A} \cdot \mathbf{u}_{3A} - c_3 = 0 \tag{3.18}$$

Consider the different sign from Equation (3.12)-(3.17). Equations of four types exist in Equation (3.18). The curve of one type of $f(\theta) = \mathbf{u}_{2A} \cdot \mathbf{u}_{3A} - c_3$ is depicted in Fig.3.15. The top panel of Fig.3.15 presents a case in which $1 - n^2 - c_1^2 = 0$ and $1 - s^2 - t^2 - c_2^2 = 0$. (The Equation (3.12)-(3.17) would have two solutions in the whole field [0,2π].) The bottom panel of Fig.3.15 is a more general case in which $\mathbf{u}_{2A}$ and $\mathbf{u}_{3A}$ would have no solution ($1 - n^2\sin^2\theta - c_1^2 < 0$ or $1 - (t\sin\theta + s\cos\theta)^2 - c_2^2 < 0$) in some field. The shapes of the other three types are similar. From Fig.3.15, it is known that the maximum number of possible solutions of each type of Equation (3.18) is four. Because $f(\theta) = f(\theta + \pi)$, only two solutions is considered in the field [0, π].

No analytical solution exists for Equation (3.18), so an iterative method is applied for solving the equation. The method of solving θ in [0, π] has the following steps. (If θ=θ' is a solution, then $\theta = \theta' + \pi$ is also a solution. Therefore the solutions in [π, 2π) are also obtained.) The initial values of θ_1 and θ_2 are set as 0 and π, respectively, in this study as shown below.

Step 1 Assume $\theta_0 = (\theta_1 + \theta_2)/2$. If $f(\theta_0)f(\theta_1) > 0$, then go to Step 2. Otherwise go to Step 4.

Step 2 If $f((\theta_0+\theta_1)/2)f(\theta_1) < 0$, then θ_0 is replaced by the value of $(\theta_0+\theta_1)/2$, otherwise if $f((\theta_0+\theta_2)/2)f(\theta_1) < 0$, then θ_0 is replaced by the value of $(\theta_0+\theta_2)/2$. Go to Step 4. Otherwise, go to Step 3.

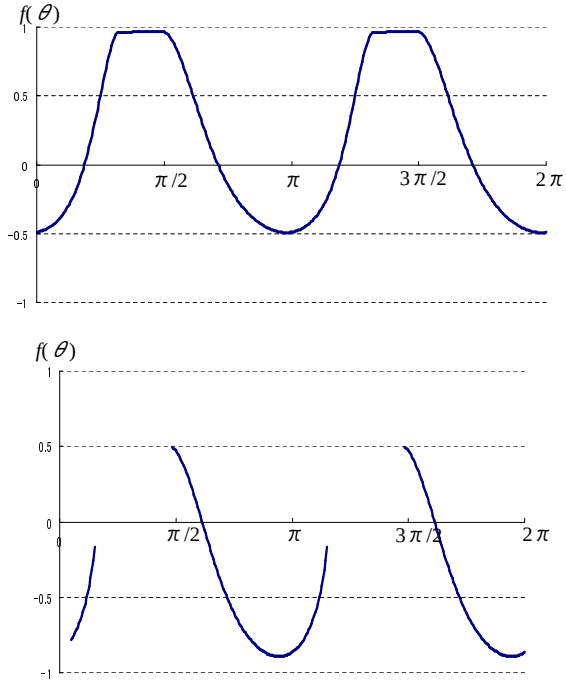

Fig. 3.15: Curve of $f(\theta)$. (Top: $1 - n^2 - c_1^2 = 0$ and $1 - s^2 - t^2 - c_2^2 = 0$. Bottom: $1 - n^2 \sin^2\theta - c_1^2 < 0$ or $1 - (t\sin\theta + s\cos\theta)^2 - c_2^2 < 0$)

Step 3 If $|f((\theta_0+\theta_1)/2)| < |f((\theta_0+\theta_2)/2)|$, then θ_2 is replaced by the value of θ_0; otherwise θ_1 is replaced by the value of θ_0. Then, if $(\theta_2 - \theta_1) > \pi/1800(0.1^\circ)$ (In this case, the value of $f(\theta_1)$ and $f(\theta_2)$ are almost not changed any more), go to Step 6; otherwise, go to Step 1.

Step 4 Assume $\theta' = (\theta_1 + \theta_0)/2$. If $|f(\theta')| < 10^{-6}$, then θ' is regarded as a solution. Go to Step 6. Otherwise go to Step 5. (It is known that the two solutions are located respectively in (θ_1, θ_0) and (θ_0, θ_2). Here only the case in (θ_1, θ_0) is discussed. The case in (θ_0, θ_2) is similar.)

Step 5 If $f(\theta_1)f(\theta') < 0$, then θ_0 is replaced by the value of θ'; otherwise θ_1 is replaced by the value of θ'. Go to Step 4.

Step 6 End.

After all solutions are solved, $\mathbf{u}_{1A}$, $\mathbf{u}_{2A}$ and $\mathbf{u}_{3A}$ are obtainable. Therefore, the rotation matrix is solved as Equation (3.19), where $\mathbf{R}_{WB}$ and $\mathbf{R}_{AB}$ are obtained as Equation (3.20) and (3.21).

$$\mathbf{R}_{WC} = \mathbf{R}_{AC}\mathbf{R}_{WA} = \mathbf{R}_{CA}^T\mathbf{R}_{AB}^T\mathbf{R}_{WB} \tag{3.19}$$

$$\mathbf{R}_{AB} = [\mathbf{u}_{1A}, (\mathbf{u}_{1A}\times\mathbf{u}_{2A})/||\mathbf{u}_{1A}\times\mathbf{u}_{2A}||, (\mathbf{u}_{1A}\times(\mathbf{u}_{1A}\times\mathbf{u}_{2A}))/||\mathbf{u}_{1A}\times(\mathbf{u}_{1A}\times\mathbf{u}_{2A})||]^T \quad (3.20)$$

$$\mathbf{R}_{WB} = [\mathbf{u}_{1W}, (\mathbf{u}_{1W}\times\mathbf{u}_{2W})/||\mathbf{u}_{1W}\times\mathbf{u}_{2W}||, (\mathbf{u}_{1W}\times(\mathbf{u}_{1W}\times\mathbf{u}_{2W}))/||\mathbf{u}_{1W}\times(\mathbf{u}_{1W}\times\mathbf{u}_{2W})||]^T \quad (3.21)$$

Then Equation (3.9) becomes a linear equation for translation $\mathbf{t}_{WC}$. After solving it, the best solution is chosen by checking the re-projection error of all solutions.

3.2.6 New Landmark Registration

If only initial landmarks are used for tracking, then it is impossible to conduct tracking in a capacious environment. In such cases, it is necessary to add new features as landmarks. A geometric method is applied to realize this function. In this method, every detected line feature on an image is a candidate or a registered landmark. This section will explain the details. As presented in Fig.3.16, two different points $\mathbf{C}_1$ and $\mathbf{C}_2$ indicate the camera positions corresponding to different frames. The two planes passing through $\mathbf{C}_1$ and $\mathbf{C}_2$ and a 3D line are represented respectively by $\mathbf{a}\cdot\mathbf{x}+a=0$ and $\mathbf{b}\cdot\mathbf{x}+b$. θ in Fig.3.16 is defined as the angle between two planes passing respectively through the 3D line and two different camera positions. The 3D landmark is obtainable from two different frames as (3.22) and (3.23):

$$\mathbf{u} = (\mathbf{a}\times\mathbf{b})/||\mathbf{a}\times\mathbf{b}|| \quad (3.22)$$

$$\mathbf{n} = (a\mathbf{b}-b\mathbf{a})/||\mathbf{a}\times\mathbf{b}|| \quad (3.23)$$

The RANSAC method was applied to optimize vectors $\mathbf{n}$ and $\mathbf{u}$ of a new landmark by choosing a model with the most inliers. If a 2D line can be detected more than 20 times in 50 continuous frames, then two frames for which the 2D line is detectable were chosen randomly between which the movement distance of camera is sufficiently large (>40 mm), and a 3D line was estimated from the two frames. Then the re-projection error of the 3D line was checked in the 50 frames. (As presented in Fig.3.17, the dashed line is a re-projection of a landmark, and solid is its corresponding 2D line detected using IEPF. The re-projection error is defined as $e=d_1+d_2$, where d_1 and d_2 are the distance from the two endpoints of the corresponding 2D line to the re-projection line.) If the error at one frame is sufficiently small (<6 pixels), then this frame would be a good frame. Repeat 50 times, and choose the result of a 3D line that has the greatest number of good frames. If the number of good frames is greater than 10, then the 3D line would be registered as a new landmark using this result, and would contribute to solving the P3L problem.

3.2.7 Accuracy Improvement of Landmarks

The registered landmarks might include some errors because the registration accuracy of the landmarks depends on the accuracy of tracking result (3D positions and orientations of

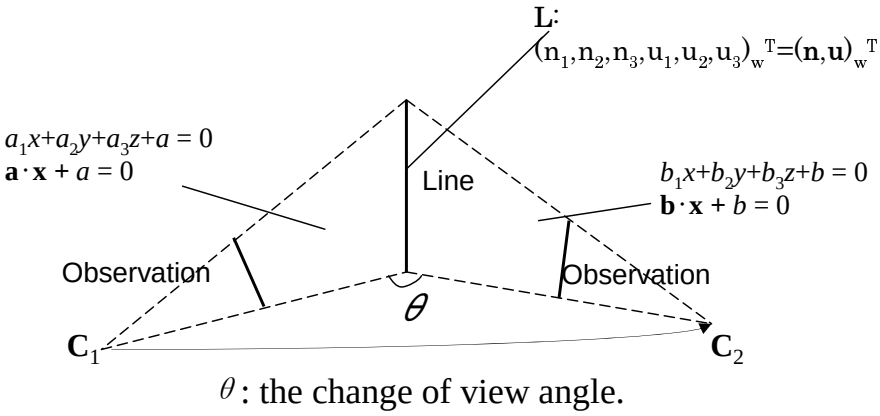

Fig. 3.16: Geometry method for new landmark registration.

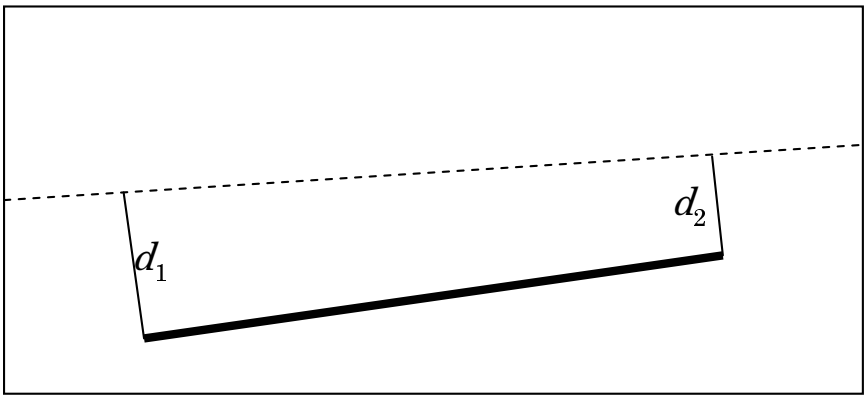

Fig. 3.17: Re-projection error between estimation and projection of a 2D line.

the camera). The errors of the tracking result, which caused by the measurement error of the initial landmarks and the detection error of 2D lines, are unavoidable. To reduce this error of landmarks, bundle adjustment[16] is applied to update the registered landmarks in a parallel thread to avoid reducing the speed of the main thread. In this study, assuming n registered landmarks and m positions and orientations of the camera, bundle adjustment is defined as a problem to minimize the total reprojection error with respect to all 3D lines and camera parameters as Equation (3.24).

$$min\Sigma_{j=1}^{m}\Sigma_{i=1}^{n}v_{ij}(d_{ij1}^2+d_{ij2}^2) \tag{3.24}$$

In that expression, v_{ij} is 1 if the ith landmark is detected when the camera is at the jth position, otherwise v_{ij} equals 0. d_{ij1} and d_{ij2} are re-projection errors of the ith landmark when the camera is at the jth position. d_{ij1} and d_{ij2} can be represented as a function with respect to $\mathbf{a}_j$ and $\mathbf{b}_i$, where $\mathbf{a}_j$ is a vector representing the jth camera position and orientation, and where $\mathbf{b}_i$ is a Plucker vector representing the ith landmark. Then Equation (3.24) can be transferred as shown in Equation (3.25).

$$min\Sigma_{j=1}^{m}\Sigma_{i=1}^{n}v_{ij}(f_1^2(a_j,b_i)+f_2^2(a_j,b_i)) \tag{3.25}$$

If all $\mathbf{a}_j$ and $\mathbf{b}_i$ are connected as a vector $\mathbf{c}$, where $\mathbf{c}=(\mathbf{a}_1,\mathbf{a}_2,...\mathbf{a}_m,\mathbf{b}_1,\mathbf{b}_2,...\mathbf{b}_n)^T$, then Equaiton (3.26) is obtainable as shown below.

$$min\Sigma_{j=1}^{m}\Sigma_{i=1}^{n}v_{ij}(f_1^2(\mathbf{c})+f_2^2(\mathbf{c})) \tag{3.26}$$

Using the Levenberg-Marquardt Algorithm[20], $\mathbf{c}$ is solvable to minimize the series sum as Equation (3.26). Therefore the registered landmarks are updated. In this study, sparse bundle adjustment[21] is applied to reduce the computing cost. If all past frames were used every time, then the computing cost would become higher and higher. Therefore, sparse bundle adjustment with a bundle of maximum of the last 50 frames was applied.

3.3 Performance Evaluation of the Line Feature-based Method in an NPP Environment

3.3.1 Purpose

To evaluate the accuracy, stability, and speed of the proposed method, an evaluation experiment was conducted in a pure-water chamber at Fugen NPP.

3.3.2 Method

The experimental area is about 8.0 m × 9.0 m. Two rectangular markers were pasted in the environment in advance, as presented in Fig.3.18 (Circular markers were used to

define the world system using MAMS. They were not used for tracking.). Their four edges were registered as initial landmarks (thick black lines). The edge length was about 0.2 m. The positions of the four corners of the rectangle were measured using MAMS beforehand so that their Plucker coordinates were calculated. A small circular marker was pasted on the camera so that its position could be measured by MAMS. The tracking results were compared with the true data measured by MAMS. The experimental environment is depicted in Fig.3.19. The camera moved along the dash arrow approximately.

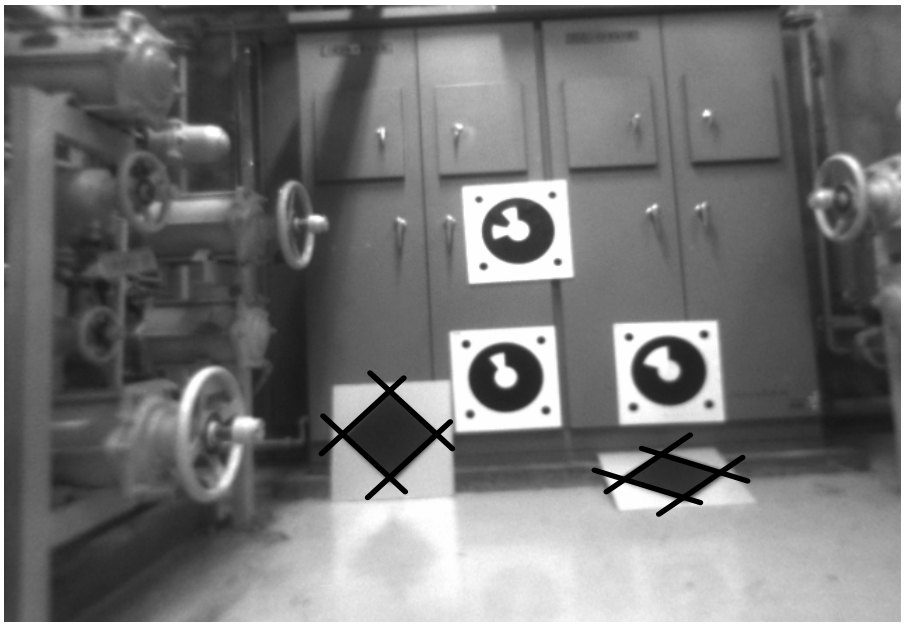

Fig. 3.18: Rectangle markers in the environment.

The experiment system includes a digital camera (IEEE-1394a, Point Grey Research, Dragonfly2; Table 4.1) with about 2.1 mm focal length and a computer connected to it. The CPU of the computer is ASUS P9X79 Corei7 3930K, Intel Corp. The program was developed using software Visual C++ 2008 (Microsoft Corp.) to realize the proposed tracking method. The capture frame rate of the camera was about 10 fps, and the resolution of the camera is 640 $\times$ 480. When tracking, the camera was fixed on a tripod, and the tripod was moved in the environment, and stopped at some sample positions. When the tripod was stopped, the true data of the camera pose at the sample position was measured by MAMS. The total path length of the camera movement was approximately 5 m. The distance between the camera and landmarks was about 2.5-5 m. When measuring the true data, it needs some time during which the tracking had to be paused. Therefore, the program processed the images later offline for convenient to avoid the pause. Images were captured when moving the camera and saved on a hard disk.

An image would be saved as a key frame when the distance between its corresponding estimated 3D position and that of the previous key frame is larger than 200 mm. In

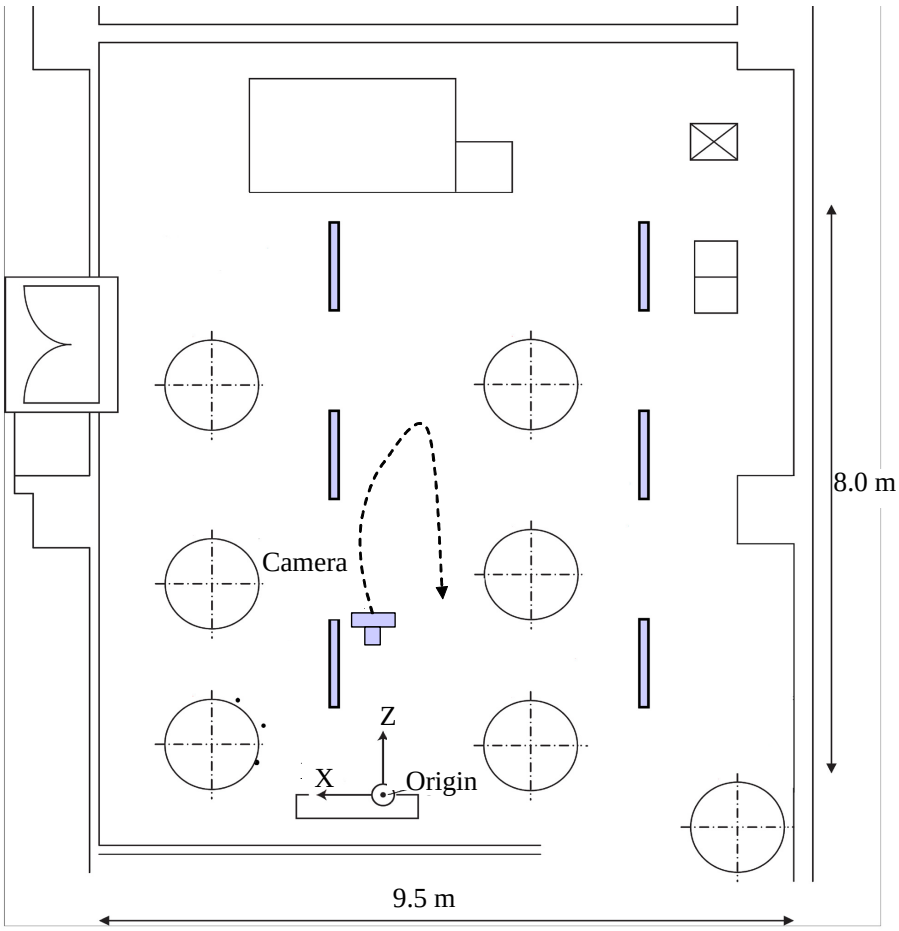

Fig. 3.19: Experimental environment.

Table 3.1: Specifications of the IEEE-1394a digital camera

Type	Dragonfly2-HIBW
Maker	Point Grey Research Inc.
Sensor	Sony 1/3" progressive scan CCDs, BW
Resolution	640 × 480
Frame Rate	10 fps
Interface	6-pin IEEE-1394a 400Mb/s interface
Pixel size	4.65 μm square pixel

Table 3.2: Threshold in the initialization and line detection

th_1	th_2	th_3	th_4	th_5
50	50	2 pixels	1°	3 pixels.

the initialization of landmarks (section 3.2.2) and the line detection (section 3.2.3), the thresholds th_1-th_5 are set by experience based on the environment, as shown in Table 3.2.

3.3.3 Result and Discussion

Total 420 frames had been captured in this experiment. Ten camera positions were measured using MAMS (It is impossible to measure the groud true data of all frames). The frame number between two adjacent measured positions was about 40. The distance between two adjacent sample positions is about 1 m.

Processing Speed

The average processing time of one frame is shown as Table 3.3. Because the proposed method for solving P3L problem can be executed in maximum four threads, the speed is faster than the existing method([13]), therefore the efficient is improved because the pose estimation is the step which consumes the most processing time. The average running speed of this method is about 10.4 frames per second in the main thread. The average cost of executing bundle adjustment once in the parallel thread is about 10 seconds. That speed is sufficient to support some field work in NPP, such as indicating the state of some equipment, or navigating the moving direction of workers.

The processing time at every frame are almost same except the time of the pose estimation, because it depends on the number of the detected landmarks and the solvable equation numbers (0,2 or 4). Fig.3.20 shows the processing time of pose estimation at every

Table 3.3: Average processing time of one frame (ms)

Process	time
Step 3-1	2.3
Step 3-2	2.2
Step 3-3	1.9
Step 3-4	3.0
line matching	19.4
Pose estimation	38.6 | 79.6([13])
New landmarks registration	28.4
Total	95.8 | 136.8

frame.

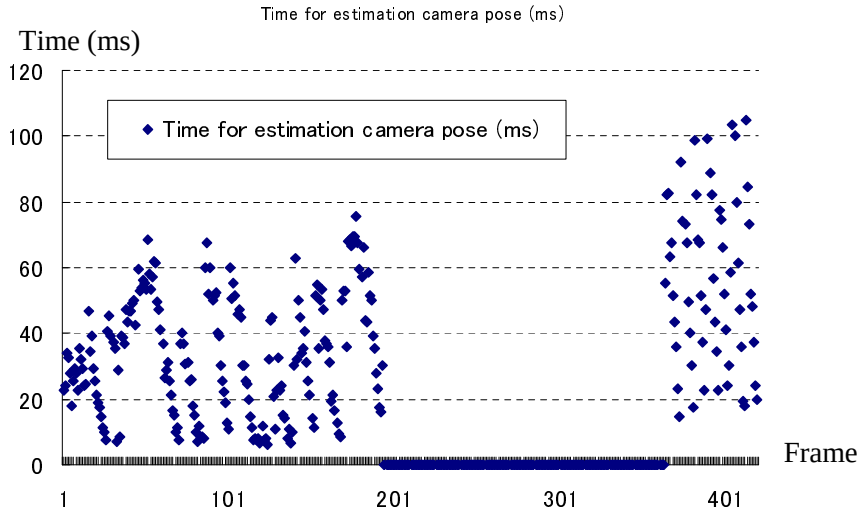

Fig. 3.20: Processing time of pose estimation.

Accuracy

The position and orientation errors of the camere pose estimation on the ten sample position is shown as Table 3.4. The error increases over time, but the error is small enough (¡60 mm) when tracking time is short using the line-based tracking method. That means the tracking cannot be applied as a primer tracking method, but by combining with the marker tracking method, it can be applied as an assistant tracking method, and reduce the needed marker number at the cases which requires lower accuracy and stability, for example, indicate the positions of some large component.

Table 3.4: Errors of the pose estimation

No.	1	2	3	4	5	6	7	8	9	10
Position error (mm)	20.1	55.3	160.4	70.5	/	/	/	/	180.0	144.7
Orientation error (degree)	5.1	7.6	13.7	10.2	/	/	/	/	15.3	13.2

Fig.3.21 shows the estimated trajectory of the camera movement. The black curve is a smooth connection of the ground true data measured using MAMS at 10 sample positions. Blue points show the estimated positions of a camera without using bundle adjustment. Red points show results with bundle adjustment. The tracking accuracy is improved when using bundle adjustment. The maximum error (the difference between estimated position and measured position of camera) is about 160 mm with bundle adjustment, and average error is about 100 mm. From 160th frame to the last frame, most of the initial landmarks (> 4) are almost not detectable. The tracking failed from the 195th frame because insufficient 2D line features were matched with 3D landmarks, and relocalization succeeded from the 364th frame. The average speed of relocalization is about 5 fps. Purple points show estimated results after relocalization when tracking failures occurred. Furthermore, green points are corresponding results obtained with bundle adjustment. In this case, the accuracy is improved when using bundle adjustment. The average error is about 150 mm after tracking fails, with matching with key frames. From Fig.3.21, it is inferred that when the tracking was successful, the estimated result was stable and accurate in short distance tracking. Camera relocalization was executed effectively.

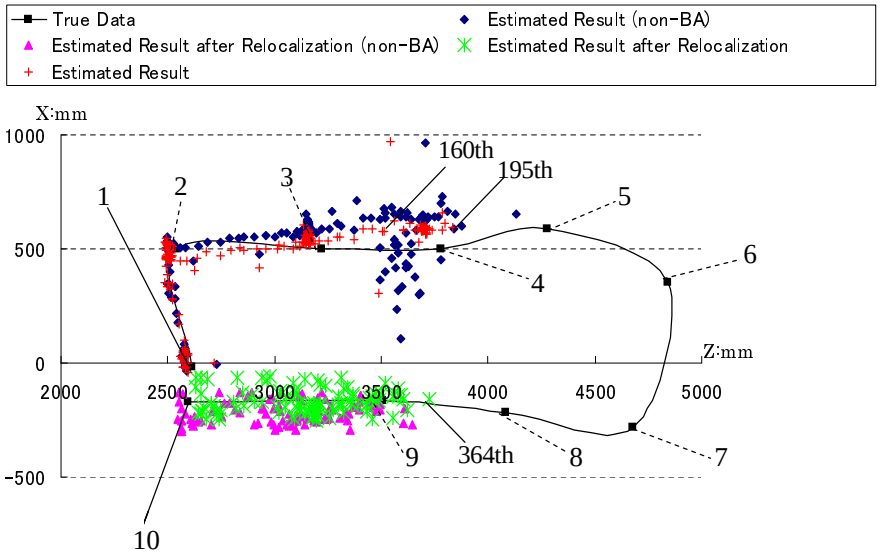

Fig. 3.21: Estimated trajectory of the camera (XZ-plane).

The result of accuracy shows that the line-based tracking is accurate enough (error ¡ 0.1 m) when the movement distance of the workers is smaller than 1 m. Therefore, the line based tracking method can be combined with the marker tracking to reduce the marker number as the following steps:

1. Paste multiple markers for tracking in the environment.
2. Capture enough markers as initial markers for tracking on the image.
3. Move the camera, until the movement distance is about 1 m.
4. Remove the markers which had been captured by the camera except the initial markers.
5. Repeat the above steps on other position until the markers cannot be reduced again.

3.4 Summary

As described in this chapter, a line-feature-based tracking method that can estimate the position and orientation of users was proposed using only a monocular camera. A RANSAC-based method for solving P3L problem in multiple threads to calculate the camera pose from correspondence lines and a geometry method to added new landmarks were applied in this method. Eight landmarks from rectangle markers were used in initial frames. This method is applied in an NPP. The result of the evaluation experiment shows that estimated results are accurate in short distance tracking. The average error of the camera position is about 100 mm. In some cases of field work in an NPP, such as the dismantling of large equipment, the accuracy of the proposed method is sufficient to apply AR for supporting field work. In some cases that require higher accuracy, such as the maintenance of small equipment, the accuracy must be improved.

In future work, firstly, the actual combination between the marker-based tracking and the line-based tracking will be realized to reduce the necessary marker number. Then the stability of line detection and the matching algorithm must be improved to make it feasible in some more complex environments. Moreover, an evaluation experiment of long-distance tracking in an NPP environment will be conducted.

Reference

[1] V. Lepetit, L.Vacchetti, D.Thalmann, P. Fua: Fully Automated and Stable Registration for Augmented Reality Applications, *Proceedings of 2nd IEEE/ACM International Symposium on Augmented Reality*, pp. 93-102, 2003.

[2] I. Skrypnyk, D. Lowe: Scene Modeling, Recognition and Tracking with Invariant Image Features, *Proceedings of 3rd IEEE/ACM International Symposium on Mixed and Augmented Reality*, pp. 110-119, 2004.

[3] J. Platonov, H. Heibel, P. Meier, B. Grollmann: A Mobile Markerless AR System for Maintenance and Rrepair, *Proceedings of 3rd IEEE/ACM International Symposium on Mixed and Augmented Reality*, pp. 105-108, 2006.

[4] M. Bosse, R. Rikoski, J. Leonard, S. Teller: Vanishing Points and 3d Lines from Omnidirectional Video, *Proceedings of IEEE International Conference on Image*, pp. 523-516, 2002.

[5] M.N. Dailey, M. Parnichkun: Landmark-based Simultaneous Localization and Mapping with Stereo Vision, *Proceedings of Asian Conference on Industrial Automation and Robotics*, pp. 108-113, 2005.

[6] E. Eade, T. Drummond: Edge Landmarks in Monocular SLAM, *Proceedings of 17th British Machine Vision Conference*, pp. 588-596, 2009.

[7] J. Zhang, D. Song: Error Aware Monocular Visual Odometry Using Vertical Line Pairs for Small Robots in Urban Areas, *Special Track on Physically Ground AI, 24th AAAI Conference on Artificial Intelligence*, 2010.

[8] J. Sola, T. Vidal-calleja, M. Devy: Undelayed Initialization of Line Segments in Monocular SLAM, *Proceedings of IEEE/RSJ International Conference on Intelligent Robots and Systems*, pp. 1553-1558, 2009.

[9] L. Zhang, R. Koch: Hand-held Monocular SLAM Based on Line Segments, *Proceedings of Irish Machine Vision and Image Processing*, pp. 7-14, 2011.

[10] T. Lemaire, S. Lacroix: Monocular-vision Based Slam using Line Segments, *Proceedings of IEEE International Conference on Robotics and Automation*, pp. 2791-2796, 2007.

[11] G. Zhang, I. Sun: Building a Partial 3D Line-based Map, *Proceedings of IEEE International Conference on Robotics and Automation*, pp. 1497-1502, 2011.

[12] H. Chen: Pose Determination from Line-to-plane Correspondences: Existence Condition and Closed-form Solutions, *IEEE Transactions on Pattern Analysis and Machine Intelligence*, Vol.13, No.6, pp. 530-541, 1991.

[13] M. Dhome, M. Richetin, J. Lapreste, G. Rives: Determination of the Attitude of 3D Objects from a Single Perspective View, *IEEE Transactions on Pattern Analysis and Machine Intelligence*, Vol.11, No.12, pp. 1265-1278, 1989.

[14] B. Triggs, P. McLauchlan, R. Hartley, A. Fitzgibbon: Bundle Adjustment - a Modern Synthesis, *Proceedings of the International Workshop on Vision Algorithms: Theory and Practice*, pp. 298-372, 1999.

[15] T. Lindeberg: Edge Detection and Ridge Detection with Automatic Scale Selection, *Proc. IEEE Computer Society Conference on Computer Vision and Pattern Recognition*, pp. 456-470, 1996.

[16] Y. Choi, T. Lee, S. Oh: A Line Feature Based Slam with Low Grade Range Sensors Using Geometric Constraints and Active Exploration for Mobile Robot, *Autonomous Robot*, Vol.24, No.1, pp. 13-27, 2008.

[17] H.P. Liu, S.D. Zhu, X.D. Wang, H.X. Wang: Research on Matching of the Remote Sensing Image Matching Based on Histogram Invariant Moments and Genetic Algorithms, *IEEE International Conference on Information Engineering and Computer Science*, pp. 1-4, 2009.

[18] B. Williams, P. Smith, I. Reid: Automatic Relocalisation for a Single-camera Simultaneous Localisation and Mapping System, *IEEE International Conference on Robotics and Automation*, pp. 2784-2790, 2007.

[19] M. Hohmeyer, S. Teller: Determining the Lines through Four Lines, *Journal of Graphics Tools*, Vol.3, No.4, pp. 11-22, 1999.

[20] J. More: The Levenberg-Marquardt Algorithm: Implementation and Theory, *Numerical Analysis*, Vol.630, No.1, pp. 105-116, 1978.

[21] M.I.A. Lourakis, A.A. Argyros: SBA: a Software Package for Generic Sparse Bundle Adjustment, *ACM Transactions on Mathematical Software*, Vol.36, No.1, pp. 1-30, 2009.

Chapter 4 Development of Temporary Placement and Conveyance Operation Simulation System

4.1 Introduction

The objective of this study is to evaluate the feasibility of AR system in an NPP. There are many tasks can be supported by AR system. In this study, the dismantling work is chosen as the support target for the feasibility evaluation. As described in chapter 1, in the immediate dismantling, the components in every part of an NPP must be dismantled one by one according to a planned dismantling procedure. In some cases, large components that are dismantled from their original locations must be cut into small pieces after they are carried to workspaces. Then the small pieces are transported to some other locations for temporary placement before their radioactivity level is checked. In an NPP, passages used for component transportation are invariably narrow, and space for the dismantling work and temporary placement is limited. Consequently, large dismantled components might collide with other components in such environments during temporary placement and conveyance operations. It is important to verify whether the space is sufficient for transporting the large components, whether the workspace is sufficient for disassembling work, and whether the space designated for temporary placement is sufficient. Because AR has two advantages: (1) it can display virtual objects at the correct position where it is excepted to be, and (2) it is more intuitive than using a legacy interface in some operation tasks, an AR supporting system is helpful to the verification by adding the virtual large components in the real environment to simulate the transportation and disassembling work.

Fugen has been developing a decommissioning engineering support system (DEXUS)[1] for support in planning the dismantling procedures using virtual reality (VR) based on a 3D computer aided design (CAD) database. This system can detect the collision between dismantled components and the around environment in a complete virtual environment. However, VR is not appropriate for supporting field work in the NPP environment, because existing 3D CAD database always includes only main components, and it is difficult to be updated. Therefore, in the virtual world, it is difficult for users to find the corresponding collision position in the real world, because many details of current environment are not represented in the existing 3d models. In fact, AR is a technology that can present the 3D position and orientation intuitively in a real environment. It can show the collision position in the actual work field so that the workers can easily refer to the collision position in actual

operation. In recent years, AR has become widely attempted for support of field work at NPPs. In the study[2], AR was applied to realize dose-rate visualization. By referring to the visualization, workers can avoid to enter dangerous regions by displaying the 3D radiation map of the environment in an NPP. In another study[3], AR was applied in a NPP dismantling supporting system. The system shows a dismantling target and whether it should be cut or not. Moreover, users can record their work progress by comparing differences between the virtual model and the real environment using the system.

The 3D models of dismantling target and work environment is necessary to simulate temporary placement and conveyance operations. Such 3D models are widely used for spatial verification. A discrepancy check is realized by comparing the 3D model of a target obtained from planned documentation and the real target to find their difference[4][5]. In the study[4], the discrepancy check is performed offline by superimposing the 3D model of a factory on images and comparing the difference between the 3D model and the images. In the study[5], the 3D model of a designed building is superimposed on the real building to find their difference in the actual field. However, the comparison is based on human subjectivity. Moreover, the 3D models of studies described above are obtained from existing CAD models. Because of the frequent renewal of the environment in NPPs, CAD updates are costly and difficult because of the complicacy of the NPP environment. Existing CAD applications can not always represent the current details of the work field.

In this chapter, a temporary placement and conveyance operation simulation system (TPCOSS) was developed for supporting NPP decommissioning. It detects the collision between the virtual dismantling target and the actual environment to verify the space during the temporary placement and conveyance operation. The 3D models of environment and the dismantling target are obtainable by scanning the work field using a laser range finder. By superimposing the virtual dismantling target on an actual object, the temporary placement and conveyance operation of the virtual dismantling target can be simulated by operating the actual object. Using the 3D models, the collision between virtual dismantling targets and the actual environment can be detected and presented intuitively in real time during the temporary placement and conveyance operation simulation. The feasibility of this system includes three aspects: (1) Whether it is reliable in actual use. (2) Whether it is easy use for workers. (3) Whether it indicates information intuitively enough for workers. The developed system was evaluated in Fugen by some field workers to examine that whether it was feasible in the actual field work.

4.2 Development of TPCOSS

In the verification of the space of actual work field, virtual objects are superimposed on the worker's view as the dismantling target, and the collision between the virtual dismantling target and the environment is detected. To represent the actual volume and shape

of the dismantling target and the environment correctly, 3D models of the target and the environment are indispensable. In this study, the 3D models were obtained based on the 3D positions of the point clouds of the dismantling target and the environment, which consist of a lot of sample points located on the dismantling target and the environment. The overall system concept is shown in Fig.4.1. (A) First, the system employs a laser range scanner to scan the environment at multiple positions to obtain the 3D positions of its point clouds. (B) Then the obtained point clouds are combined into one cloud. (C) Based on the combined cloud, the polygon models (surface model which is comprised of triangular mesh) of the dismantling target and the environment are generated. The polygon models are the 3D models used in the AR system in this study. Compare with the existing CAD models, they represents the current details of the environment better because they are obtained from the current information of the environment. (D) Then a texture is pasted on the polygon model of the dismantling target to display it upon worker's view as the actual target likes. (E) Finally the polygon model of the environment and the textured model of the dismantling target are used in the simulation of the temporary placement and conveyance operation to detect the collision between the dismantling and the environment.

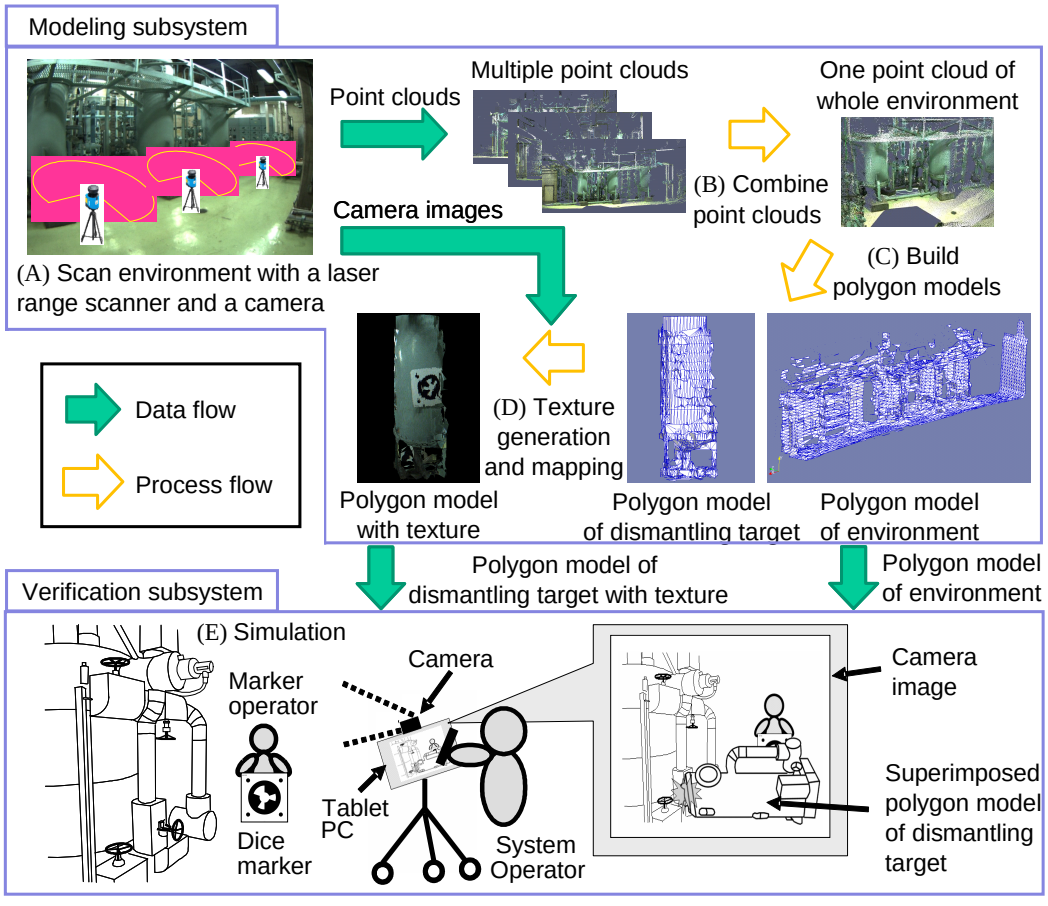

Fig. 4.1: Outline of TPCOSS.

4.2.1 System Requirements

This system was developed to support the temporary placement and conveyance operations in a work field. It makes it possible to verify whether the space of work environment is sufficient for the operation. When the operator transfers a virtual dismantling target, the location of a collision between the dismantling target and the environment is indicated intuitively if a collision occurs. For the practical use of this system in an actual work field in NPP, the Requirement A-C mentioned in chapter 1 must be satisfied. To develop TPCOSS, the following concrete requirements should be fulfilled

I The 3D model of the dismantling target must be available for reference in the work field (Requirement B).

To understand the situation of conveyance and temporary placement operation intuitively during the simulation in the work field, the virtual dismantling target must be visible in the work field. Therefore, it is necessary to superimpose the 3D model of the dismantling target on the worker's view in the work field as reference.

II The 3D model of the dismantling target must be freely movable when performing verification (Requirement B).

To simulate the conveyance and temporary placement operation, the 3D model of the dismantling target must be able to be transferred and rotated like the real dismantling target in the work field. Therefore, it must be as freely movable as the actual dismantling target.

III The collision between the dismantling target and the environment must be indicated clearly (Requirement B).

If the dismantling target collides with the environment during the simulation, then field workers must understand the collision position to avoid a similar collision during actual operation. Therefore, the collision position must be indicated clearly for intuitive understanding.

IV Operation states (3D position and orientation of the dismantling target, 3D position of collision part) must be recordable and be available for reference later as expected (Requirement B).

In some cases, for example, when the passage is very narrow, collisions often occur at some special positions in the environment. The simulation of the operation must be repeated several times in the work field to avoid the collision. Therefore, the corresponding operation state must often be referred. Furthermore, it is expected to be shown outside the work field, such as in office, so that other workers can understand where the collision occurs easily. Therefore, recording and reference functions are necessary.

V The 3D models of the dismantling target and the environment must be obtained based on the actual work field (Requirement A).

The environment often modified with the renewal of the work field. Therefore, existing 3D CAD of an NPP cannot always represent the current state of the work field. To simulate the work field operations correctly in the actual field, a 3D model that represents the current state exactly is indispensable. Therefore, a modeling function that can build models of the actual dismantling target and the environment in the work field is necessary.

VI The system must be easily installable and mobile (Requirement B).

In many cases, the work field space is narrow, and workers must move a long distance when transporting a dismantled component. Therefore the system must be as compact as possible. Moreover, it must be carried easily in the work field.

VII The system operation must be easily mastered (Requirement B).

If the system operation is overly complicated, then it would be difficult for field workers to use the system. Consequently, the operation interface of the system must be comprehensive for its acceptance by field workers.

TPCOSS was designed based on these requirements.

4.2.2 System Design

Because the 3D models must be obtained before the verification, TPCOSS is designed including two subsystems: (1) modeling subsystem for obtaining the 3D models of the dismantling target and the environment, and (2) verification subsystem for temporary placement and conveyance operation simulation. To meet the requirement VI, the two subsystems are both composed of the necessary hardwares as small-size as possible. To meet the requirement VII, the user interfaces of two subsystems are designed as comprehensive as possible.

Besides these, the modeling subsystem was designed to meet the requirement V, and the verification subsystem is designed to meet the requirement I, II, III and IV. An experiment was conducted to evaluate that whether the realized functions can meet the requirements. It will be described in later sections.

Modeling Subsystem

To meet the requirement V, the 3D models of the dismantling target and the environment must be obtained based on the actual work field. Two functions are designed following the Criterion i mentioned in chapter 1 in the modeling subsystem subsystem:

(i) Measure the 3D positions of point clouds located on the actual environment and the dismantling target. To obtain the 3D models which can represent the current state of the environment correctly, this function is necessary.

(ii) Generate 3D models from the 3D positions of the obtained point clouds. The models should be used in the verification subsystem for the simulation.

The modeling subsystem is designed as shown in Fig.4.2. To realize the function (i), a laser range scanner is applied for sampling the 3D point clouds of dismantling targets and the environment by scanning its around environment. To make the subsystem small, a small note PC is used for controlling the laser range scanner. When the laser range scanner is scanning environment, it must be fixed on a chosen position, therefore a tripod is used for fixing the laser range scanner. The 3D polygon models which are used in the verification subsystem are generated based on the point clouds. However, the polygon models can not be displayed directly because their appearances are very different from the actual dismantling target and environment for operators to understand them. Therefore, some textures are necessary to make the model more intuitive. A color camera was so employed for capturing the surface image for the texture. It was mounted on the laser scanner and its relative position and orientation to the laser range scanner were measured in advance. When a point cloud is measured using the laser scanner, the camera captures the corresponding image simultaneously, along with its position and orientation. Then every polygon of the generated model can be projected onto the corresponding image, and the color of the polygon is so obtained from its corresponding image. By painting the color on the polygon, the texture is obtained.

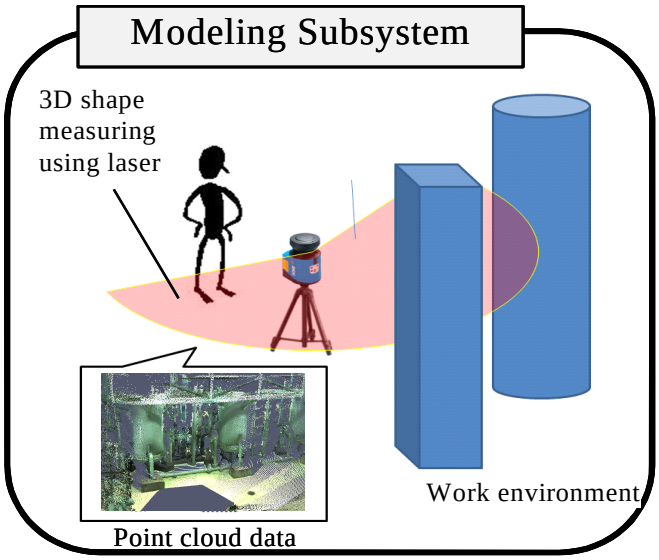

Fig. 4.2: 3D measurement of the modeling subsystem.

One measurement by the laser range scanner obtains a point cloud located on only one side of the dismantling targets and the environment. To obtain the complete model, it is indispensable to measure the point clouds at multiple positions. Each point cloud is recorded based on a local coordinate system for which the origin is the intersection of the rotation axis of the motion base when the point cloud is measured. To combine all point clouds into one cloud and build a 3D model that is useful in the verification, the coordinates of all the point clouds must be transformed into a world coordinate system. Consequently, the iterative closest point (ICP) algorithm[6], which can match two point clouds including a certain common part of the environment and can thereby obtain the transformation matrix between them, is applied to transform a point cloud (source cloud) into a world system by matching it with a target point cloud (target cloud) that is already based on a world system, as shown in Fig.4.3.

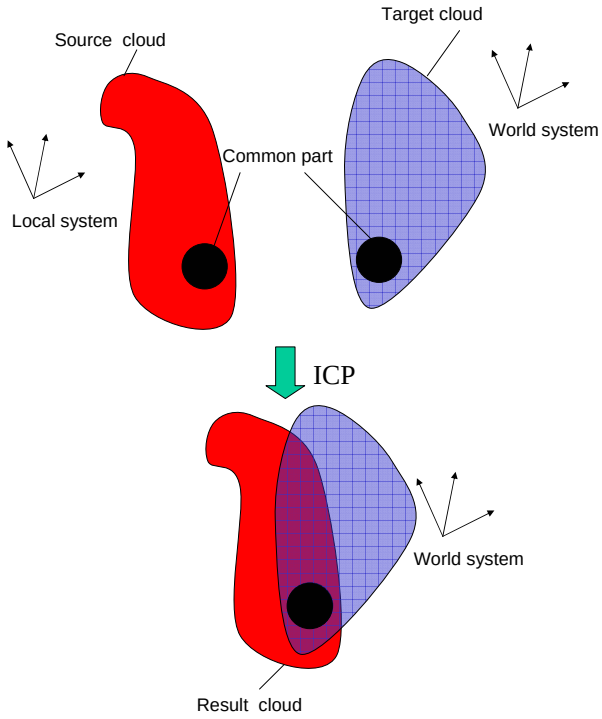

Fig. 4.3: Concept of ICP algorithm

However, ICP starts calculating from a initial guess of the transformation matrix. If the initial guess of the matrix is too far from the real value, then the algorithm might produce an incorrect result. To solve this problem, the circular marker-based camera tracking technology is applied. By capturing markers, it estimates the position and orientation of the camera mounted on the modeling subsystem based on the world coordinate system. The relative position and orientation of the camera and the laser range scanner are known. Therefore, the transformation matrix from the local system to the world system is obtainable after the position and orientation of the camera are estimated. Considering the

tracking error, the matrix is set as the initial guess in ICP instead of using it to transform the source cloud directly.

Another problem is that if the common part of environment between the source cloud and target cloud is too small compared with their respective remaining parts, the iterative result might still be wrong. Therefore, only a randomly chosen local part of the source cloud is used in ICP instead of the whole point cloud. When the chosen part is very different from the common part as shown in Fig.4.4(a), the iteration fails. On the opposite, iteration succeeds when the chosen part is one part of the common part as shown in Fig.4.4(b). (Whether the iteration result is correct or not can be examined by checking the result cloud.) A large part of a cloud is invariably measured in another cloud by the laser range scanner. If the local part of the source cloud is chosen from the area which is also measured in the target cloud, then a high probability exists that the best result is obtained using ICP.

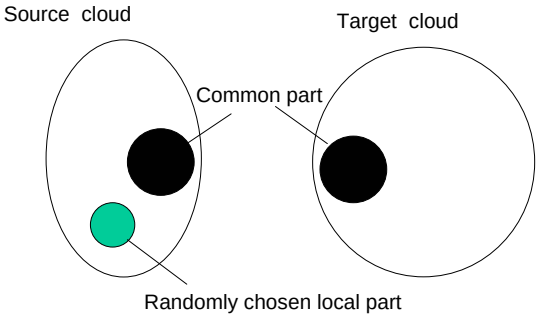

(a) Iteration fails when the chosen part is very different from the common part

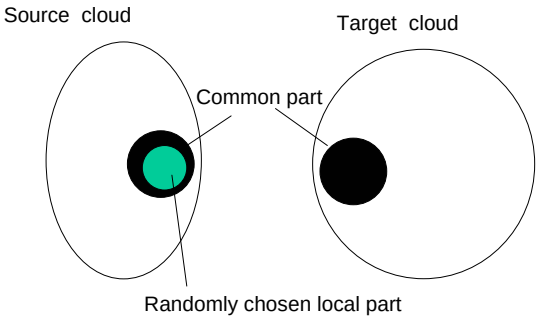

(b) Iteration succeeds when the chosen part is one part of the common part

Fig. 4.4: Realization of ICP algorithm using randomly chosen part.

The function (ii) is realized as the following steps:

Step 1-1 Smooth the obtained point clouds. Because of the measurement error by the laser range scanner, the surfaces comprised by the sample points are not smooth. It is necessary to smooth the surfaces to use these data in the ICP algorithm. The concept

of smooth is shown as Fig.4.5, the distance d between the laser range scanner and a point is corrected as d' by the adjacent 8 points of the points. (d, d_1-d_8 is measured by the laser range scanner.)

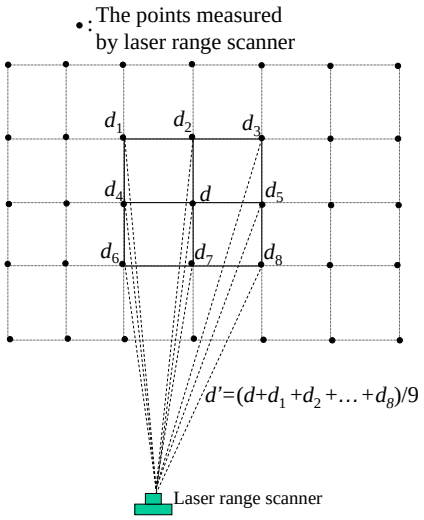

Fig. 4.5: Smoothing of a point cloud.

Step 1-2 Combine the point clouds into one cloud based on ICP algorithm.

Step 1-3 Extract the point cloud located on the dismantling target from the whole point cloud obtained in Step 1-2. It will be used to generate the 3D model of the dismantling target.

Step 1-4 Generate the 3D polygon models from the point clouds of the environment and the dismantling target respectively.

Step 1-5 Reduce the resolution of the polygon models to improve the computation speed. Because the computation cost depends on the number of the polygons.

Assuming that the target cloud is Cloud 1 and the source cloud is Cloud 2, then the Step 1-2 is actually realized as the following steps.

Step 2-1 Randomly choose a sphere with 2000 mm radius inside Cloud 2 and select the points inside the sphere. The radius is decided based on the shape of the environment and the distance between two adjacent scan positions of the laser range scanner. In this study, the distance was about 3-5 m, therefore the radius was set as 2,000 mm by experience.

Step 2-2 Match the points selected in Step 2-1 with Cloud 1 to obtain the transformation matrix of Cloud 2 using the ICP algorithm. Then transform all points of Cloud 2 into a world coordinate system.

Step 2-3 For every point of Cloud 2, find its nearest point in Cloud 1 and obtain that minimum distance between them. Count the number of points whose minimum distance is less than 50 mm (It is decided by experience based on the measurement accuracy of the laser range scanner and the distance between the laser range scanner and the measured points).

Step 2-4 Repeat from Step 2-1 to Step 2-3 for 10 iterations. Then choose the transformation matrix with the largest point number obtained in Step 2-3.

Step 2-5 Transform all points of Cloud 2 into the world coordinate system using the matrix obtained in Step 2-4.

Step 2-6 Repeat from Step 2-1 to Step 2-5 until the point number obtained in Step 2-3 does not become any larger.

Verification Subsystem

To meet the requirement I, II, III and IV, The following functions are designed following the Criterion ii-iv mentioned in chapter 1 in the verification subsystem:

(iii) The virtual model of the dismantling target can be superimposed on the camera image (Criterion iv). To understand the states of the oprations more intuitively, the virtual model of the dismantling target must be displayed as the appearance of the actual dismantling target. Using the AR technology, the function can be realized.

(iv) Users can decide whether display the virtual model of the dismantling target on the image or not (Criterion ii). To understand the environment of work field, display of the virtual model must can be canceled to check the actual environment.

(v) The virtual model of the dismantling target can be draw on the image based on the 3D position and orientation of a actual object (a dice marker in this study) (Criterion iii). To simulate the operations of dismantling work, the virtual model of the dismantling target must can be moved intuitively as the actual dismantling target. To operate the virtual model in the actual field, the 3D position and orientation of the virtual model must be input. It is most convenient to operate an actual object and obtain its 3D position and orientation as the input.

(vi) The virtual model can be moved using buttons on a interface or a stylus pen (Criterion ii, iii). In some cases, it is difficult to move the dice marker to a expected position, for example, the expected position is too high for the operator, or very small adjustment on the position and orientation of the model is expected. Considering these cases, the functions that allow the operator to move the model of the dismantling target using some buttons on the interface or using a stylus pen are designed.

(vii) The collision position between the virtual model of the dismantling target and the environment can be indicated (Criterion ii, iv). It is helpful for users to understand the collision part intuitively.

(viii) The indication of collision can be canceled (Criterion ii, iv). If the indication cannot be canceled, users would be confused by the increasing indication of collision.

(ix) The position and orientation of the virtual model of the dismantling target can be record (ii, iv). As described in Requirement IV, the operation must can be referred outside the work field. Therefore the 3D position and orientation of the virtual model is necessary for the reference.

(x) The virtual model of the dismantling target can be displayed as it was in the record (ii, iv). As described in Requirement IV, the operation must can be referred outside the work field. The display of the virtual model as the record make it intuitive to understand the operation state of the record.

4.2.3 Implementation of TPCOSS

Modeling Subsystem

Regarding hardware specifications, the laser range scanner in this system is a kind of line scanner that measures 3D positions of points that are located in a 2D plane of environment. Therefore, it was mounted on a motion base that is fixed on a tripod. By rotating the motion base, it can measure the 3D positions of point clouds of the whole surrounding environment. The hardware of the modeling subsystem is depicted in Fig.4.6. It comprises a laser range scanner, a color camera, and a motion base. Their specifications are shown in Table 4.1. The maximum error of the measured points depends on the distance between the laser range scanner and the measured points. In this study, most points are measured in a distance that is smaller than 5 m. In this case, the maximum error is about 40 mm. Comparing with the actual size of the dismantling target (about 1 m $\times$ 1 m $\times$ 3 m in this study), it is extremely small, so it only slightly affects the simulation of temporary placement and conveyance operation in the work field.

In some cases, if the tracking error is too large, alternatively if the camera cannot capture or recognize any marker, then it is difficult to obtain the initial guess of the transformation matrix for ICP. For that reason, it is necessary to set the initial guess manually to run the ICP through a software interface developed for combining the point clouds and for producing surface models. The software interface is depicted in Fig.4.7. Using the interface, a source cloud represented by its local coordinate system and a target cloud represented by the world coordinate system are input, and they are combined manually into one cloud presented by the world coordinate system. In the interface, the target cloud and source cloud can be chosen in panel (1). In addition, (2), (4), (5), (6), and (7) show buttons

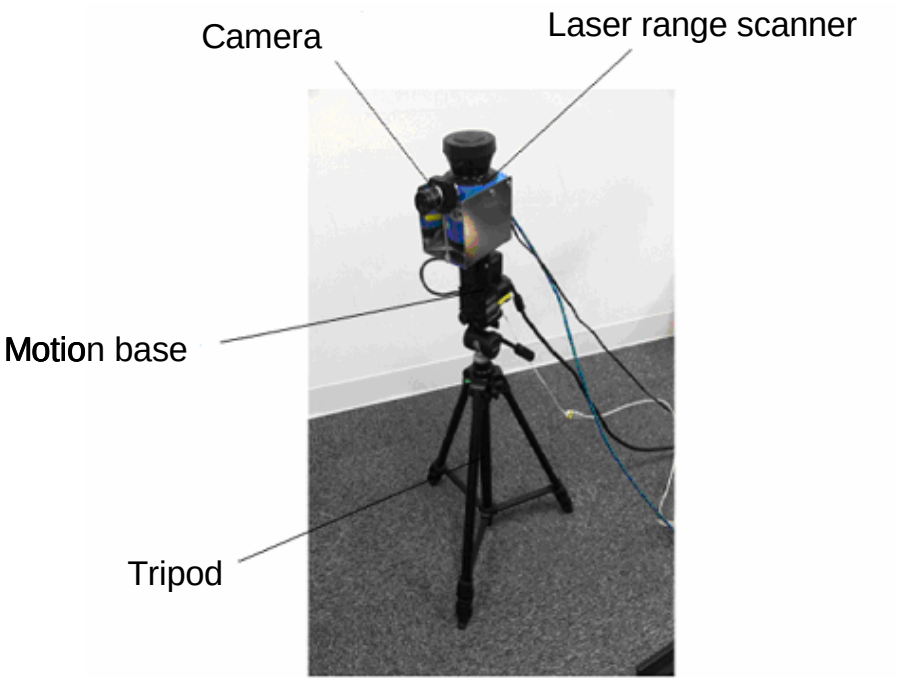

Fig. 4.6: Appearance of the modeling subsystem.

Table 4.1: Hardware specifications for the modeling subsystem

Laser range scanner	Vendor	SICK Inc.
	Model	LMS100-1000
	Scan angle	270 °
	Angular res.	0.25 °
	Max. error	40 mm
Motion base	Vendor	FLIR Systems Inc.
	Model	PTU-D46-70
	Angular res.	0.013 °
Camera	Vendor	Point Grey Research Inc.
	Model	CMLN-13S2C-CS
	Resolution	1280 × 960
	Focal length	4.15 mm

which allow the operator to run the ICP manually. The two buttons of (2) are used to control and view the position and orientation of the source cloud. Here the initial guess of transformation matrix can be set manually by controlling the source cloud. ICP is applied using button (5). Buttons (4), (6), and (7) are used, respectively, for counting the matched points, saving the transformed cloud, and saving the transformation matrix. Panel (8) shows the 3D displaying panel of the point clouds. Panel (3) is the button panel used for making surface polygon models from a point cloud.

After all measured point clouds are combined into one cloud based on world coordinates, a certain part of the cloud that is necessary for making the models of the dismantling target and the environment is chosen manually in the panel. Then the quadric clustering algorithm[7] is applied to generate the polygon models from the the points located on the chosen part. The resolution of a model needed for a dismantling work depends on the work field conditions. For example, a narrow passage for conveying the dismantling target requires high resolution of the polygon model of the dismantling target. In the quadric clustering algorithm, the polygon model resolution can be adjusted. At the cases which require high accuracy, the resolution can be increased. (But the frame rate of refreshed image will become lower, because the model with higher resolution includes more point data.) After generating the polygon models, a texture is generated from the color information of the polygon. It is used to cover the polygon model to enable more intuitive understanding of the model. The surface polygon models are depicted in Fig.4.8.

The application described above was developed using Visual Studio 2008 C++ (Microsoft Corp.) Both the rendering of 3D model and the realization of ICP algorithm was based on the Visualization Tool Kit Library[8].

Verification Subsystem

The verification subsystem is applied for simulating the temporary placement and conveyance operation in the actual work field. Its outline is depicted in Fig.4.9. The subsystem comprises a dice marker (actual object), a tablet PC (display device) and a camera fixed on the PC. The tablet PC was chosen as the display device because it is the best choice for this study. Display devices of various kinds are available for AR. The three main kinds are projection, head mounted, and handheld systems. In the temporary placement and conveyance operation, the system operator must move the display device in a large area of the work field. The projection display projects images onto an actual object using projectors. The projector is too heavy to be moved frequently with users. If it is fixed at a certain position, then the area of superimposed images is too small, so multiple projectors are needed in a large area of the work field, which increases the overall cost of the devices. Therefore, the projection display is not a good choice. The head-mounted display is also not a good choice. Its view angle is too small. Therefore, it is dangerous for operators to move themselves in the work field while many obstacles always exist in NPP. Compared

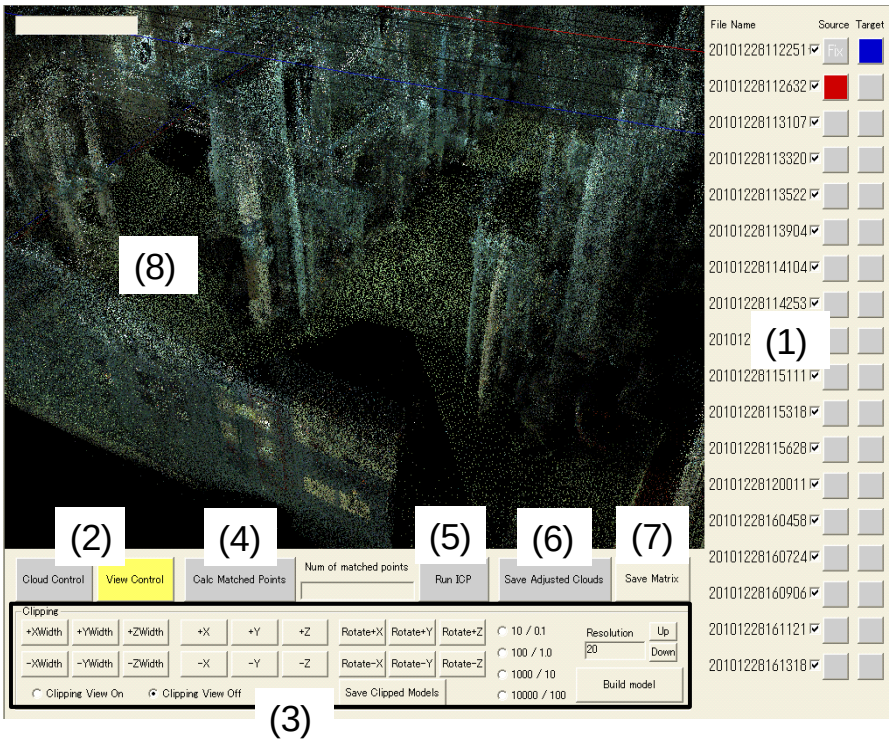

Fig. 4.7: Interface for producing a surface model.

with those systems, the handheld display presents some advantages. It does not disturb the worker's view. In addition, the displayed information related to it can be shared with other workers. Therefore, as one kind of handheld display, tablet PC was chosen for this study.

To simulate operations in the work field, a dice maker was used in this study as the actual object to operate the virtual model. Therefore, two operators are needed to use the verification subsystem. One is a system operator who performs verification through the camera and the PC. The other moves the dice marker following instructions from the system operator. The 3D model of the dismantling target can be superimposed on the dice marker if the dice marker is captured by the camera. The position and orientation of the superimposed model is changed following the movement of the dice marker. Using the camera tracking technology, the position and orientation of the camera are estimated in real time by capturing the markers pasted in the environment in advance. The relative position and orientation between the dice marker and the camera can also be calculated when the dice marker is captured by the camera. Consequently, the position and orientation of the dice marker, or in other words, the position and orientation of the virtual dismantling target, are also obtained. Referring to the 3D model of the environment obtained using the modeling subsystem, the collision position between the virtual dismantling target and real environment can be detected if the collision occurs. Then it is indicated on the tablet

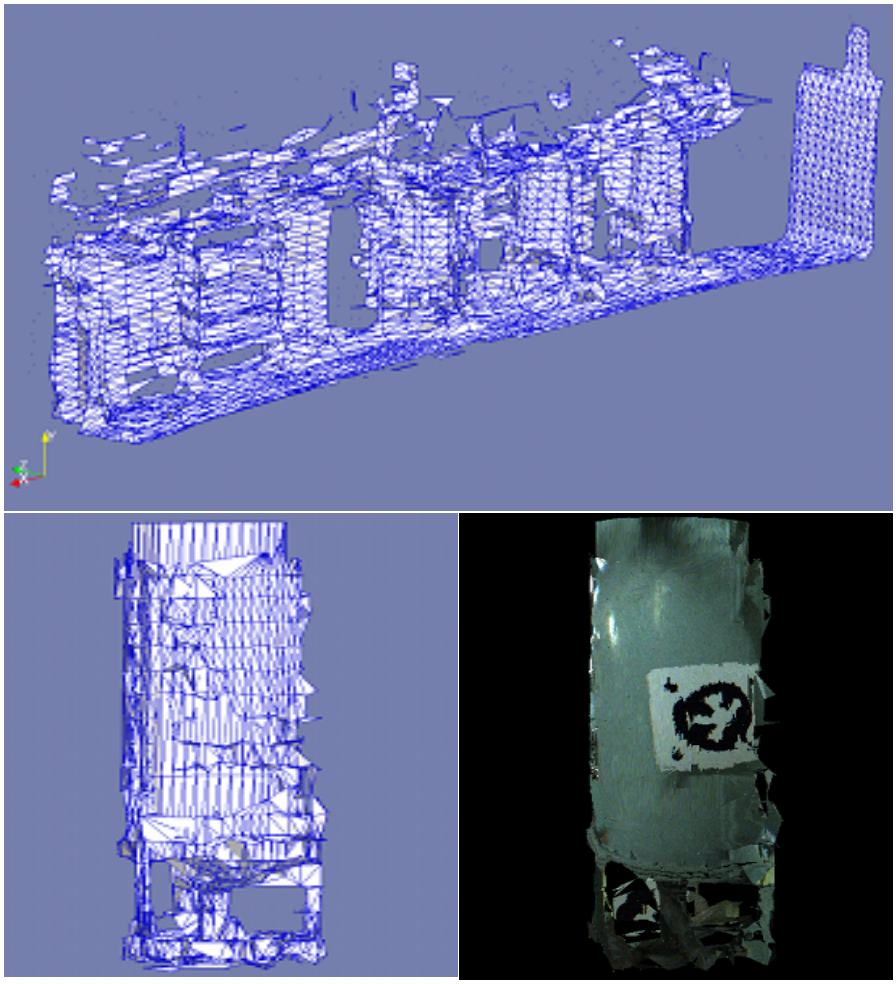

Fig. 4.8: Surface polygon models of the environment (top) and dismantling target (bottom).

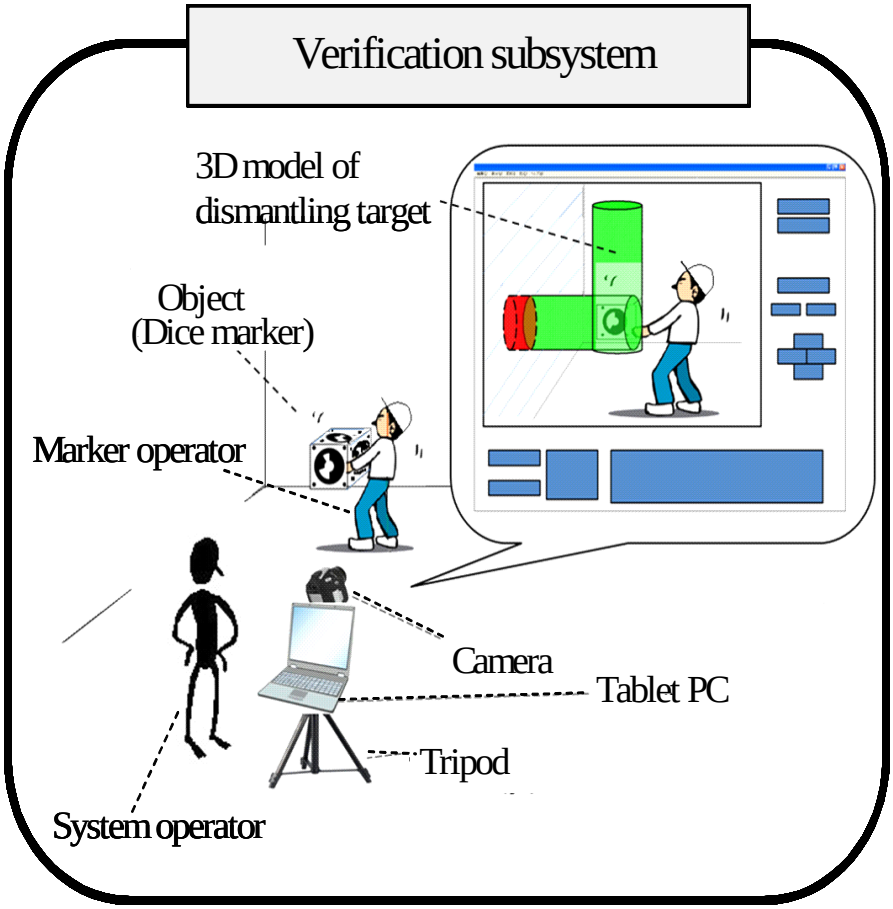

Fig. 4.9: Outline of the verification subsystem.

PC, as depicted in Fig.4.10. First, the polygon of the environment is invisible, and the dismantling target is visible with its texture. When the collision occurs, the polygons of the environment touching with the dismantling target become visible as painted red. The polygons of the dismantling target contacting the environment are painted yellow.

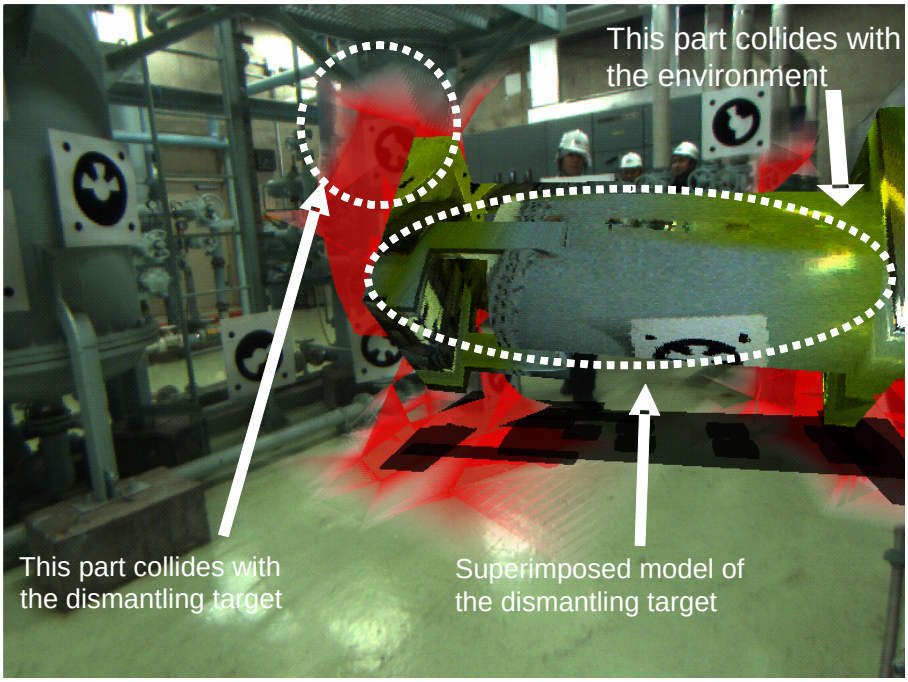

Fig. 4.10: Visualization of collided part.

In this study, to keep capturing enough markers for tracking and the operation state in the work field, a camera with a wide view angle is necessary. Therefore, a camera with a short focal length is chosen for use in this subsystem. The hardware specifications of the subsystem are shown in Table 4.2. The tablet PC is also a little too heavy to move. It is therefore mounted on a tripod. Using the screw knob of the tripod, the tablet PC can be rotated easily. Furthermore, using the caster fixed under the tripod, the tablet PC can be moved easily. The subsystem hardware is depicted in Fig.4.11.

The operation interface of the verification subsystem is designed to fulfill requirements I-IV, as presented in Fig.4.12. The buttons in panel (2) are designed to translate or rotate the model of the dismantling target. Using these buttons, the dismantling target can be moved independently of the dice marker. Moreover, a stylus pen is available to move the model by touching and dragging the dismantling target on the superimposed image directly. However, it would lose the original relative position and orientation between the dismantling target and the dice marker. Therefore, the position and orientation of the model can also be reset based on the captured dice marker by pressing a reset button in (2). Some other functions are also designed for the requirements. Corresponding to requirement

Table 4.2: Hardware specifications for the verification subsystem

Tablet PC	Vendor	Panasonic Corp.
	Model	CF-C1AEAADR
	CPU	Core i5-520M
	GPU	Intel HD Graphics
	Memory	1 GB
Camera	Vendor	Point Grey Research Inc.
	Model	CMLN-13S2C-CS
	Resolution	1280 × 960
	Focal length	3.12 mm

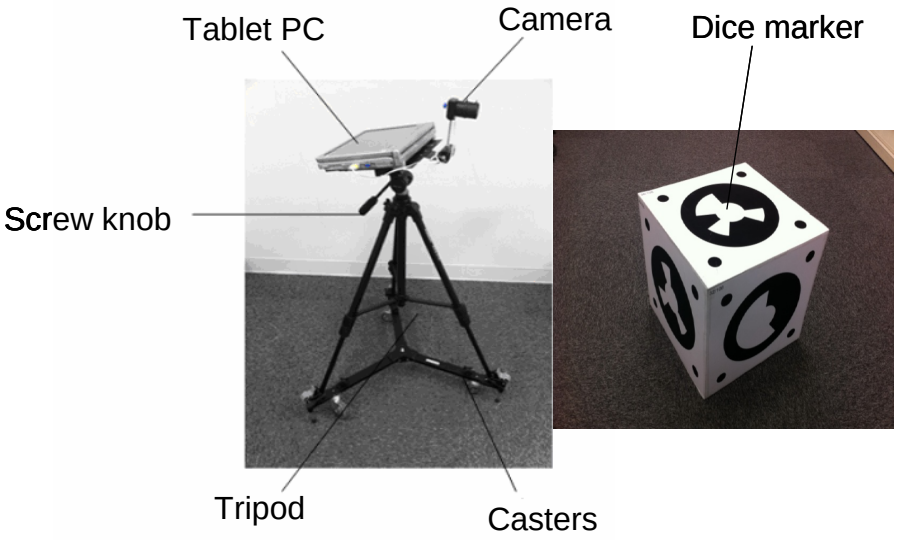

Fig. 4.11: Appearance of verification subsystem.

I, the buttons in panel (1) are designed to switch the visualization of models. Here the operator can render the model of the dismantling target visible or invisible, and cancel the color, which indicates the collided position. These two functions are necessary because the operator must know the situation behind the virtual model which will be blocked by the model when it is visible, and overly numerous indicator colors on the image might confuse the operator. Corresponding to requirement IV, panel (3) is designed to record and refer the position and orientation of the dismantling target. The corresponding superimposed image is also recorded and displayed in panel (4). Corresponding to requirement III, the superimposed imaged is displayed in panel (5) in real time.

The application was developed using Visual Studio 2008 C ++ (Microsoft Corp.). It is realized by multiple threads to increase the processing speed. The main thread is for the tracking and AR display. Another thread is used for the collision detection between the 3D models of the dismantling target and environment, as realized based on the Bullet Physics Library[9]. By displaying the virtual 3D model of the dismantling target and indicating the collision position, the frame rate of refreshed image is about 5-10 frames per second (fps). It depends on the complicacy of the dismantled target and the environment.

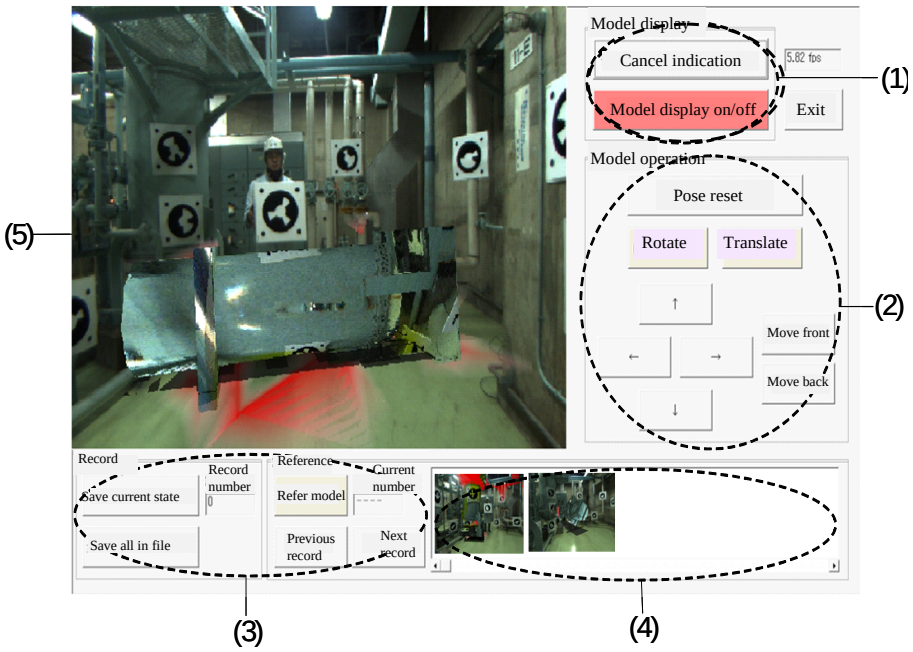

Fig. 4.12: Interface of verification subsystem.

4.3 Feasibility Evaluation of TPCOSS in an NPP Environment

4.3.1 Purpose

The developed system is anticipated for application to simulate the conveyance and temporary placement operations by field workers in an NPP. It is necessary to examine whether the system is feasible in the actual work field. The feasibility of this system includes three aspects: (1) Whether it is reliable in actual use. (2) Whether it is easy use for workers. (3) Whether it indicates information intuitively enough for workers. Therefore an experiment that evaluates the feasibility of the system and the acceptability for field workers is necessary. Some problems which might arise in practical use can also be found through the experiment. According to a pre-evaluation of the modeling subsystem, it is difficult for a beginner to combine multiple point clouds manually and to produce 3D surface polygon models using the modeling subsystem. The modeling subsystem will be improved to make it automatic to obtain the 3D surface polygon models from measured point clouds, then it will be evaluated in future studies. Therefore, although the evaluators also experienced the modeling subsystem, the emphasis of the evaluation in this study was on the verification subsystem.

4.3.2 Evaluation Method

Overview

In this study, the structured heuristic evaluation method[10] is applied in the evaluation. The method evaluates the feasibility and acceptability of the system based on the intuitive experience of the evaluators after using the system following a scenario which is decided in advance. Using the method, some problems in practical use can be identified along with some possible improvements based on advice given by the evaluators.

Evaluation Environment

The evaluation experiment was performed in a pure-water chamber of Fugen. Fig.4.13 presents the appearance of the work environment in the chamber. The preparation in the work field for camera tracking is necessary before the evaluation. For this study, a circular marker with 147 mm radius was adopted for tracking. The marker was pasted on a square panel whose edge length is 405 mm. 24 square panels were pasted in the work environment in advance. Their position and orientation were measured using MAMS; then it is input into the verification subsystem for the camera tracking. The sketch map of the pasted marker in environment is depicted in Fig.4.14. Six square panels were pasted on

each side of the dice marker used in the verification subsystem, as shown in the right image of Fig.4.11. The top view on the environment is depicted in Fig.4.15, in which the large ellipse shows the position of temporary placement of the dismantling target. The arrows indicate the moving direction of the dismantling target.

Fig. 4.13: Pure-water chamber pasted with markers.

Evaluators

There were four evaluators in the evaluation. One of the evaluators (Evaluator A) is an expert of human interface, and others are field works of Fugen who are familiar with the field work in an NPP.

Evaluation Procedure

In this experiment, one evaluator was the system operator to operate the verification subsystem and instruct how to move the dice marker, whereas the experimenter was the dice marker operator who followed instructions from the system operator. Because the evaluation about the interface of TPCOSS is important in the feasibility evaluation, the four evaluators operate the system and evaluate it in order.

A tank about 1 m $\times$ 1 m $\times$ 3 m (height) was chosen as the equipment designated for dismantlement, as portrayed in Fig.4.8 (the dismantling target with texture at the bottom right image). It was assumed to be dismantled and temporarily placed; then it was transported through a passage in this experiment. Evaluators conducted the evaluation

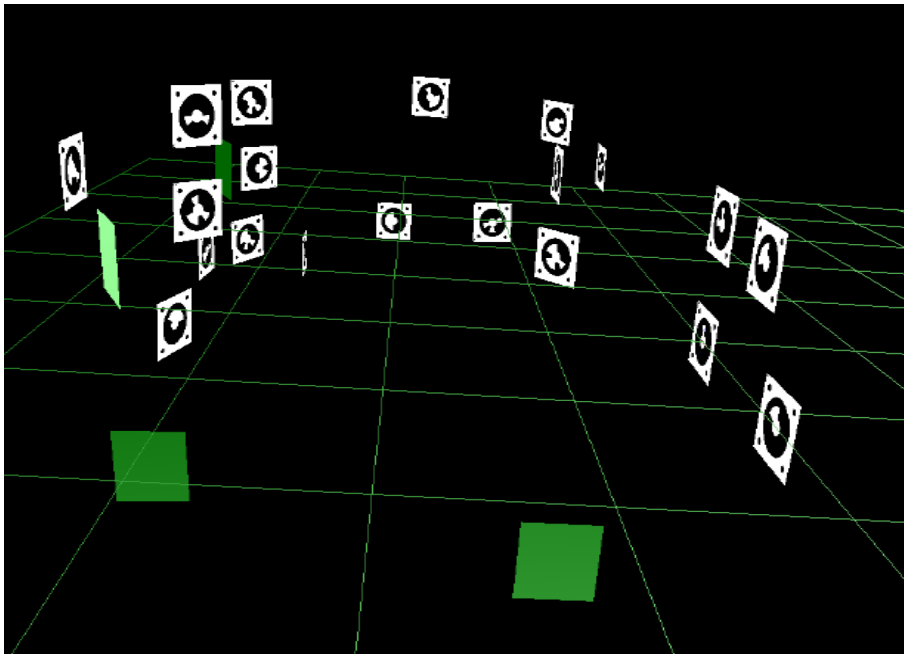

Fig. 4.14: Sketch map of the pasted markers.

by following the steps presented in Fig.4.16. First, an evaluator was explained how to use the system: about 10 minutes were necessary for the instructions. Then the evaluator respectively operated the two subsystems following the work scenario. The work scenario comprises two parts: a scanning part and verification part. In the scanning part, the evaluator used the modeling subsystem to elucidate how to obtain the 3D point cloud of environment and dismantling target. Details of the scan procedure are as described below, it took about 20 minutes.

Step 1 Following the instructions of the experimenter, the evaluator assembled the hardware (laser range scanner, motion base, tripod, and control PC) of the modeling subsystem.

Step 2 Measure the 3D point clouds of the work environment using the modeling subsystem.

Step 3 Save the measured data. Confirm the 3D surface polygon model, which would be used in the verification subsystem. Because it is difficult for a beginner to combine measured point clouds into one cloud and produce the 3D model, the 3D model in this experiment was not made from the point clouds measured by the operator, but was instead made by the experimenter in advance.

Step 4 Uninstall the subsystem as its initial state before Step 1.

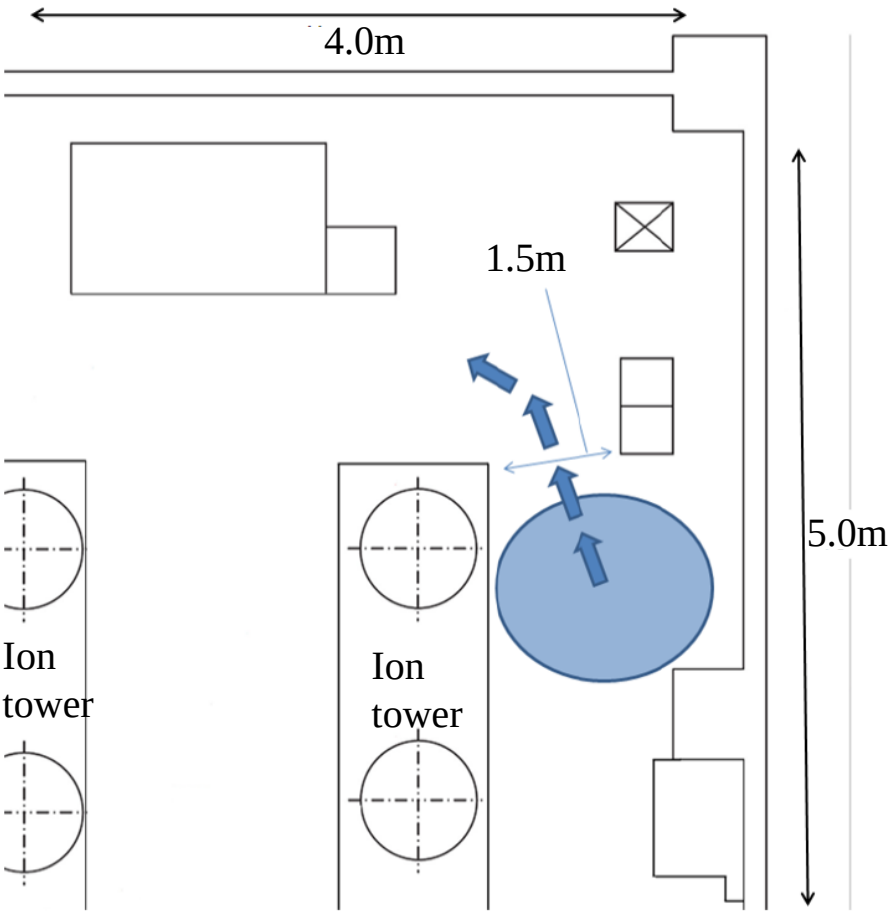

Fig. 4.15: Top view of the simulation environment.

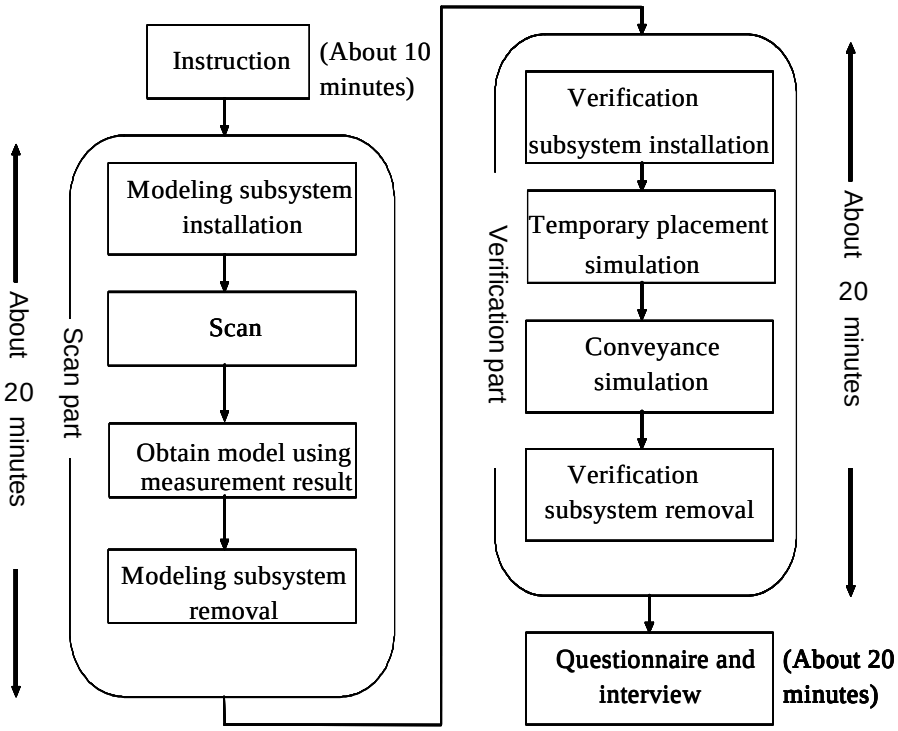

Fig. 4.16: Evaluation flow.

In the verification part, the evaluator simulated the temporary placement and conveyance operations using the 3D surface model obtained from the modeling subsystem. The dice marker was placed on ground to simulate the placement, then it was moved through a narrow passage by the dice marker operator to simulate the conveyance (Fig.4.17). The superimposed image of the temporary placement and conveyance operation simulation are depicted in Fig.4.18 and Fig.4.19, in which the dash ellipse indicates the superimposed virtual 3D model of the dismantling target. Actually, the dash ellipse does not exist in the actual image. It is superimposed only in this paper for convenience of explanation. Details of the verification part are explained below. This part took about 20 minutes.

Step 1 Following the instructions of the experimenter, the evaluator assembled the hardware (tripod, PC, camera) of the verification subsystem.

Step 2 Simulate the temporary placement operation by keeping the 3D model at a given position.

Step 3 Simulate the conveyance operation by moving the 3D model.

Step 4 Uninstall the subsystem as its initial state before Step 1.

Finally a questionnaire and an individual interview about the system feasibility and acceptability were administered by the evaluators. The evaluation items are shown in Table

4.3-Table 4.7. Because the emphasis of the evaluation was on the verification subsustem, they are decided based on the Requirement I - Requirement VII and the Function iii - Function x. It took about 20 minutes for each evaluator. After all evaluators had finished their evaluations, a group discussion was conducted between them and the experimenter.

Fig. 4.17: Conveyance operation simulation with a dice marker.

4.3.3 Result and Discussion

Corresponding to requirement I, all the evaluation items received a high rank (Rank 4 or 5), as shown in Table 4.3. Consequently, it is known to be effective to refer to the surface model of the dismantling target in the work field. However, Evaluator A found that the model was swaying slightly, even if the dice marker and camera did not move at all in some cases. That apparent motion occurred by the slight instability of the camera tracking. Although it affected the verification little in this study, it would be better to improve it in future work. Evaluator A also suggested that the superimposed dismantling target can be made transparent because the arrangement of objects behind the dismantling target is not visible when the dismantling target is superimposed. Although the function to make the dismantling target invisible is designed to solve this problem, if the transparent model will not reduce the intuitive characteristics of the system, it can be incorporated as a point of improvement in future versions.

The items corresponding to requirement II are shown in Table 4.4. Low rank (Rank

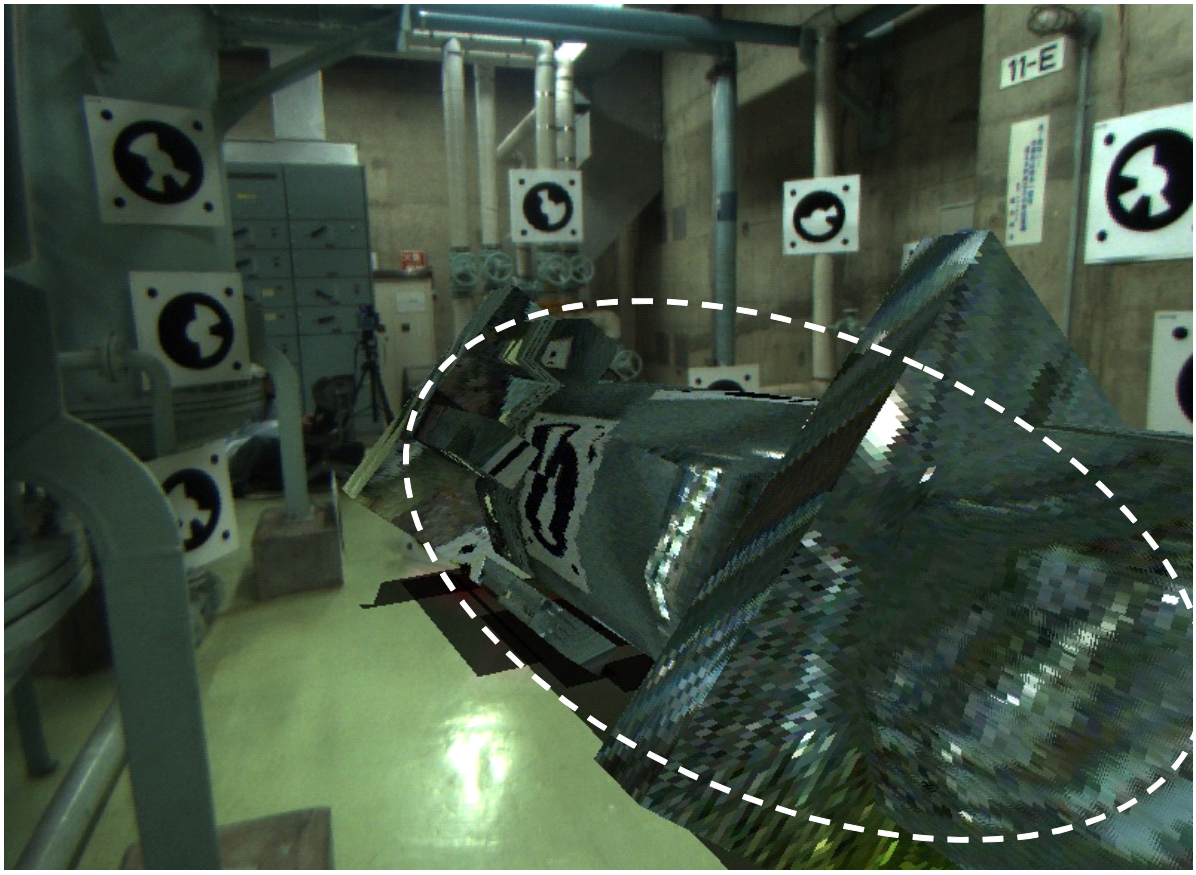

Fig. 4.18: Simulation of temporary placement.

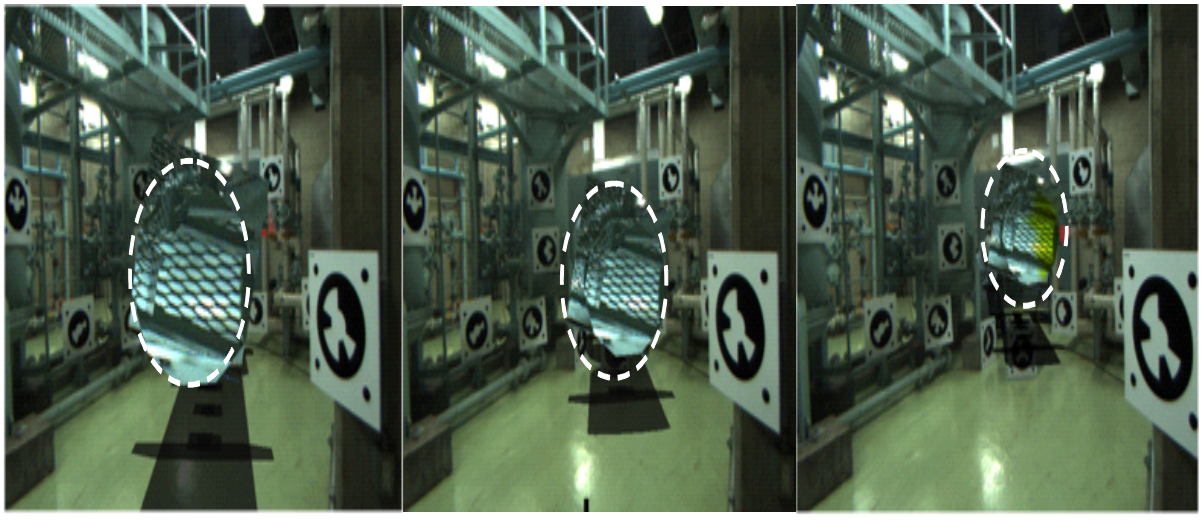

Fig. 4.19: Simulation of conveyance. (From left column to right: The dismantling target is moved far away from the evaluator.)

2 or 3) on Items No.7-No.9, which evaluate the operation method of dismantling target using the dice marker, was obtained from Evaluators A, B, and C. Evaluator A thought it was inconvenient to instruct the dice marker operator in how to move the dice marker by oral communication because of the noise in actual work field. Therefore, a set of gestures that can be understood between the dice marker operator and system operator is necessary. He also pointed out that it was difficult to move the dismantling target with a small amount of distance using the dice marker. He suggested that after moving the dismantling target to an approximate position using the dice marker, the smart movement of the dismantling target should be done using the interface. Evaluator B pointed out that the movement of the dismantling target has a slight delay after moving the dice marker in some cases. Especially, Evaluator B assigned the lowest rank to Item No.8. As the youngest of the evaluators, he might be very familiar with computers and might therefore preferred moving the dismantling target using the software interface instead of using the dice marker. Evaluator C thought that the dice marker was too large to move easily. The marker size was determined depending on the distance between the camera and marker to assure tracking stability in this study. If a tracking technology with higher stability in long distance tracking were available, then this problem could be solved. On Item No.13, Evaluator A and D assigned a low rank (Rank 3). They felt a little trouble in rotating the dismantling target using the stylus pen. Evaluator A also pointed out that the dismantling target cannot be rotated around the direction parallel with the image. On Item No.14, Evaluator B assigned Rank 3 because he thought the translation amount of the dismantling target was too small after pressing an arrow button once. That is troublesome when translation of a large distance is expected. Therefore, some function is necessary to allow the operator to adjust the translation amount as expected.

The two items corresponding to requirement III are shown in Table 4.5. Evaluator B assigned Rank 2 to Item No.17. He reported that the superimposed colors would cause confusion in the operators' view. It was better to paint color only on the dismantling target or only on the environment. Moreover, he suggested using some superimposed arrows to indicate the collision position, thereby making it possible to distinguish the current collision position from that which occurred before to make the simulation more intuitive. Therefore, a superimposing method that can realize the suggested functions without confusing operators is necessary.

Items corresponding to the requirement IV are presented in Table 4.6. They all were assigned Rank 5 except Item No.22, with Rank 4 from Evaluator D, who did not understand the referring function very well at first. Results show that the record and reference functions are effective and easy.

The items corresponding to requirements VI and VII are presented in Table 4.7. Evaluators B and C assigned Rank 3 to Item No.27. They felt it somewhat inconvenient to use the stylus pen. Evaluator B reported that the movement of the dismantling target corresponding to the slide of the stylus pen is too slow to perform the operation. Evaluator

A and B gave Rank 3 to Item No.36. Especially, Item No.32 is the only item which did not receive a Rank 5 from any evaluator. These show that the system is not understood so easily by a beginner. Evaluator D thought it was better to do training before actual operation. Evaluator C also assigned Rank 3 to Item No.31 because he reported that the buttons were small. Furthermore, some disadvantages of the system were pointed out. Evaluator A thought it was difficult to move the system using casters when the ground had some hollows. Evaluator B thought it was difficult to move the system with the tripod in some cases when the space was too narrow. Consequently, the system will be accepted easily if the user interface and the pre-instruction of how to using the system is sufficiently comprehensible. To use the system in most cases in an NPP, miniaturization of the system for its easy movement by workers is also expected.

In addition to the valuable knowledge related to the items listed above, the evaluators provided some useful comments. Evaluator C pointed out that the image is difficult to view on the Tablet PC when the environment is too bright. To solve this problem, some other display device should be prepared. For example, the HMD is useful in some cases in which an operator need not move in a large area. Therefore, the small view angle will not affect the operation. To make the simulation more intuitive and similar to actual operations, Evaluator D suggested that not only the dismantling target, but also workers and equipment such as cranes for carrying the dismantled components should be superimposed on the image when moving the dismantling target. It would be better if the distance between the environment and the moving dismantling target could be shown. Moreover, Evaluator D thought the system would be more useful if it could be used by multiple workers simultaneously. If that were possible, the situation of the operation could be shared and checked from different positions so that the efficiency and safety could be improved. This is possible using multiple systems with mutual exchange of information through a wireless network.

4.4 Summary

For the attempt of realizing an appropriate AR support system for the decommissioning work of NPP, using the developed technology in chapter 2, TPCOSS is developed in this chapter. The system includes two subsystems: a modeling subsystem for obtaining the surface polygon models of dismantling targets and environment, and a verification subsystem for simulating the temporary placement and conveyance operation. The feasibility and acceptability of this system were evaluated at Fugen by investigating whether the requirement for actual operation in the work field of NPP is satisfied by the system. As far as the evaluation result by the 4 evaluators is regarded, the following requirements are fulfilled.

(1) A 3D model of the dismantling target can be referred easily in this system. (2) A 3D model of the dismantling target can be moved freely but not easily in this system.

Table 4.3: Evaluation result of the verification subsystem (1/5)

No.	Evaluation item	Requirements and functions	Evaluation			
			A	B	C	D
1	The situation of temporary placement becomes easy to understand by superimposing the dismantling target over the camera view.	Requirement I, Function iii,iv	5	4	4	5
2	Situation of transportation becomes easy to understand by superimposing the dismantling target over the camera view.	Requirement I, Function iii,iv	5	5	4	5
3	Function is effective to make the dismantling target invisible.	Requirement I, Function iii,iv	5	5	5	5
4	Function is effective to reset the color of the dismantling target.	Requirement I, Function iii,iv	5	5	5	5
5	It is effective to make dismantling target models by measurement with the system and to use them for verification.	Requirement I, Function iii,iv	5	4	5	5
6	It is effective to verify temporary placement and transportation work by referring to the dismantling target model in the actual work environment.	Requirement I, Function iii,iv	5	4	5	5

Table 4.4: Evaluation result of the verification subsystem (2/5)

No.	Evaluation item	Requirements and functions	Evaluation			
			A	B	C	D
7	It is effective to make it possible to change the position and orientation of dismantling target by moving the dice marker.	Requirement II, Function v,vi	4	4	4	5
8	It is easy to translate the dismantling target using the dice marker.	Requirement II, Function v,vi	4	2	3	5
9	It is easy to rotate the dismantling target using the dice marker.	Requirement II, Function v,vi	2	4	3	5
10	It is effective to translate the dismantling target using a stylus pen.	Requirement II, Function v,vi	5	4	5	5
11	It is effective to rotate the dismantling target using a stylus pen.	Requirement II, Function v,vi	5	4	5	5
12	It is easy to translate the dismantling target using a stylus pen.	Requirement II, Function v,vi	5	4	5	5
13	It is easy to rotate the dismantling target using a stylus pen.	Requirement II, Function v,vi	3	5	5	3
14	It is effective to translate the dismantling target using the buttons. ($\rightarrow$, $\leftarrow$, $\uparrow$, $\downarrow$)	Requirement II, Function v,vi	5	3	4	5
15	It is easy to translate the dismantling target using the buttons. ($\rightarrow$, $\leftarrow$, $\uparrow$, $\downarrow$)	Requirement II, Function v,vi	5	4	5	5
16	It is effective to set the position and orientation of the dismantling target at its initial position using the button.	Requirement II, Function v,vi	4	5	5	5

Table 4.5: Evaluation result of the verification subsystem (3/5)

No.	Evaluation item	Requirements and functions	Evaluation			
			A	B	C	D
17	It is easy to recognize the collided position on the dismantling target by making the collided position yellow.	Requirement III, Function vii,viii	4	2	5	4
18	It is easy to recognize the collided position in the work environment by making the collided position red.	Requirement III, Function vii,viii	5	4	5	5

Table 4.6: Evaluation result of the verification subsystem (4/5)

No.	Evaluation item	Requirement and functions	Evaluation			
			A	B	C	D
19	It is effective to record the position and orientation of the dismantling target.	Requirement IV, Function ix,x	5	5	5	5
20	It is easy to record the position and orientation of the dismantling target.	Requirement IV, Function ix,x	5	5	5	5
21	It is effective to refer to the recorded position and orientation of the dismantling target visually.	Requirement IV, Function ix,x	5	5	5	5
22	It is easy to refer to the recorded position and orientation of the dismantling target visually.	Requirement IV, Function ix,x	5	5	5	4
23	It is effective to choose the recorded capture images using the buttons.	Requirement IV, Function ix,x	5	5	5	5
24	It is easy to choose the recorded capture images using the buttons.	Requirement IV, Function ix,x	5	5	5	5

(3) Collision of positions between the dismantling target and environment is indicated intuitively. (4) The operation state (position and orientation of the dismantling target, and the corresponding superimposed image) can be recorded and referred easily. The functions are effective. (5) 3D models of the dismantling target and environment are obtainable in the work field, but it is difficult now for field workers. (6) The system is installed and moved easily, except in certain cases. (7) The system is easy for a field worker who has operation experience using the system. However, prior instruction is necessary for beginners. As far as the evaluation result by the 4 evaluators is regarded, the system is feasible for supporting the actual conveyance and temporary placement operation in a work field of an NPP, except in some cases. Such cases might be those in which the ground has hollows that complicate the passage of an item on casters, or where the work space is too narrow to move the system with a tripod. To make the system useful in more cases, system miniaturization is necessary to allow it to be moved more easily in future work. The system is accepted well by field workers after pre-instruction about the system. However, some problems remain for practical use. They must be resolved in future work. The main problems are the following.

(1) In some cases, if the dismantling target is blocked by some component, then it is difficult to measure the dismantling target using the laser range scanner. Other modeling methods should be considered in these cases. For example, a camera might be used to build the 3D model of the target from extended image sequences[11]. (2) Special skills are necessary to generate the 3D surface models in the current system. Therefore, such

Table 4.7: Evaluation result of the verification subsystem (5/5)

No.	Evaluation item	Requirements and functions	Evaluation			
			A	B	C	D
25	It is easy to set up the system.	Requirement VI	5	4	5	5
26	It is easy to remove the system.	Requirement VI	5	4	5	5
27	It is easy to operate the system using a stylus pen.	Requirement VII	5	3	3	4
28	The size of the area to display the camera image is adequate.	Requirement VII	5	3	4	5
29	The PC display size is adequate.	Requirement VII	5	5	4	5
30	The system size is adequate and it is easy to carry in.	Requirement VI	5	4	4	5
31	The button size is adequate.	Requirement VII	5	5	3	5
32	The system is useful easily even if it is the first use.	Requirement VII	4	4	4	4
33	The system response is sufficiently quick.	Requirement VII	5	4	5	5
34	It is easy to rotate the system to change your viewpoint.	Requirement VII	5	4	4	5
35	It is easy to move the system to change your viewpoint.	Requirement VII	4	5	4	5
36	I was able to use the system without feeling stress.	Requirement VII	3	3	5	4

generation is necessary to make it completely automatic in building models in future work. (3) Intuitive use of the superimposed image should be improved. The arrow to indicate the collision position, and the difference between a collided part and a touching part were suggested by the evaluators. Realization of the use without confusing the operator should be explored in future work. (4) The user interface must be improved to make it as easily comprehensible and operator-friendly as possible. (5) Making the system more useful by multiple workers simultaneously, with multiple systems and their wireless communication must be considered.

In addition to the points explained above, a tracking method with less preparation, for example, natural feature based tracking, and more compact devices such as the iPad is expected to be obtainable in the future work. Simpler operation methods of the virtual dismantling target should also be explored.

Reference

[1] Y. Iguchi, Y. Kanehira, M. Tachibana, T. Johnsen: Development of Decommissioning Engineering Support System (DEXUS) of the Fugen Nuclear Power Station, *Journal of Nuclear Science and Technology*, vol. 41, pp. 367-375, 2004.

[2] R. Vabo, L. Piotrowski, G. Rindahl: Representation of Radioisotopic Dose Rates within Nuclear Plants for Improved Radioprotection and Plant Safety, *International Journal of Nuclear Safety and Simulation*, vol. 1, pp. 127-133, 2010.

[3] H. Ishii, H. Shimoda, T. Nakai, M. Izumi, Z. Bian, Y. Morishita: Proposal and Evaluation of a Supporting Method for NPP Decommissioning Work by Augmented Reality, *12th World Multi-Conference on Systemics*, 2008.

[4] P. Georgel, P. Schroeder, S. Benhimane, S. Hinterstoisser, M. Appel, N. Navab: An Industrial Augmented Reality Solution for Discrepancy Check, *Proceedings of Sixth IEEE/ACM International Symposium on Mixed and Augmented Reality*, 2007.

[5] R. Schoenfelder, D. Schmalstieg: Augmented Reality for Industrial Building Acceptance, *Proc. IEEE Virtual Reality Conference*, 2008.

[6] P. J. Besl, N. D. McKay: A Method for Registration of 3-D Shapes, *IEEE Trans. on Pattern Analysis and Machine Intelligence*, vol. 14, pp. 239-254, 1992.

[7] P. Lindstrom: Out-of-core Simplification of Large Polygonal Models, *27th Annual Conference on Computer Graphics and Interactive Techniques*, 2000.

[8] Visualization Tool Kit, http://www.vtk.org/, November 1, 2012.

[9] Bullet Physics Library, http://bulletphysics.org/, November 1, 2012.

[10] M. Kurosu, M. Sugizaki, S. Matsuura: Structured Heuristic Evaluation, *UPA Seventh Proceedings*, 1998.

[11] P. Beardsley, P. Torr, A. Zisserman: 3D Model Acquisition from Extended Image Sequences, *Proceedings of European Conference on Computer Vision*, vol. 2, pp. 683-695, 1996.

Chapter 5 Conclusion

5.1 Summary of the Study

In the decommissioning work of an NPP, dismantled components must be transported to some other location for temporary placement before their radioactivity level is checked. Therefore, it is important to verify whether the space in a narrow passage is sufficient for transporting large components, whether the workspace is sufficient for field work, and whether the space designated for temporary placement is sufficient. To develop an AR system for supporting the verification of the NPP dismantling work, a tracking method which estimates the 3D position and orientation of the workers in real time is necessary. The marker-based tracking technology is chosen as the primer tracking method in this study. To realize the marker-based tracking method, the following problems must be solved for the practical use of the AR support system in an NPP.

Problem 1 NPP is an indoor environment with wide area. When using the marker-based tracking method, it is necessary to paste a large number of markers in advance to cover the whole tracking area, and their 3D position and orientation must be measured. It is a very heavy workload by measuring so many markers manually, and it is very difficult to avoid human error of the measurement.

Problem 2 The tracking method must applicable in both long distance tracking for supporting navigation task, and short distance tracking for supporting operation task in field work with high accuracy and stability in the wide area. The current marker-based method cannot meet this requirement by using a small number of markers.

Problem 3 In some case, it is very difficult to paste markers, for example, the space is too narrow or the position is too high. To cover the whole environment, a marker-less tracking method is also necessary as an assistant of the marker-based tracking method.

In chapter 2, a new circular marker is designed which is effective in long distance tracking in an NPP environment. Then, to solve the problem 1, MAMS is developed which can measure the 3D position and orientation of the circular markers pasted in the environment automatically with high accuracy and stability.

MAMS is composed of a camera and a laser range finder and a computer. When it starts working, the camera recognizes the pasted markers in the environment, and the relative positions and directions between them are estimated. Then the computer controls the laser

range finder to measure the markers one by one. When measuring a marker, the camera is monitoring the marker to detected the laser dot. The laser range finder is adjusted by computer to move the laser dot. When the dot is covered with the marker center, the measurement is successful. Because of the automatic, the human error is avoided. A performance experiment of MAMS was conducted in lab environment to evaluate its accuracy and stability. Result shows that the average system error is 7.6mm, and the random error is 3.5mm. Another experiment is conducted in NPP environment to evaluate its feasibility by some field workers of the NPP. Result shows that the system can largely reduce the preparatory workload of AR application in an NPP, and its installation, uninstallation and operation are easily understandable by workers through a pre-instruction about MAMS.

It is difficult for current marker-based method to solve the problem 2. Because when the camera is near with the markers, there are few markers can be detected on the image, which means there might be no enough feature points for tracking. But this problem cannot be solved by reducing the marker size because the marker recognition would become unstable when it is far from the camera. In this study, the marker design was improved by adding four additional small circles on the marker. In this case, if the distance between camera and markers are short, the projection of the marker on image is with large area, and its four small circle can be easily detected as feature points. If the distance between camera and markers are long, although the small circles are difficult to be detected, the detectable marker number becomes large. Therefore the long distance tracking is also successful. The practical use of this marker shows that it is effective in both long distance and short distance tracking.

In chapter 3, a line feature-based markerless tracking method is proposed to solve the problem 3. This method uses only two rectangle markers as initial landmark, and registers the 3D position and direction of the edge lines of the markers into database as initial data in advance. This method estimates the position and orientation of camera through registered landmarks which position and direction is known. In order to make it possible to use the tracking in a capacious space, not only initial registered landmarks, but also new landmarks are necessary to be registered into database. To add new landmarks, a line registration method is realized. The method applies RANSAC to calculated 3D position of a 2D line on image. If a new line is registered as a landmark, it will be used for tracking. When tracking, natural line features are detected from image captured by a camera. At every frame, after matching 2D lines on an image with 3D line landmarks in the environment whose position and orientation are registered in database, RANSAC-based method for solving P3L problem which is newly proposed in this study is applied to calculate the position and orientation of the camera. Then new line features are registered into the database using a triangulation method. Bundle adjustment is applied in a parallel thread to improve the accuracy of the position and direction of registered line landmarks by minimizing their total re-projection error. An evaluation experiment was conducted using an image series captured from an NPP. The result shows that the tracking frame rate is about 10.4 fps, and the average error

of camera position is about 100 mm.

In chapter 4, TPCOSS is developed to support dismantling work by simulating temporary placement and conveyance operations using AR with the circular marker-based tracking. TPCOSS includes two subsystems. The modeling subsystems employs a laser range scanner to measure the 3D information of the environment and a dismantling target to produce 3D surface polygon models. Then, the operator simulates temporary placement and conveyance operations using the verification subsystem by manipulating the obtained 3D model of the dismantling target in the work field. Referring to the obtained 3D model of the environment, the possible collisions between the dismantling target and the environment are detectable. Using AR, the collision positions are presented intuitively. After field workers evaluated TPCOSS, the result shows that it is feasible and acceptable to verify whether spaces for passage and temporary storage are sufficient for temporary placement and conveyance operations.

For the practical use of AR support system in an NPP, the future work includes the following aspects: (1) Improvement of the tracking method and AR system. (2)Expansion of the system in other field.

In chapter 2, the MAMS should be improved as following aspects:

1. Compact. Current system is a little large so that it is difficult to be used in some narrow space. In future, the wireless communication between the computer and the laser range finder and the camera is expected.

2. Speed. Although current speed is much faster than manual measurement, it still spends too long time for preparation.

3. Recognizable marker type. Current system is only for the designed circular marker in this study. If necessary, it can be update for any other type of markers in future.

In chapter 3, the line feature-based tracking should be improved as following aspects:

1. Accuracy and stability. The accuracy and stability is lower than the marker-based tracking now, so it is difficult to apply in a long distance tracking in current stage.

2. Speed. Although current speed is about 10 fps, it still not so comfortable for users.

In chapter 4, TPCOSS should be improved as following aspects:

1. Compact. Current system is too large to be moved with workers. In future, iPad is considered to replace the Tablet PC, so it will be moved easily.

2. Acceptability. Although a pre-struction of the system is helpful, the interface is expected to more understandable.

5.2 Applicable Fields

This study is not limited in NPP environment although it is proposed for supporting NPP field work.

1. The circular marker is applicable in any indoor environment with good illumination, such as industrial plant, museum, lab, etc. for navigation, instruction and education. And MAMS is also applicable in the same environment to reduce the preparation workload and human error. It is applicable for any type of markers by updating the program.

2. Line feature-based tracking is applicable in any environment where are abundant of line features, such as industrial plant which has many pipes or other components with straight edges, the urban environment with many buildings, etc.

3. TPCOSS is applicable in other industrial plant for verification simulation.

5.3 Perspective for Integration of the Researches

Tracking in the NPP environment can be realized by integrating the methods proposed in chapter 2 and chapter 3. Then, using TPCOSS developed in chapter 4, an AR system for supporting the temporary placement and conveyance operation of the decommissioning work of an NPP can be obtained.

1. Firstly, a circular marker is designed for both long distance tracking and short distance tracking. Before using the AR system, Some preparation of pasting the markers in environment and measuring them is necessary. MAMS can realize the automatic measurement with high accuracy, stability and efficiency. The human error is also avoided.

2. Line feature-based tracking can be used as an assistant of the marker-based tracking when it is difficult to paste marker in some case. In future, if the accuracy and stability of line feature based tracking method can be improved, it can even replace the marker-based tracking.

3. Using the MAMS for praparation work, and the marker-based and markerless tracking method for the realization of AR, TPCOSS can simulate the temporary placement and conveyance operations in the field.

5.4 Future Perspective

The future perspective of the AR system for supporting the dismantling work is based on the integration of the develop methods: using the designed multiple distance circular marker, the marker-based tracking method is applied in the AR system. MAMS is used in the preparation to reduce the workload and human error, and line feature-based tracking is used as an assistant of the marker-based tracking. Because the dismantling work always needs the cooperation of multiple workers, the AR system is expected to be used by the multiple workers at the same time. Fig.5.1 shows the concept of the AR system. All the operators can simulate the dismantling work through an iPad, for example, allocate a chain block and some chains which connect the dismantling target and the chain block, and move the dismantling target. The operations of the operators are communicated by wireless LAN. Therefore, the current state of the dismantling work is comprehensive by all the operators. Using the modeling subsystem of TPCOSS to obtain the 3D model of the dismantling target and the environment, the collision between the virtual dismantling target and the environment can be detected and indicated on each iPad, so every operator can understand the state of the dismantling target when moving it even if some parts of the dismantling target are occluded on the operator's view.

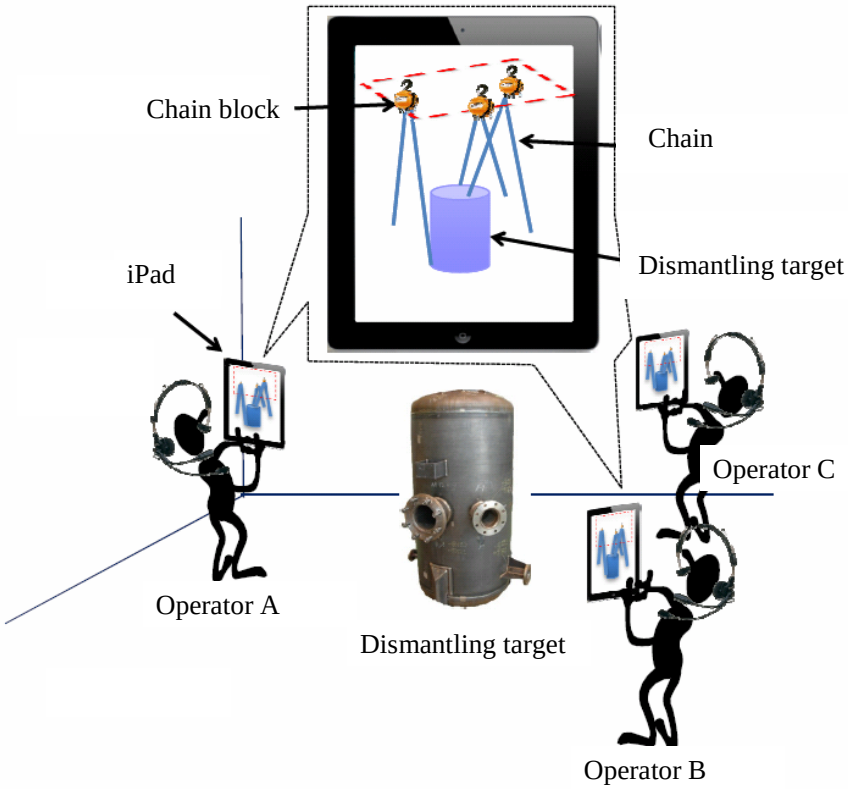

Fig. 5.1: Cooperation system in future.

To realize the cooperation AR system, the future work is focuses on the following aspects:

1. The transplantation of the verification subsystem onto iPad.
2. The wireless communication between multiple iPads.
3. The simulation of allocating some tools (such as chain blocks and chains) for moving the dismantling target, and the simulation of moving the dismantling target without any actual object.

Acknowledgment

This dissertation represents my culmination of research efforts in Energy and Information Laboratory, Graduate School of Energy Science, Kyoto University. During the PhD period, I am very fortunate to have been guided, supported and assisted by a great number of friendly professors, colleagues, staffs and friends. I want to express my profound gratitude to all of them.

First of all, I would like to express my great appreciation to my supervisor, Professor Hiroshi Shimoda for his guidance, support and encouragement throughout my doctoral research and life. Great thanks for your kindness to give me the chance to come to study in Japan. Thank you for your great help on my research task.

I want to express my deep respect to my supervisor, Assistant Professor Hirotake Ishii for his guidance, support and encouragement throughout my doctoral research and life. All my dissertation is based on his great researches in the past years. I will never forget your great efforts, the day and night on my every papers and the dissertation. Your talent programs have helped and inspired me in many research tasks.

I would like to take this opportunity to thank my dissertation committee members, Professor Tetsuo Tezuka and Professor Katsuhiro Kamae, for their valuable suggestions and supports throughout my doctoral dissertation.

I must thank Mr. Masanori Izumi, from Fugen nuclear power plant, for his consistent support and assistance during my doctoral research and experiment.

I want to express my great appreciation for being supported by several Japanese students in the laboratory: Mr. Satoshi Oshita and Mr. Shuhei Aoyama for supporting my research in augmented reality.

I also want to express my great appreciation for Chinese students: Thanks for their helps on my research and life.

I am grateful to the secretaries in the laboratory, Ms.Yamashita, Ms. Tani and Ms. Fusho for their kind helps during my doctoral research.

I want to express my thank to Mr. Zhiqiang Bian, Mr. Shoufeng Yang, Mr. Qi Zhang, Mr. Hongzhe Jin, Ms. Yue Zhao, Mr. Zhiyuan Man and Mr. Yingcheng Gu for their helps on my research and life. Great thanks for Mr. Qi Zhang for his tutorial in my first year in Japan.

Thanks to the Japanese government for the Monbusho Scholarship from the Jananese government, which is much appreciated as the financial support for my research and my life in Japan.

I want to thank my family for their love and support. I would like to express my deep

gratitude and love to my parents, who wholeheartedly support me in my work even though they are thousands of kilometers away from me. I would like to express my deep gratitude and love to my wife and daughter, who wholeheartedly support me in both work and life.

I might not finish writing this acknowledgment if I list all the people who I greatly owed to. Therefore, I would like to say thank to all the people who I should take the opportunity to thank.

At last I want to express my profound appreciation again for spending the 5-year doctoral period in Kyoto University with my dear supervisors, Professor Hiroshi Shimoda, and Assistant Professor Hirotake Ishii.

List of Publications

Chapter 2

Origional Journal Paper

[1] Hirotake Ishii, Hidenori Fujino, **Weida Yan**, Shoufeng Yang, Hiroshi Shimoda, Masanori Izumi: Development of Wide Area Tracking Method for Augmented Reality using Multi-Range Fiducials, *Japan Society of Maintenology*, Vol.8, No.2, pp.43-50, 2009. (In Japanese)

[2] Hirotake Ishii, **Weida Yan**, Shoufeng Yang, Hiroshi Shimoda, Masanori Izumi: Wide Area Tracking Method for Augmented Reality Supporting Nuclear Power Plant Maintenance Work, *International Journal of Nuclear Safety and Simulation*, Vol.1, No.1, pp.45-51, 2010.

[3] **Weida Yan**, Shoufeng Yang, Hirotake Ishii, Hiroshi Shimoda, Masanori Izumi: Development and Experimental Evaluation of an Automatic Marker Registration System for Tracking of Augmented Reality, *International Journal of Nuclear Safety and Simulation*, Vol.1, No.1, pp.52-62, 2010.

International Conference Paper

[1] **Weida Yan**, Shoufeng Yang, Hirotake Ishii, Hiroshi Shimoda, Masanori Izumi: Development and Experimental Evaluation of Automatic Marker Registration System for Tracking of Augmented Reality, *Proceedings of Joint International Symposium of ISSNP2008/CSEPC2008/ISOFIC2008*, Vol.1, CD-ROM, pp.35-41, 2008.

[2] Hirotake Ishii, **Weida Yan**, Shoufeng Yang, Hiroshi Shimoda, Masanori Izumi: Wide Area Tracking Method for Augmented Reality Supporting Nuclear Plant Maintenance Work, *Proceedings of Joint International Symposium of ISSNP2008/CSEPC2008/ISOFIC2008*, Vol.1, CD-ROM, pp.22-28, 2008.

Patent

[1] Hirotake Ishii, Hiroshi Shimoda, Shoufeng Yang, **Weida Yan**, Masanori Izumi: 3D Position Measurement Method and System of Marker, No. 2008-193047, July 28th, 2008. (In Japanese)

[2] Hirotake Ishii, Hiroshi Shimoda, Shoufeng Yang, **Weida Yan**, Masanori Izumi: Automatic Registration Method and System of Marker, No. 2008-247348, September 26th, 2008. (In Japanese)

Chapter 3

Original Journal Paper

[1] **Weida Yan**, Hirotake Ishii, Hiroshi Shimoda, Masanori Izumi: A Line Feature-based Tracking Method of Augmented Reality for Supporting Fieldwork of Nuclear Power Plants, *IEICE Transactions on Information and Systems*. Preparing

International Conference Paper

[1] **Weida Yan**, Hirotake Ishii, Hiroshi Shimoda, Masanori Izumi: A Feasible Tracking Method of Augmented Reality for Supporting Fieldwork of Nuclear Power Plant, *HCI International*, DVD, 2009.

[2] **Weida Yan**, Hirotake Ishii, Hiroshi Shimoda, Masanori Izumi: A Line Feature-based Tracking Method of Augmented Reality for Supporting Fieldwork of Nuclear Power Plants, *International Symposium on Symbiotic Nuclear Power Systems for 21st Century*, CD-ROM, 2010.

[3] **Weida Yan**, Hirotake Ishii, Hiroshi Shimoda, Masanori Izumi: A Line Feature-based Tracking Method of Augmented Reality for Supporting Fieldwork of Nuclear Power Plants, *First International Symposium on Socially and Technically Symbiotic System*, DVD, 2012.

Chapter 4

Original Journal Paper

[1] **Weida Yan**, Shuhei Aoyama, Hirotake Ishii, Hiroshi Shimoda, Tran Sang, Solhaug Inge, Toppe Lygren, Johnsen Terje, Masanori Izumi: Development and Evaluation of a Temporary Placement and Conveyance Operation Simulation System Using Augmented Reality, *Nuclear Engineering and Technology*, Vol.44, No.5, pp.507-522, 2012.

International Conference Paper

[1] Hirotake Ishii, Shuhei Aoyama, Yoshihito Ono, **Weida Yan**, Hiroshi Shimoda, Masanori Izumi: Spatial Clearance Verification Using 3D Laser Range Scanner and Augmented

Reality, *HCI International*, Vol.1, Paper No.LNCS 6773, pp.45-54, 2011.

Other

Original Journal Paper

[1] Hirotake Ishii, Satoshi Oshita, **Weida Yan**, Hiroshi Shimoda, Masanori Izumi: Development and Evaluation of a Dismantling Planning Support System Based on Augmented Reality Technology, *International Journal of Nuclear Safety and Simulation*, Vol.2, No.1, pp.52-60, 2011.

[2] Hiroshi Shimoda, Yue Zhao, **Weida Yan**, Hirotake Ishii: A Radiation Learning Support System by Tri-sensory Augmented Reality Using a Mobile Phone, *International Journal of Nuclear Safety and Simulation*, Vol.2, No.4, pp.350-359, 2011.

International Conference Paper

[1] Hirotake Ishii, Satoshi Oshita, **Weida Yan**, Hiroshi Shimoda, Masanori Izumi: Development and Evaluation of a Dismantling Planning Support System Based on Augmented Reality Technology, *International Symposium on Symbiotic Nuclear Power Systems for 21st Century*, CD-ROM, 2010.

[2] Hiroshi Shimoda, Yue Zhao, **Weida Yan**, Hirotake Ishii: A Radiation Learning Support System by Tri-sensory Augmented Reality Using a Mobile Phone, *International Symposium on Future I& C for Nuclear Power Plants, Cognitive Systems Engineering in Process Control, and International Symposium on Symbiotic Nuclear Power Systems*, Paper No.1102, 2011.